UNIVERSITY OF NOVA GORICA
GRADUATE SCHOOL
STUDY PROGRAMME: ENVIRONMENTAL SCIENCES

DEVELOPMENT AND APPLIACTION OF NEW LASER METHODS IN ENVIRONMENTAL AND BIOMEDICAL RESEARCH

Azamela MADŽGALJ

Master Thesis

Mentor: prof. dr. Mladen Franko

Nova Gorica, 2007

ACKNOWLEDGMENTS

My years at the Laboratory for Environmental Research have given me a remarkable opportunity to work with and learn from a range of bright and interesting people. It is a pleasure to convey my gratitude to them all in my humble acknowledgment.

In the first place I would like to express my gratitude to Prof. Mladen Franko for being an outstanding advisor and excellent professor. His constant encouragement, support and invaluable suggestions made this work successful.
I would like to thank the other members of my committee: Prof. Janez Štupar, Prof. Corrado Sarzanini and Asst. Prof. Milko Novič for their time and effort in reviewing this work.

I wish to acknowledge and thank to Prof. Sabina Passamonti and her PhD student Alessandra Meastro (University of Trieste) for their help and cooperation.
A very special thanks goes to Maja who has lived with me during this two years, encouraged me and was there for me whenever I needed her.
I feel most grateful to my officemates Mojca and Aleš, with whom I started to feel a bit at home with at the university. Mojca thank you for introducing me to the world of analytical chemistry, for being my friend and the source of great emotional support.
Branka thank you for your advice and willingness to share your bright thoughts with me.
Thanks to my lab-mates Urh, Malgorzata, Ana, Ksenija, Dunja, Kristina, Romina, Jana and Martina for the fun, support and pleasant working environment.
Ana, Veronika, Renata, Vanesa and Mirjana thanks for the lunch meeting and exhilarating time we spend together.

I am deeply and forever indebted to my parents for their love, support and encouragement throughout my entire life. I am also very grateful to Lejla and Fatima for being supportive and caring siblings.

ABSTRACT

This thesis describes the development and application of thermal lens spectrometry (TLS) to the analysis of photo-labile analytes (such us Cr(VI)-DPC and bilirubin) and neonicotinoids (relatively new class of insecticides) in environmental and biological samples. TLS is well known as highly sensitive technique enabling measurements of absorbencies as low as 10^{-7}, and determination of low concentrations of various compounds. It was however noticed that measurements of photo-labile compounds by this technique are hindered due to decomposition of analytes induced by intensive excitation laser source. Flow injection analysis, which minimizes the exposure of the sample to the excitation beam light, contributes to minimization of the influence of photochemical processes on the TLS signal.
For this purpose a system for flow injection analysis with thermal lens spectrometric detection (FIA-TLS) was assembled and determination of photolabile analytes was investigated under various experimental conditions to overcome or minimize the problems associated with photodegradation.
Cr(VI) was determined following on-line generation of Cr(VI)-DPC complexes, or by injection of Cr(VI)-DPC into the FIA system after complete development of color (20 min). In the first case acidified diphenylcarbazide as reagent was injected through a 20 µL injection loop and was further mixed with the carrier solution spiked with Cr(VI), while in the second case the carrier solution was not spiked with Cr(VI) and Cr-DPC was injected directly through a 0.5 mL injection loop. The carrier solution consisted of water, acetone and 25 % H_3PO_4 in the volume ratio of 22 : 2 : 1. Under optimized conditions, a linear calibration graph was obtained in both cases for the range of 1-20 µg/L. The LODs (limits of detection) of 0.067 µg/L for on-line generation of Cr-DPC and 0.065 µg/L for injection of pre-reacted Cr-DPC were achieved. The results indicate that in the case of Cr(VI) determination by on-line generation of Cr(VI)-DPC complexes the time of analysis and the consumption of reagent are significantly reduced. The sensitivity is comparable to Cr(VI) determination in batch mode, while the LODs are lowered below 0.1 due to reduced standard deviation in case of FIA-TLS.

The effect of added methanol on the sensitivity and the detection limits (LODs) of the determination of bilirubin by FIA-TLS technique was investigated. Different amounts of organic solvent were added directly to the carrier solution and to the sample to improve the thermooptical properties of the solvents. Consequently, the sensitivity of the technique was increased by a factor of 2.9 and an LOD of 0.4 nM bilirubin was achieved. The developed method enables sensitive, rapid and reproducible determination of real physiological concentrations of bilirubin in biological samples, which is not accessible by conventional transmission spectrometric techniques due to low solubility of bilirubin (70 nM) under physiological conditions.

The performance of the FIA-TLS technique for photolabile analytes was verified by the determination of Cr(VI) in spiked drinking water and was exploited further for investigations of bilirubin uptake into endothelial cells.

A new HPLC-TLS method for determination of selected neonicotinoids (imidacloprid, thiamethoxam, acetamiprid and thiacloprid) in water samples was developed. The method is based on the reversed phase separation (C_{18} column), isocratic elution (with 7:3 (v/v) water (0.2% phosphoric acid):acetonitrile as eluent, 1 mL/min flow rate), and collinear dual beam TLS detection at 244 nm. Achieved LODs for thiamethoxam, imidacloprid, acetamiprid and thiacloprid were 15, 27, 3.2, and 7.5 µg/L, respectively. The LOD and related LOQ values are lower by 2.5–8.5 times for thiamethoxam, acetamiprid and thiacloprid, compared to HPLC/DAD, with similar RSDs. The applicability of the developed procedure was tested on spiked river water samples.

This work confirms the applicability of TLS detection in flowing samples and for determination of photolabile analytes in particular. The developed FIA-TLS and HPLC-TLS methods allow sensitive, selective, and reproducible trace-level determination of Cr(VI), bilirubin and selected neonicotinoids. The FIA-TLS method reduces the time of analysis, sample and reagent consumption and offers higher reliability relative to batch mode TLS, while the HPLC-TLS method offers important improvements in sensitivity and LOD's compared to HPLC/DAD detection of some neonicotinoids.

POVZETEK

V pričujočem magistrskem delu je opisana uporaba spektrometrije s termičnimi lečami (TLS) pri razvoju novih analiznih metod za določevanje svetlobno občutljivih snovi kot sta kromov difenilkarbazidni kompleks (Cr-DPC, uporabljen za določevanje Cr(VI)) in bilirubin ter neonikotinoidov (nove skupine insekticidov) v okoljskih in bioloških vzorcih.
Spektrometrija TLS je visoko občutljiva analizna tehnika, ki omogoča določevanje različnih spojin v zelo nizkih koncentracijah, saj merilno območje TLS sega nižje od 10^{-7} absorpcijskih enot. V znanstveni literaturi pa so opisali tudi slabosti TLS pri določevanju svetlobno občutljivih spojin, ki so povezane z visoko intenziteto vzbujevalne laserske svetlobe in posledično z razkrojem analita med detekcijo. Z uporabo pretočne injekcijske analize (FIA) pri meritvah s TLS smo vpliv opisanih pomanjkljivosti uspešno zmanjšali. Na ta način je kontaktni čas med vzorcem in svetlobnim snopom tudi do tisočkrat krajši, vendar še zagotavlja visoko občutljive meritve in izboljšanje spodnje meje določljivosti.

Cr(VI) smo določali po tvorbi kompleksa Cr-DPC.To smo dosegli na dva načina. Pri prvem smo skozi sistem FIA kot nosilno raztopino črpali vzorec, ki je vsebovala Cr(VI), z dodatkom acetona in nakisano s H_3PO_4 ter skozi 20 µL zanko vbrizgali reagent DPC. V drugem primeru smo v sistem z nosilno tekočino brez Cr(VI) skozi 500 µL zanko vbrizgali kompleks Cr(VI)-DPC, ki je bil predhodno pripravljen z dodatkom reagenta DPC vzorcu., Nosilna tekočina je bila sestavljena iz vode, acetona in 25 % H_3PO_4 v volumskem razmerju 22 : 2 : 1. V obeh primerih smo dosegli linearnost v območju uporabljenih koncentracij 1-20 µg/L. Dosežene meje zaznavnosti za Cr(VI) pa so bile v prvem primeru 0,067 µg/L v drugem pa 0,065 µg Cr/L. Z direktno reakcijo Cr(VI)-DPC smo dodatno znižali spodnjo mejo zaznavnosti (doslej 0,1 ng/mL) ter obenem pomembno skrajšali čas analize (50 s namesto 20 min.) in zmanjšali porabo reagenta. Metodo smo uspešno uporabili za določevanje nizkih koncentracij Cr(VI) v vzorcih pitne vode.

Pri določevanju bilirubina s pomočjo tehnike FIA-TLS smo z dodajanjem metanola dosegli zvišanje občutljivosti saj organska topila izboljšajo optotermične lastnosti raztopin za meritve s TLS. Na ta način smo občutljivost za določevanje bilirubina zvišali za 2,9-krat, obenem pa smo z meritvami v sistemu FIA-TLS izboljšali ponovljivost meritev. S tem smo dosegli znižanje meje zaznavnosti na 0,4 nM koncentracijo bilirubina, kar pomeni petkratno izboljšanje dosedanje meje zaznavnosti s TLS v stacionarnih vzorcih ter omogoča hitro in zanesljivo detekcijo fizioloških koncentracij bilirubina v bioloških vzorcih.

Metodo smo uspešno uporabili pri raziskavah privzema bilirubina v endotelijske celice v realnih fizioloških pogojih, kjer uporabo transmisijskih tehnik za merjenje absorbance omejuje nizka topnost bilirubina.

V nadaljevanju smo razvili metodo kromatografije visoke ločjivosti HPLC z detekcijo s TLS za določevanja neonikotinoidov (imidakloprida, tiametoksama, acetamiprida in tiakloprida) v vodnih vzorcih. Ločbo izbranih insekticidov smo dosegli na koloni C_{18} z izokratsko elucijo z raztopino vode in acetonitrila (7:3 (v/v) voda (0.2% fosforna kislina) : acetonitril; pretok 1 mL/min). Za detekcijo s TLS smo uporabili valovno dolžino 244 nm in za tiametoksam, imidakloprid, acetamiprid in tiakloprid dosegli nizke meje zaznavnosti 15, 27, 3.2, in 7.5 µg/L. S tem smo 2.5–8.5 krat znižali meje zaznavnosti za tiametoksam, acetamiprid in tiakloprid v primerjavi s tehniko HPLC-DAD pri enaki merski negotovorsti. Uporabnost metode smo uspešno testirali z določevanjem neonikotinoidov v rečni vodi.

Dokazali smo prednosti in uporabnost detekcije s spektrometrijo TLS v pretočnih sistemih, posebno še pri določevanju svetlobno občutljivih spojin. Razvite metode FIA-TLS in HPLC-TLS omogočajo občutljivo, selektivno in ponovljivo določevanje Cr(VI) v sledovih ter nizkih koncentracij bilirubina in neonikotinoidov. Čas analize se z uporabo tehnike FIA-TLS učinkovito zmanjša, enako tudi poraba reagentov. Občutljivost in meje zaznavnosti pri določevanju neonikotinoidov po postopkih za HPLC-DAD smo tudi občutno izboljšali z uporabo tehnike HPLC-TLS.

CONTENTS

LIST OF TABLES

LIST OF FIGURES

1 INTRODUCTION

Rapid population growth combined with industrialization, urbanization and agricultural intensification, has resulted in an increased consumption of natural resources and energy, massive waste production, and steadily growing environmental pollution. Availability and use of chemicals, exposure to pesticides, heavy metals and small particulates, emission of hazardous substances in the air, soil and water, pose an increasing threat to the health of humans and their environment. Owing to governmental and public concern over the extent of environmental pollution considerable effort has recently been directed towards developing advanced sensitive techniques capable of determining ultra trace amounts of substances in various samples. In this regard, not only detection of organic and inorganic pollutants in environmental and biological samples, but also understudying of their mechanisms of action has distinct importance.

Typical example of a pollutant whose toxicity depends on its chemical form and concentration is chromium. Chromium (III) is considered an essential micronutrient for humans (Hambidge, 1971), whereas chromium (VI) is a potential carcinogenic agent (Littig, 1980). This leads to a great interest in the speciation and determination of chromium in biological and environmental samples, especially chromium (VI), due to its potential toxicity. Chromium is present in biological tissues, fluids and in the environment at trace levels. In most easily accessible biological samples from humans, like blood, serum/plasma, urine, etc, the levels of chromium (Cr) are less than 1 ng/g, and in many cases closer to 0.1 ng/g (Veillon et al., 1999). Total Cr content in surface water is typically between 0.3 and 6.0 µg/L (Bowen, 1979).
Spectrophotometry is often favored for detection of individual Cr species (particularly Cr(VI)), but the applicability of this technique is limited due to its relatively low sensitivity, compared to species non-specific techniques (AAS, ICP-AES).

Among the new organic pollutants appearing in the environment, neonicotinoids have received particular attention. Neonicotinoids are a relatively new class of insecticides with a distinct mode of action. They act as antagonists by binding to postsynaptic nicotinic receptors in the insect's central nervous system. This leads to the accumulation of acetylcholine, resulting in the paralysis and death of insects (Suchail, 2000). Neonicotinoids are intensively used for crop protection because of their excellent systemic properties, but are unfortunately suspected as major cause of observed massive killings of honeybees. Since physiological effects on honeybees are possible at concentrations of neonicotinoids much lower than LD_{50} values (40-100 ng/bee) (Bonmatin et al., 2003). Development of highly sensitive analytical methods is needed for monitoring the low levels of neonicotinoids in various matrices.

With relation to possible effects of various toxic substances on human health it is essential to understand the mechanisms of activity and transport pathways into cells of various systems that protect the body. To prevent the formation of oxidants as well as to repair oxidative damage to tissues, all aerobic living organisms posses a complex arsenal of enzymatic and nonenzymatic antioxidant defenses to protect themselves against reactive oxygen species (Young and Woodside, 2001). Bilirubin is a potent physiological antioxidant, which is supposed to provide important protection against many diseases (Sedlak and Snyder, 2004). The solubility of bilirubin under physiological conditions is extremly low, quoted 70 nM, which is not accessible by conventional transmission spectrometric techniques. Therefore, highly sensitive analytical methods, which enable the determination of real physiological concentrations of bilirubin in biological samples are needed in studies of antioxidant transport across the cellular membrane under physiological conditions.

Measurements of absorbance through photothermal effects, i.e. thermal lens spectrometry (TLS) was proven to provide better sensitivity and in principle lower LODs compared to spectrophotometry and enables detection of absorbance as low as 10^{-7} (Dovichi and Harris, 1981). Recently, highly sensitive photothermal techniques, including TLS, have evolved and have been attracting attention for trace-level analysis of different biological and environmental samples (Franko, 2001, Luterotti et al., 2002, Pogačnik and Franko, 2003). It was however noticed that TLS measurements of photo-labile compounds (Cr(VI)-DPC and bilirubin) are hindered due to decomposition of analytes induced by intensive excitation laser source (Pedreira et al., 2004, 2006). Consequently, an abnormal decrease of the TLS transient signal due to a fast photochemical reaction is observed during a TLS measurement of Cr-DPC in solution, as it was demonstrated experimentally and described theoretically (Pedreiraa et al., 2004, 2006).

In a flow injection mode the decomposition of photo-labile analyte could be avoided or significantly reduced. FIA-TLS technique should offer a reproducible, rapid and rather convenient procedure for routine determination of trace amount of photolabile analytes.

TLS is a non-specific detection technique and therefore requires prior separation of analytes species. It has alredy been applied for the detection of different compounds in HPLC with UV-Vis detection. For determination of low levels of neonicotinoids a new HPLC method with TLS-UV detection is needed.

The aim of my work was:

- Development and application of FIA-TLS method for determination of trace levels of photo-labile analytes (Cr(VI)-DPC, bilirubin) in environmental and biological samples.
- Optimization and validation of a novel thermal lens spectrometer for detection in UV region and its use as detection unit in liquid chromatography.

2 THEORETICAL BACKGROUND

2.1 Thermal Lens Spectrometry

The basic principle of photothermal methods is the measurement of the amount of thermal energy released by chemical species when excited by a laser beam. The heat generated from non-radiative relaxation processes leads to a temperature rise in the medium in which the absorbing compound is contained. When the radial energy distribution of the excitation beam has a Gaussian profile, the temperature within the sample will also follow a similar profile. Therefore, a refractive index gradient, $\partial n/\partial T$, is produced and the sample behaves like an optical lens. Practically, a second laser, the probe beam, probes the thermal lens effect by measuring the far-field variation in beam centre intensity.
The first photothermal spectroscopic method to be applied for sensitive chemical analysis was photothermal lens spectroscopy. The photothermal lens effect was discovered by Gordon et al. 1964-1965, while carrying out an intracavity excitation of a liquid sample for Raman spectroscopy. The authors observed time-dependent changes in the laser intensity, which they could attribute to localized heating of the sample.
Since the discovery of the thermal lens effect several works have been done in order to derive a theoretical relationship between the sample concentration and the analytical signal. The focal length of the thermal lens was first expressed by Gordon, using a parabolic approximation for the temperature rise within the sample. The expression for the variation of the far-field intensity at the centre of a Gaussian beam after passing through the thermal lens was then derived by several authors (Gordon et al., 1965; Hu and Whinnery, 1973; Whinnery, 1974).

In this work, the derivation of an expression for the thermal lens signal on a mode-mismatched dual beam device (Figure 1) with modulated continuous excitation will be presented, based mainly on the theoretical considerations discussed in the book of Bialkowski (Bialkowski, 1996) and other reviews (Gupta, 1992; Franko, 1996; Dovichi, 1987; Sheldon et al., 1982).
The mode-mismatched dual beam TLS spectrometer is a thermal lens instrument, were two laser beam generates and detect the TLS signal: a more powerful laser (pump laser) is used to excite the sample and a low power laser (probe laser), is used to probe the generated thermal lens. Focuses of the two lasers are mismatched, that is the focal points of two lasers are not at the same position.

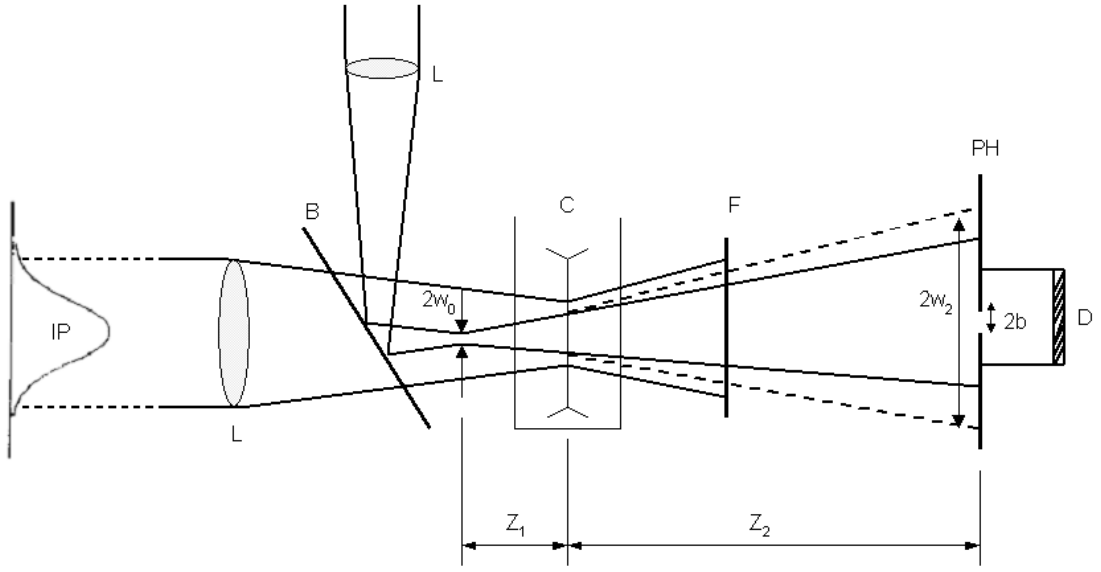

Figure 1: *Scheme of the geometric position of the beams in a mode-mismatched dual beam thermal lens spectrometry (TLS).*
IP = intensity profile of the pump beam; L = lens; B = beamsplitter; C = cell; F = filter; PH = pinhole; D = photodetector; w_0 = radius of beam waist of the probe beam; w_2 = radius of the probe beam at the pinhole position; Z_1 = distance between the focus of the probe beam and the sample cell; Z_2 = distance between the sample and the pinhole, b =radius of pinhole before the photodiode.

2.1.1 Temeperature changes from Gaussian excitation sources

A common thermal diffusion problem encountered in the all photothermal techniques is that arising from sample excitation with a Gaussian spatial profile laser. Solutions to this problem have been summarized by Dovichi (1987) and Gupta (1989). The derivations assume that:

- The laser beam is cylindrically symmetric and attenuation along the path of the laser does not result in a significant difference in the temperature change
- An infinite sample (the infinite sample extent approximation is valid when relatively large volume samples are excite with focused laser sources. The sample observation time is less than the time required for heat to diffuse to the cell walls, $t \leq r^2/4D_T$ where r is the minimum distance between the laser focus location and the cell wall and t is the time of observation)
- Thermal diffusion at the sample cell windows is neglected (the relative contribution of this loss mechanism to the total thermal diffusion can be minimized using sample cells with relativly long pathlenghts)
- The sample is optically thin (little attenuation of the excitation source occurs upon passing through the sample. The energy or power absorbed by the sample per unit length is essentially independent of pathlenght)
- All absorbed energy is converted to heat.

Consider a weakly absorbing sample being irradiated with a Gaussian or TEM_{00} laser beam. The laser light is propagating along the *z*-axis direction. The irradiance at any point through the homogeneous sample can be found from differential expression for absorption along the sample path

$$-\frac{dE(x,y,z,t)}{dz} = \alpha E(x,y,z,t) \qquad (1)$$

E(x,y,z,t) (W m^{-2}) is the irradiance in the sample at a distance *z* past the origin, and α (m^{-1}) is the absorption coefficient. For an optically thin sample the irradiance does not change significantly on pass-

ing through the sample. The irradiance on the right hand side of Eq. (1) is thus approximately constant and may be substituted for by $E_0(x,y,t)$, the irradiance incident on the sample. The power delivered tothe sample is

$$E_l(x,y,t) - E_0(x,y,t) \approx E_0(x,y,t)\alpha l \tag{2}$$

where l (m) is the sample pathlenght and $E_l(x,y,t)$ is the irradiance leaving the sample.
The irradiance of the Gaussian laser used to excite the sample is expressed as

$$E_0(x,y,t) = \frac{2\phi(t)}{\pi\omega^2} e^{-\frac{2(x^2+y^2)}{\omega^2}} \tag{3}$$

The expression factor Φ(t) is the time-dependent power and *w* is the Gaussian beam waist radius. The factor $2/\pi w^2$ is a normalization factor. The Gaussian irradiance is normalized such that integration of $E_0(x,y,t)$ over x and y space is equal to Φ(t), the total power of the beam.

The time-dependent temperature change is found by solving the thermal diffusion equation,

$$\frac{\partial}{\partial t}\delta T(x,y,t) = D_T \nabla^2 \delta T(x,y,t) + \frac{\alpha E_0(x,y,t)}{\rho C_p} \tag{4}$$

where T(x,y,t) is a temperature, D is thermal diffusivity, ρ is the density, C_p is the specific heat at a constant pressure of the medium, E_0 is the irradiance of the Gaussian laser.

Assuming that the homogeneous sample is of infinite extent, the solution to the thermal diffusion equation can be obtained using a Furrier transformation in space and a Laplace transformation in time (Bialkowski, 1996, p. 142). The solution can be expressed as the convolution of the point-source solution with the heat source:

$$\delta T(x,y,t) = \phi(t) * \left[\frac{2\alpha}{\pi\rho C_p} \frac{1}{\omega^2(1+2t/t_c)} e^{-\frac{2(x^2+y^2)}{\omega^2(1+2t/t_c)}} \right] \tag{5}$$

where t_c is the characteristic thermal diffusion time defined as $t_c = w^2 \rho C_p / 4k$, k is thermal conductivity.

The temperature change induced by a modulated continous Gaussian laser excitation source (which was used in this study) can be described by convoluting the laser-induced heating and cooling cycle with a repetition function C(t). For a chopper with a duty cycle such that t_1 is the time that chopper allows the beam to pass and t_2 is the time that chopper blocks the beam, a repetition function for a periodic source can be cast in terms of delta functions

$$C(t) = \sum_{m=1}^{M} \delta(t - m\tau) \tag{6}$$

where τ is the cycle period and a total of M cycles have occurred since the start of the experiment. The cycle period is $\tau = t_1 + t_2$, t_1 is time of excitation and t_2 is cooling time. The temperature change at the end of the M th cycle is

$$\delta T_{chopped}(x,y,M\tau) = \delta T_{cw}(x,y,t) * C(t) \tag{7}$$

where $\delta T_{cw}(x,y,t)$ for continuous excitation can be derived from Eq. (5) considering Φ(t) as a constant. The solution for the on-axis temperature change at the end of the M[th] cycle of the chopper is (Bialkowski, 1996, p.281)

$$\delta T_{choppeed}(0,0,M\tau) = \frac{\phi_0 \alpha}{4\pi\kappa} \sum_{m=1}^{M} \ln \frac{t_c + 2m\tau}{t_c + 2(m\tau - t_1)} \tag{8}$$

The on-axis temperature change apparently has a finite limiting value since

$$\lim_{m\to\infty} \ln \frac{t_c + 2m\tau}{t_c + 2(2m\tau - t_1)} = \ln \frac{t_c + 2m\tau}{t_c + 2m\tau} = 0 \tag{9}$$

However, model calculations show that a steady state on axis temperature change is not reached even with as many as 10^8 cycles, even for favourable values of t_1 and t_c. The infinite medium approximation breaks down with these long times since the diffusion distance would be greater than the sample cell dimensions. In this case the maximum temperature is reached when the rate of heat transfer from the sample cell to the surroundings equals the rate at which heat is added to the sample by laser excitation. The differential temperature change resulting from each individual cycle is independent of the initial temperature.

The average temperature continues to increase, although the temperature change produced for a single chopper cycle is about the same after the first few excitation/cooling cycles. The temperature change can be thought of a sum of two components: an average temperature increase, proportional to the average excitation power, and an oscillating component. The average temperature increase will be logarithmic and the magnitude of the oscillating component is approximately constant.

The heat resulting from the absorbed energy causes changes in the temperature distribution within the medium and to the change of thermodynamic properties of the sample. Refractive index is one such property. A time dependent refractive index gradient formed inside the sample can be described as:

$$n(x,y,t) = n_0 + \left(\frac{\partial n}{\partial T}\right)_{T_A} T(x,y,t) \tag{10}$$

where n_0 is the refractive index at room temperature T_A. Equation (15) assumes a decrease in refractive index with increased temperature, and $\partial n/\partial T$ is an absolute value. Consequently, the irradiated sample acts as a lens like element, which causes the laser beam to diverge. The increased divergence of the beam may be observed some distance beyond the sample as a larger spot size or a lower intensity at the beam center.

2.1.2 Propagation of Gaussian Beam and Predicting Thermal Lens Behavior

The effect of an optical element such as a lens on the propagation of the laser beam is conventionally determined using ABCD law (Harris, xxx), where A, B, C, and D are the elements of a ray transfer matrix for the optical element in question. For example, the ray transfer matrix of a free-space propagation of length Z is

$$\begin{bmatrix} A & B \\ C & D \end{bmatrix} = \begin{bmatrix} 1 & Z \\ 0 & 1 \end{bmatrix} \tag{11}$$

And that of a thin lens of focal length f is

$$\begin{bmatrix} A & B \\ C & D \end{bmatrix} = \begin{bmatrix} 1 & 0 \\ -1/f & 1 \end{bmatrix} \tag{12}$$

The ray transfer matrix of any system composed of N optical elements is the product, in reverse order of propagation, of the individual ray transfer matrices of each element:

$$\begin{bmatrix} A & B \\ C & D \end{bmatrix} = \begin{bmatrix} A_N & B_N \\ C_N & D_N \end{bmatrix} \cdots\cdots \begin{bmatrix} A_2 & B_2 \\ C_2 & D_2 \end{bmatrix} \begin{bmatrix} A_1 & B_1 \\ C_1 & D_1 \end{bmatrix} \tag{13}$$

When the origin of the optical system correspondents to the waist of a laser beam and when the refractive index at the end of the optical system is the same as the origin, the spot size of the emerging beam may be contently determined by (Piepmeier, 1986)

$$w^2 = w_0^2 \frac{A^2 + B^2}{Z_c^2} \tag{14}$$

where w_0 and $Z_c = \pi w_0/\lambda$ are the spot size (the beam radius) and confocal distance at the waist. A typical optical system to observe a thermal lens is shown in figure 1, which corresponds to a ray transfer matrix given by product

$$\begin{bmatrix} A & B \\ C & D \end{bmatrix} = \begin{bmatrix} 1 & Z_2 \\ 0 & 1 \end{bmatrix} \begin{bmatrix} 1 & 0 \\ -1/f(t) & 1 \end{bmatrix} \begin{bmatrix} 1 & Z_1 \\ 0 & 1 \end{bmatrix} \tag{15}$$

Substituing A and B from the above system matrix into Eq. (14) and allowing Z_2 to increase without bound so that the divergence of the beam becomes constant, yields the following expression for the far-field spot size:

$$w_2^2(t) = w_0^2 Z_2^2 \left[\left(\frac{1}{f(t)} \right)^2 + \left(1 - \frac{Z_1}{f(t)} \right)^2 / Z_c^2 \right] \tag{16}$$

where Z_1 is a distance between the focus of the probe beam and the sample, Z_2 is a distance beetwen the sample and pinhole and f(t) is focal length of a thermal lens.

Finally, the relative change to the far field spot size ($Z_2 >> Z_1$ and $Z_2 >> Z_c$) with the assumption that thermal lens is weak ($f(t) >> Z_1$ and Z_c) is found by substitution, recalling that the sample focal length at the onset of illumination would be $f(0) = \infty$,

$$\frac{\Delta w^2}{w_2^2} = \frac{w_2^2(o) - w_2^2(t)}{w_2^2(t)} \approx \frac{-2Z_1}{f(t)} \tag{17}$$

2.1.3 Detection of TLS signal

The pinhole with the radius b is positioned at the center of the beam and the transmitted power is

$$\phi_{\det}(t) = 2\pi \frac{2\phi_{probe}}{\pi w^2(t)} \int_0^b e^{-\frac{2r^2}{w_2^2(t)}} r dr = \phi_{probe}\left(1 - e^{-\frac{2r^2}{w_2^2(t)}}\right) \tag{18}$$

For a relatively small pinhole radius it can be rewritten as

$$\lim_{b/w_2(t)} \phi_{\det}(t) = \frac{2\phi_{probe} b^2}{w_2^2(t)} \tag{19}$$

Thermal lens signal s(t) for chopped or periodic excitation is defined as (Bialkowski 1996, p.377)

$$s(t) = \frac{\phi_{\det}(t) - \phi_{\det}(0)}{\phi_{\det}(0)} = \frac{w_2^2(0) - w_2^2(t)}{w_2^2(t)} \tag{20}$$

from Eq. (17) it is evident that

$$s(t) = \frac{-2Z_1}{f(t)} \tag{21}$$

When calculating the focal length of the thermal lens, which is needed to evaluate the thermal lens strength it is necessary to consider different possible geometrical configurations of pump and probe beams. Most frequently, collinear and transverse configurations are used.
For the collinear configuration (which was used in our experiments) the focal length of a thermal lens can be obtained from

$$\frac{1}{f} = -l \frac{\partial n}{\partial T}\left(\frac{\partial^2 \delta T}{\partial r^2}\right)_{r=0} \tag{22}$$

where l is the interaction length and $r^2 = x^2 + y^2$.
The magnitude of the inverse focal length in the position r = 0, which contributes to the measurable thermal lens signal, can be obtained by calculating the difference in focal lengths heating between the maximum heating and minimum cooling times (Bialkowski, 1996; p. 367).

$$\frac{1}{|\delta f|} \approx \left(\frac{\partial n}{\partial T}\right) \frac{8\phi_0 \alpha l}{\pi k w^2} \frac{(t_1/t_c)^2}{(1 + 2t_1/t_c)(1 + 4t_1/t_c)} \tag{23}$$

Substituting Eq. (23) into Eq. (21) yields the following expression for thermal lens signal in a case of collinear configuration and chopped continuous excitation

$$s(t) = -Z_1 \frac{8\phi_0 \alpha l}{\pi k w^2}\left(\frac{\partial n}{\partial T}\right) \frac{(t_1/t_c)^2}{(1 + 2t_1/t_c)(1 + 4t_1/t_c)} \tag{24}$$

The ratio in expression (24) with t_1 and t_c is a constant for a particular measurement, characteristic for the particular experimental set-up (t_1) and the sample parameters (t_c).

The thermal lens signal is linearly dependent on the power of a laser used for excitation and it is strongly dependent on the size of the pump beam. For this reasons tightly focused and high power

laser beams are preferred for excitation. Equation (24) demonstrates that a mode-mismatched (the focus of probe and pump beam laser are not at the same place) dual beam thermal lens experiment is more sensitive than the single beam or mode-matched dual beam methods. From Eq. (24) it is assumed that an increase in Z_1 will result in a higher signal, which is not the case. The probe laser beam radius must be less than the dimension of the thermal perturbation and this does not allow Z_1 to be large. Through dependence of t_c on $w(Z_1)$ ($t_c=w^2\rho C_p/4k$) and the dependence of $s(t)$ on Z_1, both the magnitude and time dependence of the thermal lens effect are sensitive to the location of the cell with respect to the waist. It was proven that the sample position for maximum response is at $Z_1 = Z_c\sqrt{3}$ (Sheldon, 1982).

The model derived above is the simplest model describing a thermal lens behavior in a motionless sample. A quantitative model of thermal lens behavior for a flowing sample is considerably more complex. Bulk flow effecting thermal lens response in a typical flow cell may be divided into two components: one directed parallel to the cell axis (z direction), and the other directed transverse to the cell axis (Dovichi and Harris, 1981). Axial bulk flow cools the sample by removing heated metarial from the exit and introducing unheated material at the entrance. The time scale necessary for axial flow to influence thermal lens behavior is given by the residence time of the cell (cell volume divided by the flow rate). If the residence time is much longer than the time constant t_c, flow has little influence on the thermal lens. The secondary flow, arising from the destabilizing effect of the velocity difference across the cell corners, takes the form of motion in vortices, which results in efficient mixing within the cell. This mixing is superimposed upon the bulk from the cell. This secondary flow could be indetified as a major heat conduction mechanism affecting the thermal lens response. The thermal lens effect of a flowing sample influenced by mixing is considerably more complex than for simple bulk flow. The time dependence of the effect could be obtained by convolution of the thermal lens impulse response (Twarowski and Kliger, 1977) for a static sample with a correlation function which describes the time-dependence decrease in coherence of the temperature distribution due to random mixing within the cell (Dovichi and Harris, 1981).
Nevertheless, both flows act as an additional thermal transport mechanism, which has two effects: the increased rate of thermal transport produces a steady state signal more rapidly, and change in the stady-state probe beam intensity is smaller than that observed from a static thermal diffusion case (Dovichi and Harris, 1981).
In all the experiments presented in this work, the samples were flowing in z-direction. Under such flow condition the heat is carried along the probe beam axis. The refractive index gradient therefore overlaps constantly with the probe axis, which is not the case for the sample flow, perpendicular to the pump and probe beam propagation. As flow in a medium of constant refractive index does not affect beam propagation, the initial probe beam intensity is indenpendent of flow rate (Dovichi and Harris, 1981).
Overall, flowing the sample will, in general, decrease the enchancement relative to the transmmison mode measurements and consequently result in a loss of sensitivity. At excessive flow rates a loss of sensitivity due to increased thermal conduction and an additional source of proportional noise from flow pulsations is observed. At low flow rates suitable for most applications performance is not severely degraded and a thermal diffusion time response can still be used to fit the data (Dovichi and Harris, 1981). The loss of sensitivity could be overcome by an increase in laser power or the use of a solvent having more favourable thermooptical properties.

2.1.4 Sensitivity

The best-known property of thermal lens spectrometry is its high sensitivity. The relative merit of using thermal lens spectrometry for trace measurements is encompassed in the theoretical enhancement factor. By definition (Dovichi and Harris, 1979) the enhancement factor is the ratio of the photothermal signal to that obtained using transmission spectrophotometry under the assumption that both measurements have the same limiting noise.
In conventional absorption spectrometry, the transmitted signal is given by Lambert-Beer's law:

$$\phi = \phi_0 10^{-\varepsilon c l} \tag{25}$$

where Φ_0 is the incident beam power, Φ the transmitted power, ε the molar extinction coefficient, c the concentration of the analyte and l the optical pathlenght.
For weakly absorbing analyte, $10^{-\varepsilon cl}$ can be approximated by (1-ln 10εcl) so that the relative change in intensity, can be written as:

$$\phi_A = \frac{\phi_0 - \phi}{\phi_0} = \frac{\phi_0 - \phi_0\left(1 - \ln 10 \cdot \varepsilon cl\right)}{\phi_0} = \ln 10 \cdot \varepsilon cl \tag{26}$$

In TLS there are two causes of intensity changes. One is the intensity reduction due to absorption of light by the analyte - the same as in absorption detection. The other is the decrease due to beam de-focusing which causes less power to strike the photodetecor. This explains why in TLS the measured value of relative change in intensity is higher than the value calculated on the basis of Eq. (26).
The intensity decrease due to the defocusing effect of the induced thermal lens in the sample cell at the optimal position is given by:

$$\phi_{TL} = -\frac{\ln 10 \cdot \phi_0 \varepsilon cl}{k\lambda} \frac{\partial n}{\partial T} \tag{27}$$

and the total TLS signal by:

$$\phi_{tot} = \phi_{TL} + \phi_A \tag{28}$$

Usually, in the literature dealing with TLS, Eq. (28) is written as:

$$\phi_{TOT} = \phi_A\left(1 + E\right) \tag{29}$$

where E is the enhancement factor of the response compared to Lamber-Beer's law. That is, E can be written as:

$$E = -\frac{\phi_0 \dfrac{\partial n}{\partial T}}{k\lambda} \tag{30}$$

Therefore, the sensitivity of a thermal lens measurement depends linearly on laser power. The choise of solvent can greatly influence the enhancement one observers for the laser power available, as shown in Table 1 (data are from Bialkowski, 1996). Non-polar solvents are particularly useful for trace analysis because of their relatively high ∂n/∂T and low *k* values.

Table 1: *Opthothermal properties of solvents*

	Thermooptical properties of solvents at 293 K				
Solvent	k ($W\ m^{-1}K^{-1}$)	C_p ($J\ kg^{-1}K^{-1}$)	ρ ($kg\ m^{-3}$)	∂n/∂T ($10^4\ K^{-1}$)	n_D^{20}
Water	0,598	4180	1000	-0,91	1,333
Methanol	0,202	2460	790	-3,94	1,329
Acetone	0,190	2180	800	-5,42	1,359
Acethonitrile	0,188	2230	780	-4,50	1,342
THF	0,141	1590	889	-4,40	1,407
CCl_4	0,103	850	1600	-6,12	1,460

2.1.5 Analytical applications of thermal lens spectrometry

Indirect measurement of absorbance through the changes of temperature-dependent refractive index of the sample, which is exploited in TLS, offers two major advantages of this technique over conventional spectrometry, which is based on the measurement of light transmitted through the sample.

1. The heat released inside the absorbing sample during the radiation-less de-excitation of excited species is proportional to the power of the excitation laser. This provides an inherently high sensitivity of the TLS technique, which was demonstrated capable of measuring absorbences as low as 10^{-7} –10^{-8} (Dovichi and Harris, 1980, 1981; Erskine and Bobbitt, 1989).
2. Compared to conventional transmission techniques, TLS is much less subject to errors resulting from frequently present light scattering (Thorne and Bobbit, 1993) in environmental and food samples (Power et al., 1988; Gutzman et al., 1993; Khuen et al., 1994).

These characteristics resulted in many applications of TLS in chemical analysis, which were extensively reviewed (Georges, 1999; Snook and Lowe, 1995; Franko, 1996; Bicanic et al., 1996). TLS technique has found many applications in the analysis of environmental and food samples, which vary in complexity from drinking water to analytically very demanding samples of oils, fruit juices and extracts from biological fluids and tissues. Various organic pollutants, heavy metals and biologically active compounds can be detected with high sensitivity, which enables their determination at ppb concentration levels. Furthermore, the high sensitivity of the TLS technique has been successfully combined with the high selectivity of separation techniques such as HPLC and ion chromatography or biorecognition methods such as biosensors.

2.1.5.1 Analysis of environmental samples

TLS is the best suited for the analysis of liquid samples. It is therefore not surprising that in the case of environmental samples it has found the most applications in the analysis of waters.
Due to high toxicity of various pesticides and the possibility of their accumulation in body tissues, the permitted concentrations, as recommended by the world health organizations (EPA, WHO) are very low and require detection limits of 0.1 mg/mL for pesticides in drinking water (Faubel, 1996). This requirement has probably contributed to the fact that determination of pesticides represents one of the first applications of TLS for determination of environmentally relevant organic compounds in liquid samples.
It was reporded that TLS determination of a single dinitrophenol pesticide in static non-flowing samples, is superior and provide three times lower LOD (0.1 µg/mL) compares to various photothermal techniques including PAS, PDS, PTPS and spectrophotometry (Faubel, 1996; Faubel et al., 1994). Because of high baseline noise in flowing samples TLS detection of a mixture of DNOC and 2,4 dinitrophenol (DNP), after HPLC isocratic separation, has higher LOD values (0.7 µg/mL) compared to non-flowing samples. But this values still compare favorably to spectrophotometric detection (LOD = 10 µg/kg).
To achieve required selectivity a new bioanalytical method which unable simple and rapid detection of organophosphate and carbamate pesticides was developed. Enzyme acetylcholinesteraze imobilizated on control porosity glass beads contained in a small-size reactor (200 µl) and incorporated into a TLS flow injection system unable measurements of pesticide concentrations due to enzyme inhibition (Pogačnik and Franko, 1999). Besides adequate selectivity and high sensitivity in the case of some pesticide, the novel biosensor-FIA system enabled determination of pesticide toxicity.
Other applications of TLS in environmental analysis is detection of heavy metals and several other metal species. Chromium is a typical example of an element where the analysis requires not just accurate determination of its total concentration, but also the determination of its species Cr(VI), and Cr(III), since the former is highly toxic and carcinogenic, while the latter is considered essential to humans. It was demonstrated by the determination of Cr(VI) in potentially contaminated water samples using spectrophotometry (SPEC), TLS and ion chromatography with SPEC or TLS detection, that in addition to low LODs, which compare favorably with SPEC, the TLS technique is less subject to errors arising from light scattering in the sample (Šikovec et al., 2000). The effects of light scattering, which are encountered in direct determination of Cr(VI) with DPC, as well as the effects of interfering strong oxidants (Fe(III), V(V)) were avoided by the ion chromatographic separation of Cr species prior to the coloring reaction with DPC (Šikovec et al., 1995, 2000). Besides the elimination of interferences, this also enabled simultaneous

determination of both Cr species with LOD = 0.3 ng/ml for Cr(VI) and LOD = 30 ng/mL for Cr(III). The most recent measurements have confirmed that the improved sensitivity in IC eluents containing 30% acetonitrile offers LODs of 0.1 and 10 ng/mL for Cr(VI) and Cr(III), respectively (Šikovec et al., 2001).
The coupling of ion chromatography to TLS detection was also shown advantageous in determination of several other metal species like Pb^{2+}, Ni^{2+}, Cu^{2+}, Cd^{2+}, Mn^{2+}, Fe^{2+}, and Fe^{3+} (Šikovec et al., 1996). This was performed by using an excimer-pumped dye laser or an Ar-ion laser to excite the complexes of metal ions with PAR reagent, which are formed by post column derivatization and exhibit maximum absorbance at 520 nm. Despite the relatively high background absorption due to PAR reagent, LODs of 4 and 5 ng/ml were achieved for Co^{2+} and Cu^{2+}, respectively, after optimizing the concentration of PAR.
Thermal lens determination of a wide range of transition metals (Al (III), Bi(III), Cd(II), Co(II), Cr(III), Cu(II), Fe(III), Mn(II), Nd(III), Ni(II), Pb(II), Pr(III), Zn(II), Ni(II)) in the flow injection mode using Xylenol Orange and 4-(2-thiazolylazo)resorcinol (TAR) as sensitive reagents was demonstrate (Proskurnin et al. 2000). Low limits of detection (n x 10^{-8} - n x 10^{-7} mol/L) and wide linear calibration ranges (about three orders of magnitude) were achived.
The first application of TLS for analysis of biological tissues and fluids, related to environmental research and food analysis, was the determination of carotenoids in blood plasma by a combined HPLC–TLS method relying on a pump beam from an Ar-ion laser providing 60 mW excitation at 476 nm (Franko 1998). The reported LOD values ranged from 70 to 120 pg/ml for compounds such as β-cryptoxanthin, α-carotene, *trans*-β carotene, and lycopene. What represents a 100-fold improvement compared to the HPLC analysis with UV–Vis detection.
In reality, the proper operation of HPLC–TLS was confirmed by the determination of carotenoids from various species of marine phytoplankton and by the determination of carotenoids from phytoplankton in different physiological conditions (Logar et al. 1999; Šikovec et al. 2001).
The possibility of focusing laser beams to points smaller than 1 µm in diameter opens an area for new applications of TLS. This includes the measurements of absorbance on the microscopic scale and eventually inside a single living cell. The tight focusing of the laser beams results in much higher power densities compared to conventional TLS instruments. As a result, lasers with powers of only a few milliwatts can provide higher sensitivities relative to TLS instruments relying on the focusing with regular optics.
A miniature flow injection analysis FIA system with TLS detection was shown capable of detecting a single atom of lead in 7 fL of water samples after the appropriate derivatization of lead with octaethylporphyrin (Saito et al., 1999; Saito et al., 2001). The potentials of microscopic TLS for measurements on living cells and tissues were demonstrated by measurements of pigments and color distribution in a 5-µm-thick slice of human hair measuring 125 µm in diameter (Harata et al., 1995).

2.1.5.2 Foodstuff analysis

Applications of TLS to foodstuff analysis were governed by the need for new analytical tools to control the quality of foodstuffs and their authenticity or eventual adulteration. New sensitive analytical methods were needed for detection of undesired compounds such as various pollutants, which are already toxic when present in very low concentrations.
Various compounds that are occurring naturally in our diet, such as trans unsaturated fatty acids, are considered harmful to human health and should not be present in foodstuffs in high concentrations. Trans unsaturated fatty acids (TFA) and so called free fatty acids (FFA) were however identified among the compounds, which should be avoided. Standard techniques for determination of those compounds include IR spectrometry at 935 cm^{-1} for FFA (Chapman et al., 1965) and 965 cm^{-1} for TFA (Kochar and Rossel, 1987). These techniques suffer from relatively low sensitivity, which hardly enables determination of FFA and TFA at concentration levels below 1%. TLS detection of fatty acids was carried out in the region covered by CO and CO_2 laser emission (Franko, 1996). Limits of detection of 0.002% for trans fatty acids and 1.4 µg/mL for oleic acid were achieved. To circumvent the relatively high background absorbences of solvents in this spectral region and to improve the LODs a novel differential IR TLS spectrometer has been constructed (Franko and Bicanic, 1998). It operates on the basis of the positional dependence of the thermal lens signal, which enables up to 95% or better cancellation of the blank signal when two identical sample cells, containing the solvent in which the analyte is dissolved, are placed symmetrically with respect to the probe beam waist.
TLS enables determination of parameters such as thermal diffusivity and thermal conductivity of the sample and not just the concentration of a particular compound. These are important parameters needed to optimize the processing, packaging and storage of fatty acids, oils and fats. The applicabil-

ity of TLS for measurements of thermal conductivity and the related thermal diffusivity of various liquids and other materials (Franko et al., 1991; Baesso et al., 1994) has been well documented.
Among several methods used to identify the authenticity of various food products, the fingerprints of pigments such as carotenoids and flavonoids, present in foodstuffs, were found very useful (Simpkins et al, 1995; Luterotti et al., 1999). In the case of olive and fish oils TLS was used in combination with HPLC to identify differences in concentrations and ratios of carotenoid compounds in oils of different quality. Similarly to the characteristic pigment fingerprints in oils, this feature was frequently used in characterization of beverages such as citrus fruit juices and tannins in white wines (Philip et al. 1989, Caldera-Forteza et al. 1995). The procedure relying on TLS detection (Šikovec et al., 1999) was however much faster, due to smaller sample volumes needed for analysis compared to analytical procedures using less sensitive detection schemes.

2.2 Chromium in general

Chromium is a steel-gray, lustrous, hard metal that takes a high polish and has a high melting point 2176 K. Its density is 7,18 g/cm^3 at 293 K and atomic mass is 51.996 g/mol. Chromium main uses are in alloys such as stainless steel, in chrome plating and in metal ceramics. It is used in metallurgy to impart corrosion resistance and a shiny finish; in dyes and paints, as a catalyst in dyeing and in the tanning of leather; to make molds for the firing of bricks (Chromium Lenntech, 2006).
Chromium occurs naturally and most abundantly as the mineral chromite. This ore, $FeCr_2O_4$ is a spinel and is the only commercial source of chromium. Chromium occurs in minor amounts in many minerals where Cr(III) replaces iron or aluminium. The colours of rubies and emeralds for example are due to the incorporation of small amounts of chromium (Cotton and Wilkinson, 1988).

2.2.1 Chromium chemistry

Chromium can exist in several chemical forms, which have oxidation states ranging from 0 to VI. However, only trivalent and hexavalent chromium are stable enough to occur in the environment.
Cr(III) is the most stable and best known oxidation state of chromium. Thousands of chromium(III) complexes exist and most of them are found to be hexacoordinate and octahedral. The kinetic inertness of Cr(III) complexes permits the isolation of these complexes as solids and also allows the complexes to be stable for long periods of time in solution.
The presence, concentration and form of chromium(III) in the environment depends on various chemical and physical processes including hydrolysis, complexation, redox reactions and adsorption.
Cr(III) forms stable salts with all the common anions and is able to complex with most species that are capable of donating an electron pair. Trivalent chromium complexes with a variety of ligands such as water, ammonia, urea, ethylenediamine and other organic ligands containing oxygen, nitrogen or sulphur donor atoms (Encyclopedia of Chemical Technology, 1979).

In the pH range of water hexavalent chromium exists as CrO_4^{2-}, $HCrO_4^-$ and $Cr_2O_7^{2-}$ ions. These form part of many Cr(VI) compounds, which are relatively soluble and thus mobile in the environment.
The tetrahedral, yellow chromate ion CrO_4^{2-} is formed by CrO_3 in basic solutions above pH 6 whereas $HCrO_4^-$ and the orange-red dichromate ion $Cr_2O_7^{2-}$ are in equilibrium between pH 2 and 6. At pH values of below 1 the main specie present is H_2CrO_4.
The species present in solution depend on the acid used. For HNO_3 and $HClO_4$ the only equilibria are

$$HCrO_4^- \longleftrightarrow CrO_4^{2-} + H^+ \qquad K = 10^{-5.9}$$

$$Cr_2O_7^{2-} + H2O \longleftrightarrow 2HCrO_4^- \qquad K = 10^{-2.2}$$

$$H_2CrO_4 \longleftrightarrow HCrO_4^- + H^+ \qquad K = 4.1$$

Cr(VI) oxyanions are readily reduced to the Cr(III) form by electron donors such as organic matter or reduced inorganic species, which are extensive in soil, water and atmospheric systems (Encyclopedia of Chemical Technology, 1979; Kotaś, 2000).

2.2.2 Chromium Biochemistry

Chromium is known to be an essential trace element but is found to be toxic at high levels.

Essentiality of Chromium

a. Function

Chromium is an essential nutrient required for normal glucose and lipid metabolism as it enhances the effect of insulin. Insulin is secreted by the pancreas in response to increased blood glucose levels. Insulin binds to receptors on cell surfaces, which cause the uptake of glucose by the cells. Thus insulin provides the cells with glucose and also prevents blood glucose levels from becoming elevated. Insulin also plays a role in the metabolism of fat and protein. Thus chromium plays an important role in the body as it behaves as a cofactor by enhancing the response of the insulin receptor to insulin (Anderson, 1989; Barrett et al., 1985).

b. Sources

Chromium is found in most fresh foods and drinking water. Sources rich in chromium include breads, cereals, spices, fresh vegetables, meats, fish, brewer's yeast and beer (Chromium. Micronutrient Information Center, 2006).

c. Deficiency

Chromium deficiency has been associated with impaired glucose tolerance, fasting hyperglycemia, glucosuria, elevated percent body fat, decreased lean body mass, maturity-onset diabetes, cardiovascular disease and impaired fertility. Thus it can be seen that it is an essential nutrient. There is no recommended dietary allowance for chromium however a safe and adequate daily intake of 50-200 µg/day has been set (Chromium. Micronutrient Information Center, 2006).

Toxicity of Chromium

Chromium enters the body through inhalation, ingestion and dermal absorption. The general population is exposed to chromium through ingestion of chromium in food and water while occupational exposure occurs predominantly through inhalation and dermal contact. Workers exposed to chromium are at risk of developing lung cancer as well as nasal, pharyngeal and gastrointestinal carcinomas.

The uptake rate of chromium from the gastrointestinal tract is relatively low and depends on the valence state (Cr(VI) is more readily absorbed than Cr(III)), the chemical form (organic chromium is more readily absorbed than inorganic chromium), the solubility of the chromium compound, and the gastrointestinal transit time.

Cr(III) does not readily cross cell membranes when entering the body from an exogeneous source. It is however able to bind to transferring, an iron-transporting protein in the plasma. Cr(VI) is able to permeate nuclear membranes. Cr(VI) undergoes enzymatic reduction, which results in the formation of free radicals and Cr(III). Ascorbic acid, the thiols, glutathione, cysteine, cysteamine, lipoic acid, coenzyme A and coenzyme M reduce Cr(VI) at a significant rate. Cr(III) ion can bind to DNA and protein. Thus it inhibits critical enzymes and alters the 3-dimensional geometry of DNA, which has mutagenic and carcinogenic consequences. Thus although Cr(III) causes the harm in the end, it originates as Cr(VI) which is able to permeate membranes therefore Cr(VI) is seen as the toxic species.

Chromium is widely distributed in the body and is found in the lungs, liver, kidney, spleen, adrenals, plasma, bone marrow and the red blood cells (Chromium Toxcity, 2006).

2.2.3 Chrmoium in the water and soil systems

Chromium occurs in water systems from natural sources such as weathering of rocks, run-off from terrestrial systems as well as wet precipitation and dry fallout from the atmosphere. The concentration of chromium in rivers and lakes is usually between 1 – 10 µg/l. The chromium content of polluted waters is much higher due to discharge of wastewater from various industries. The number and type of chromium species present in effluents depend on the industrial process using the chromium.

Chromium exists as two stable oxidation states in natural water, namely Cr(III) and Cr(VI). Various processes in the water system which include chemical and photochemical redox transformation, pre-

cipitation/ dissolution and adsorption/ desorption reactions determine the presence and ratio of the two oxidation states.
Under anoxic or suboxic conditions, trivalent chromium is the only form that occurs. In oxygenated aqueous solutions, Cr(III) is the stable species at pH ≤ 6 whereas CrO_4^{2-} ions predominate at pH ≥ 7. The Cr(III)/Cr(VI) ratio is not only dependant on pH but also on oxygen concentration, the nature and concentration of reducers, oxidation mediators and complexing agents for example Cr(III) is easily oxidised to Cr(VI) in the presence of manganese oxides.
Aquo/hydroxo complexes of Cr(III) are dominant in natural waters, however, Cr(III) can form many different complexes with naturally occurring organic materials such as amino, fulvic, humic and other acids. These complexes have a strong tendency to be absorbed by solids and macromolecular compounds thus decreasing the mobility and bioavailability of Cr(III) in waters.
Unlike Cr(III) complexes, Cr(VI) species are only weakly sorbed to inorganic surfaces and are thus the most mobile form of chromium.
The behavior of chromium species originating from industrial waste differs to that of natural waters due to the altered physicochemical conditions of the eluents used. These different conditions occur due to the different chromium compounds used, the pH as well as organic and/or inorganic ligands used in the various industrial processes and influence the solubility, sorption and redox reactions of the chromium. Hexavalent chromium for example, is found mainly in metallurgical, chromium plating, refractory and pigment production waste solutions. Trivalent chromium on the other hand is found prominently in tannery, dying, printing and decorative plating wastewater. This is demonstrated in the following example where Cr(III) is the expected form of chromium in tannery wastewater although the hexavalent form can also be present due to redox reactions that occur in the sludge. In addition to this the trivalent chromium should occur as the poorly soluble $Cr(OH)_3$.aq form but due to a high content of organic matter from the hides, soluble organic Cr(III) complexes form (Kotaś and Stasicka, 2000).

In soil systems chromium occurs predominantly as insoluble $Cr(OH)_3$. or as Cr(III) adsorbed to soil components, such that it does not leach into the groundwater and is not taken up by plants. The dominant form of chromium in the soil depends on the pH of the soil. $Cr(H2O)^{3+}$ is found mainly in acidic soils whereas the hydrolysis products such as $CrOH^{2+}$ occur at a pH of below 5.5. Both of these forms are easily adsorbed by macromolecular clay compounds, which render the Cr(III) insoluble, immobile and unreactive. However, mobile ligands such as citric acid, diethylenetriaminepentaacetic acid and fulvic acid form soluble Cr(III) complexes, which can relocate and oxidize to Cr(VI). In alkaline soils the precipitation of Cr(III) competes with complexation.
Hexavalent chromium occurs mostly as soluble chromates e.g. Na_2CrO_4 as well as the moderately-to-sparingly soluble chromates in neutral-to-alkaline soils. In more acidic soils $HCrO_4^-$ becomes the dominant form. CrO_4^{2-} and $HCrO_4^-$ are the most mobile forms of chromium in soil systems. These forms are easily taken up by plants and can leach out into deeper soil layers causing ground and surface water pollution.
Oxidation and reduction reactions can interconvert Cr(III) and Cr(VI) but these processes are dependant on the pH, oxygen concentration and the presence of reducers and mediators, which act as ligands or catalysts (Kotaś and Stasicka, 2000).

2.2.4 Detection methods

Cr in water can be determined by a number of standard analytical methods (Clesceri et al., 1989), including atomic absorption (AAS) and emission spectrometry (AES), inductively coupled plasma-atomic emission spectrometry (ICP-AES), flame atomic absorption spectrometry (FAAS), and spectrophotometry (SPEC). The latter being favored for rapid analysis in view of its ease of automation and simple low-cost instrumentation. On the other hand, the applicability of the spectrophotometry is limited due to its relatively low sensitivity, compared to non species specific techniques such as AAS and ICP-AES. However, these techniques require some means of separation prior to the measurement in order to distinguish different species of the same element, and are, therefore, less selective compared to spectrophotometry with DPC.
Several different chromatographic procedures have been applied for separation of chromium species including high-performance ion chromatography (HPIC) with TLS detection (Šikovec et al., 1995).
Thermal lens spectrometry is sensitive and reliable method, appropriate for determination of hexavalent chromium in liquid samples, such as real water samples. The performance of TLS method for the determination of Cr(VI) as Cr-diphenylcarbazone complex (Cr-DPC) was verified by the determination

of Cr(VI) in drinking water (Šikovec et al., 2000) and standard reference water samples (Šikovec et al., 1996) and by comparing the results to those obtained by other techniques such as atomic absorption spectrometry.
It offers several advantages over the spectrophotometry method, this includes higher sensitivity and lower limits of detection (10-times lower compared to SPEC) (Šikovec et al., 2000).

2.3 Bilirubin

Bilirubin is the breakdown product of the heam moiety of hemoglobin and other haemoproteins in mammals. Approximatly 4 mg/kg body weight of bilirubin is produced daily. About 70 to 80% of the total daily bilirubin production is derived from the breakdown of hemoglobin in senescent red blood cells. The remainder comes from prematurely destroyed erythroid cells in bone marrow and from the turnover of hemoproteines such as myoglobin and cytochromes found in tissues throughout the body. Due to its structure, bilirubin is poorly soluble in water and requires enzyme-mediated glucuronidation in the liver for biliary excretion. In normal circumstances, plasma bilirubin is mostly unconjugated (UCB) and is tighlty bound to circulating albumin. Disorders of bilirubin metabolism leading to unconjugated hyperbilirubinemia. Very high levels of serum bilirubin lead to its accumulation in the brain, causing encephalopathy (kernicterus) (Lucey, 1972; Gourley 1997).

2.3.1 Enzymatic mechanism of bilirubin formation

Haem is a tetrapyrrole, the four pyrrole rings being connected by methane bridges. The four bridges are not equivalent because the side chains are asymmetrically distributed (Figure 3). Haem is cleaved specifically at the α-methene bridge by a reaction catalysed by microsomal haem oxygenases, resulting in the formation of biliverdin and 1 mole of CO, and the release of an iron molecule. The reaction consumes three molecules of oxygen and requires a reducing agent, such as NADPH. The α-methene-bridge carbon is eliminated as CO, and the iron molecule is released (Chowdhury et al., 2001). There are three known isoforms of haem oxygenase (HO). The ubiquitous isoform HO-1 is inducible by haem and stress.HO-2 is a constitutive protein present mainly in the brain and the testis. HO-3 has a very low catalytic activity and may function mainly as a haem-binding protein. Subsequently, biliverdin is reduced to bilirubin by the action of cytosolic biliverdin reductase. The vasodilatory effect of CO regulates the vascular tone in the liver, heart and other organs during stress. The other products of haem breakdown, namely biliverdin and bilirubin, are potent antioxidants, which may protect tissues under oxidative stress.

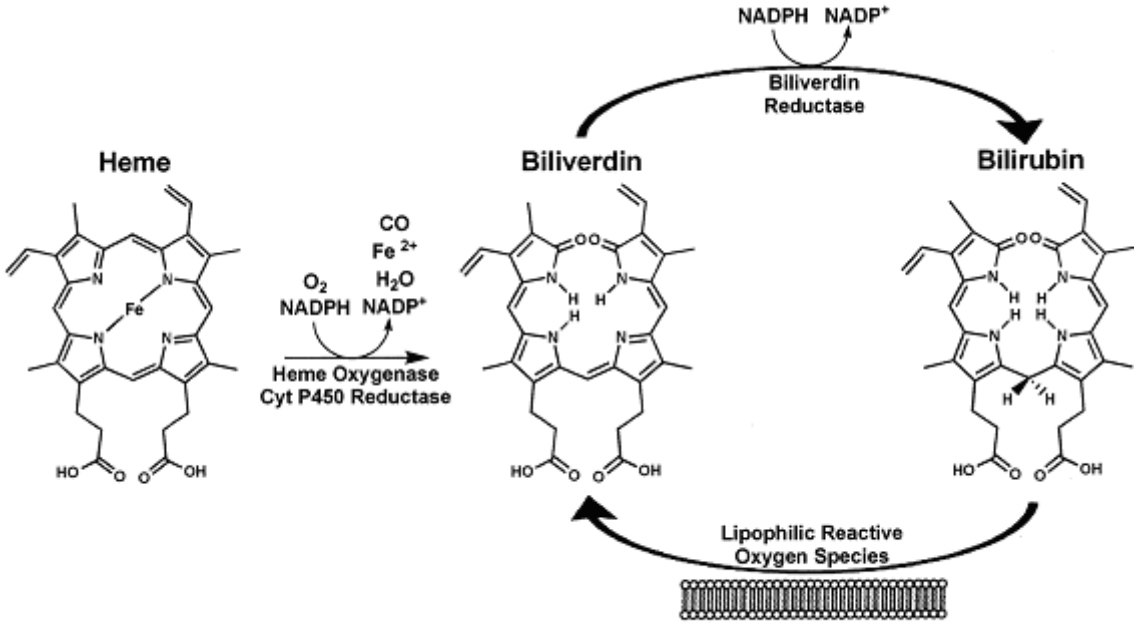

Figure 2: *Enzymatic mechanism of bilirubin formation (taken after Sedlak et al., 2004)*

2.3.2 Bilirubin structure and solubility

The main isomer in humans is bilirubin IXα, which, at physiological pH, exists mainly as a dianion or as a bilirubin acid (Figure 3). It is nearly symmetrical tetrapyrrole, consisting of two rigid, planar dipyrroles units (dipyrrinones), joined by a methylene (-CH_2-) bridge at carbon 10. At physiological pH values in plasma tissues (7.0), and bile (6.0 to 8.0) there is significant ionization of the –COOH groups of the natural IXα isomer of UCB, so that in addition to the diacid (H_2B), a proportion of UCB is present as the monoanion (HB^-) and dianion (B^{2-}) (Ostrow et al., 1994).

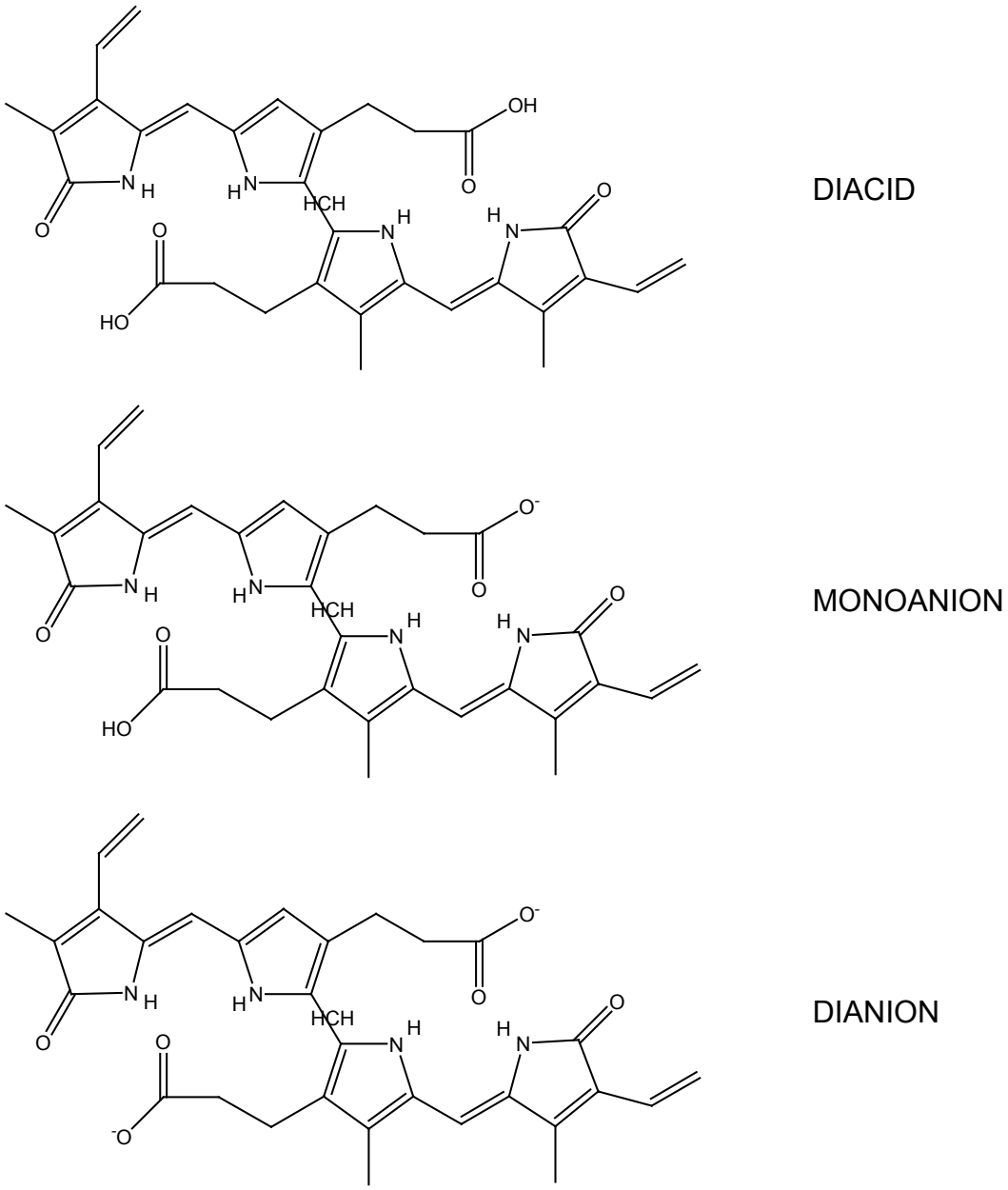

Figure 3: *The structures of unconjugated bilirubin IXα-Z,Z diacid (H_2B, top), monoanion (HB^-, middle), and dianion (B^{2-}, bottom)*

Despite the presence of several polar groups, such as the propionic acid side-chains and the amino groups, bilirubin is insoluble in water. This apparent paradox is explained by internal hydrogen bonds between the propionic acid cyrboxyls and the contralateral amino and lactam groups (Figur 4) (Bonnet et al., 1976). In nature, the hydrogen bonds are disrupted by glucuronidation of the propionic acid carboxyls. As a result, conjugated bilirubin is water-soluble and readily extractable in bile. The hydrogen bonds of unconjugated bilirubin bury the central methane bridge that connects the two dipyrrolic halves.

Experimental solubilities near neutral pH, however, derived from studies of crystal dissolution or acidification of H_2B , have varied extensively (10 nM to 15 mM). Much more reliable values, determined by chloroform-to-water partition**,** indicate that the maximum aqueous solubility of H_2B, at 25°C and ionic strength 0.15 is about 70 nM. The partition data (3) show that total UCB solubility increases with increasing pH. Since the solubility of H_2B is the same at all pH values,

the increase in overall UCB solubility with increasing pH is due to successive ionization of H_2B to HB^- and B^{2-}. Ionization removes the proton that, in H_2B, hydrogen bonds the -COOH group to the lactam

>C=O of the opposite dipyrrole and renders these groups available for interaction with water, and also generates a negatively charged -COO- group (Figure 4).

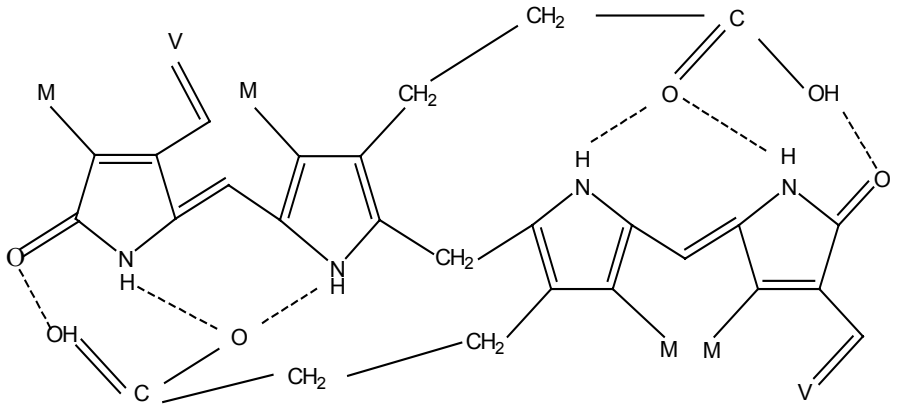

Figure 4: *Internal hydrogen bonding of bilirubin IXα*

2.3.3 Bilirubin metabolism

Bilirubin produced in the periphery is transported to the liver within the plasma, where, due to its insolubility in aqueous solutions, it is tightly bound to albumin. In the liver bilirubin is taken up by hepatocytes via a process that at least partly involves carrier-mediated membrane transport. After entering the hepatocyte, unconjugated bilirubin is bound to the cytosolic protein ligandin, or gluthatione S-transferase B. Whereas ligandin was initially thought to be a transport protein, responsible for delivering unconjugated bilirubin from the plasma membrane to the endoplasmic reticulum, itnow appears that its role may in fact be to reduce bilirubin afflux back into the plasma. Studies suggested that unconjugated bilirubin may well rapidly diffuse unaided through the aqueous cytosol between membranes. In the endoplasmic reticulum, bilirubin is solubilized by conjugation to glucuronic acid, aprocess that disrupts the internal hydrogen bonds and yields bilirubin monoglucuronide and diglucuronide. The conjugation of glucuronic acid to bilirubin is catalyzed by bilirubin uridine-diphosphate (UDP) glucuronosyltransferase. The now hydrophilic bilirubin conjgates diffuse from the endoplasmic reticulum to the canalicular membrane, where bilirubin monoglucuronide and diglucuronide are actively transported into canalicular bile by energy-dependent mechanism involving the multiple drug resistence protein.
The conjugated bilirubin excreted into bile drains into the duodenum and passes unchanged through the proximal small bowel. Conjugated bilirubin is not taken up by the intenstinal mucosa. When the conjugated bilirubin reaches the distal ileum and colon, it is hydrolyzed to unconjugated bilirubin by bacterial β-glucuronidases. The unconjugated bilirubin is reduced by normal gut bacteria to form a group of colorless tetrapyrroles called urobilinogens. About 80 to 90% of these products are excreted in feces, either unchanged or oxidized to orange derivatives called urobilins. The remaining 10 to 20% of the urobilinogens are passively absorbed, enter the portal venous blood, and are reexcreded by the liver. A small fraction (<3 mg/dL) escapes hepatic uptake, filters across the renal glomerulus, and is excreted in urine (Braunwald et al., 2004)

2.3.4 Bilirubin as a toxin

Free unconjugated bilirubin exhibits a wide range of toxicity to many cell types, particularly neuronal cells. All known toxic effects of bilirubin are abrogated by binding to albumin. Cerebral toxicity (kernicterus) from bilirubin occurs when the molar ratio between bilirubin and albumin exceeds 1.0. Bilirubin toxicity is usually seen during exaggerated neonatal hyperbilirubinaemia end in patients with Crigler–Najjar syndrome at all ages (Hansen, 1986). In neonates, serum unconjugated bilirubin levels above 20 mg/dL are generally considered dangerous. Kernicterus can, however, occur at lower levels in the presence of sulphonamides, radiographic contrast media, coumarins and antiinflammatory drugs that displace bilirubin from its albuminbinding sites, thereby increasing the level of unbound bilirubin. The immaturity of the blood–brain barrier in neonates has traditionally been implicated as a cause of susceptibility to kernicterus, but lower bilirubin clearance from the brain may play an important role.
Hyperbilirubinemia in absence of liver disease or increased bilirubin production is characteristic for some inherited disorders. In this case, the transfer of bilirubin from blood to bile is disrupted at a specific step (Bosma, 2003). Three familiar disorders, Crigler-Najjar syndromes type I (CN-I), Crigler-Najjar syndromes type II (CN-II) and Gilbert's syndrom characterized by differing degrees of unconjugated hyperbilirubinemia have long been recognised.
CN-I is characterized by striking unconjugated hyperbilirubinemia of about 20 to 45 mg/dL that appears in the neonatal periodpersist for life. The clinical course of the Crigler-Najjar syndrome (type I) disease is characterized by the development of a progressive and severe neurological syndrom, usually leading the affected subjects to death within the first two years of life. Thy symptoms are caused by massive deposition of bilirubin in organs and tissues, deep jaundice of the cerebral cortex and other structures of the central nervous system, and neuronal loss (Sampietro and Iolascon, 1999).
The CN-II is less severe and more common that CN-I. The bilirubin levels are significantly lower than those in CN-I (10-20 mg/dL) and central nervous system damage is rare (Sampietro and Iolascon, 1999). In patients with CN-II, glucuronyl transferase activity is severely reduced but not absent. The mode of inheritance of CN-II is not clear. A recent hypothesis suggests CN-II could represent the homozygous state for the Gilbert's syndrome gene (Sampietro and Iolascon, 1999).
Gilbert's syndrome is characterized by mild unconjugated hyperbilirubinemia, normal values for standard hepatic biochemical tests, and normal hepatic histology other than a modest increase of lipofuscion pigment in some patients. Serum bilirubin concetrations are most often < 3 mg/dL, although both higher and lower values are frequent. The clinical spectrun of hyperbilirubinemia fades into that of CN-II at serum bilirubin concentration of 5 to 8 mg/dL. At the other end of the scale, the distinction between mild cases of GS and a normal state is often blurred. Bilirubin concentrations may fluctuate substantially in any given individual, and at least 25% of patients will exhibit temporarily normal values during prolonged follow-up. Compartmental analysis of bilirubin kinetic data suggests that GS patients have a defect in bilirubin uptake as well as in conjugation (Braunwald et al., 2004).

2.3.5 Bilirubin as an antioxidant

Bilirubin has long been considered just a toxic waste product formed during heme catabolism. Nevertheless, more recent evidence suggests that it is in fact a potent physiological antioxidant, which is supposed to provide important protection against many diseases (Seadlak and Snyder, 2004). As early as the 1950s, bilirubin was reported to protect against the oxidation of lipids such as linoleic acid and vitamin A (Bernhard et al., 1954; Beer et al., 1959). In the late 1980s, Ames and colleagues (Stocker et al., 1987) demonstrated that the antioxidant effect of bilirubin exceeds that of vitamin E toward lipid peroxidation. Serum concentrations of bilirubin are high enough to account for a substantial portion of the total antioxidant capacity of serum (Gopinathan et al., 1994). Thus, bilirubin might alleviate oxidant stress in the blood. However, what matters most is what goes on inside cells. During the oxidant stress associated with myocardial and cerebral infarcts, infection, inflammation, and various causes of ischemia, the intracellular environment is exposed to high concentrations of reactive oxygen species. It has long been assumed that the principal cellular antioxidant is the peptide glutathione (GSH), whose tissue concentrations are millimolar, presumably sufficient to cope with most instances of oxidative stress. By contrast, levels of bilirubin in rodent tissues are only 10 to 50 nanomolar, at least 10000 times lower than concentrations of GSH (Seadlak and Snyder, 2004).
Mild hyperbilirubinaemia may have a protective effect against ischemic cardiovascular disease and cancer. Higher bilirubin levels ~ 0.9 mg/dL were associated with lowered risk of myocardial infraction

and other cardiovascular disease events compared with individuals with lower bilirubin levels of 0.5 mg/dL (Djousse et al., 2001). In a recent study on a large population, the odds ratios for a history of colorectal cancer were reported to be reduced to 0.295 in men and 0.186 in women per 1 mg/dl increment in serum bilirubin levels (Zucker et al. 2004). An inverse relationship between serum bilirubin levels and cancer mortality has also been reported. Such negative associations do not, however, conclusively establish a cause-and-effect relationship because of the presence of many potentially confounding variables.

2.4 Neonicotinoid pesticides

Neonicotinoid products were the first new major chemical family of insecticides introduced within the past 20 years in the Europe. Classified as “Nicotine Acetylcholine Receptor Agonists / Antagonists” as their mode of action, they work on very specific nerves areas (nicotine receptors that many insects have in abundance) in the region of the mouth and they paralyze the associated muscles thus causing the insect to starve to death. They also have a rather low mammalian toxicity.
The first of these compounds to reach the market was a chloronicotinyl now well known as Imidacloprid. This compound has been widely used for many insects that have a piercing-sucking mouth type as well as certain grub pests in turf. Although labeled for certain “chewers” like caterpillars, Imidacloprid has not been nearly as successful at controlling such pests as some of the newer Neonicotinoids that are now becoming available.
Recently, what is being referred to as the “second generation of Neonicotinoids”, are now becoming available to professionals. These new active ingredients, in addition to Imidacloprid, are: Clothoinidin, Thiamethoxam, Dinotefuran, Acetamiprid and Thiacloprid. All of these have the same mode of action as Imidacloprid and are labeled for many of the same pest groups. However, some of these newer products are active as contact sprays, have systemic action within plants and a few have translaminar capabilities, which means that when applied as a foliar spray, the compound moves into the foliage. They do not then become systemic but they do come into contact with those hard to reach pests such as armored scales (Acetamiprid) and those pests that feed within the non-transport cells where systemic products generally do not reach.
Some of the key points for consideration about the Neonicotinoids, in general:
- they work by contact and ingestion
- most have a long residual time
- they may act as a contact, systemic and / or translaminar pesticide
- they can be toxic to bees at the time of application and for as long as 5 days after application
- overall, they are relatively non-phytotoxic
- when used repeatedly on evergreens (in particular) there is a risk of developing serious outbreaks of spider mites.

2.4.1 Structural properties of neonicotinoids

The new generations of nicotine-related insecticides, sometimes referred to as neonicotinoids, possess either a nitromethylene, nitroimine or cyanoimine group (Figure 5). Nitromethylenes are derived from the 2-(nitromethyl)pyridine structure, which itself shows weak insecticidal activity. An early structure–activity study based on this prototype led to the discovery of 2-(nitromethylene)-tetrahydro-1,3-thiazine (nithiazin) (Soloway et. al., 1979). Although nithiazin has improved insecticidal activity compared with 2-(nitromethyl)pyridine, nithiazin was not developed commercially, in part, because of its photo-instability (Kagabu and Medej, 1995). Substitution of nithiazin at the 1-position led first to the development of PMNI [1-(3-pyridylmethyl)-2-nitromethylene-imidazolidine], which possessed enhanced insecticidal activity compared with nithiazin, and then to imidacloprid, first synthesized by Kagabu, and related nitroimines, all of which possessed enhanced photo stability (Kagabu and Medej, 1995; Kagabu, 1997).
The commercially important neonicotinoids, such as imidacloprid, nitenpyram and acetamiprid, all contain a 6-chloro-3-pyridyl moiety and therefore resemble nicotine and epibatidine, both of which are potent agonists of nAChRs (Figure 6). Liu *et* al., 1993 and Buckingham *et* al., 1995 showed that the relative toxicity of several neonicotinoids correlates closely with their relative affinity for insect nAChRs, which suggests that nAChRs are likely to represent the principal sites of action of these compounds.

To date, neonicotinoids with diverse structures have been synthesized and their structure–activity relationships have been discussed in terms of physicochemical and structural properties.

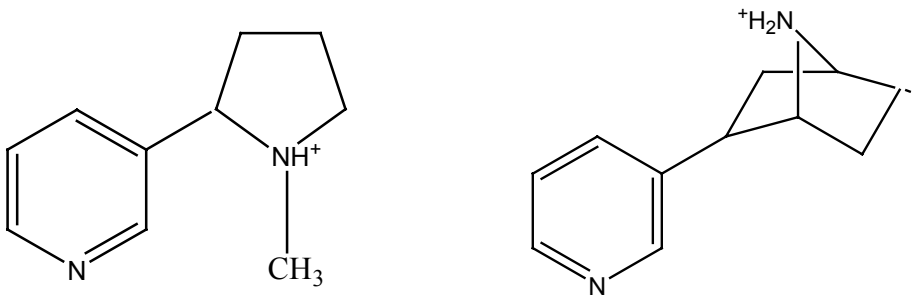

Nicotine Epibatidine

Figure 5: *Natural nicotinic agonists*

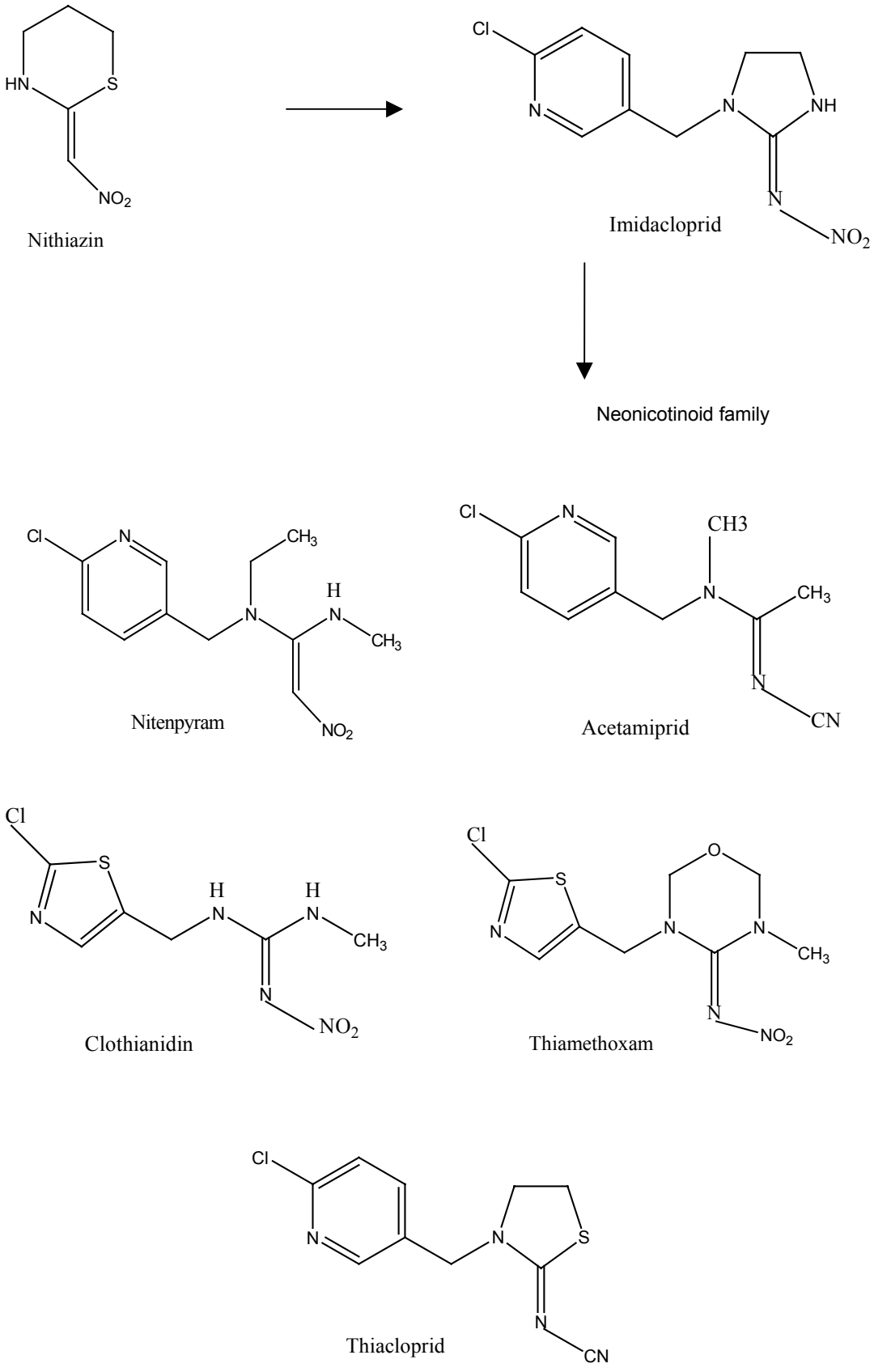

Figure 6: *The structures of neonicotinoid insecticides and nithiazin*

2.4.2 Imidacloprid

Imidacloprid 1-[(6-chloro-3-pyridinyl)methyl]-N-nitro-2-imidazolidinimine is a general use pesticide, and is classified by EPA as both a toxicity class II and class III agent.There are tolerances for residues of imidacloprid and its metabolites on food/feed additives ranging from 0.02 ppm in eggs, to 3.0 ppm in hops (U.S. Environmental Protection Agency, 1995).
Imidacloprid is a systemic, chloro-nicotinyl insecticide with soil, seed and foliar uses for the control of sucking insects including rice hoppers, aphids, thrips, whiteflies, termites, turf insects, soil insects and some beetles. It is most commonly used on rice, cereal, maize, potatoes, vegetables, sugar beets, fruit, cotton, hops and turf, and is especially systemic when used as a seed or soil treatment. The chemical works by interfering with the transmission of stimuli in the insect nervous system. Specifically, it causes a blockage in a type of neuronal pathway (nicotinergic) that is more abundant in insects than in warm-blooded animals (making the chemical selectively more toxic to insects than warm-blooded animals). This blockage leads to the accumulation of acetylcholine, an important neurotransmitter, resulting in the insect's paralysis, and eventually death. It is effective on contact and via stomach action (Kidd and James, 1994).
Imidacloprid based insecticide formu-lations are available as dustable powder, granular, seed dressing (flowable slurry concentrate), soluble concentrate, suspension concentrate, and wettable powder (Meister, 1995). Typical application rates range from 0.05 - 0.125 pounds/acre. These application rates are considerably lower than older, traditionally used insecticides. It can be phytotoxic if it is not used according to manufacturer's specifications, and has been shown to be compatible with fungicides when used as a seed treatment to control insect pests (Pike et. al., 1993).

2.4.2.1 Physical properties

Imidacloprid is colourless crystals or beige powder with molecular mass 255,7 g/mol and density 1,542 g/L. Solubility in water 0.51 g/L (20 °C). Solubility in other solvents at 20 °C: dichloromethane - 50.0 - 100.0 g/l; isopropanol - 1.0-2.0 g/l; toluene - 0.5-1.0 g/l; n-hexane - <0.1 g/l; fat - 0.061 g/100g. Melting point 136.4-143.8 degrees C. Octanol/water partition coefficient as log P_{ow} is 0.57. Vapour pressure, Pa at 20°C is negligible. Stable to hydrolysis at pH 5-11 (U.S. Environmental Protection Agency, 1995).

2.4.2.2 Toxicological effects

Acute toxicity
Imidacloprid is moderately toxic. The oral dose of technical grade imidacloprid that resulted in mortality to half of the test animals (LD_{50}) is 450 mg/kg body weight in rats (Meister, 1995), and 131 mg/kg in mice (Kidd and James, 1994). The 24-hour dermal LD_{50} in rats is >5,000 mg/kg. It is considered non-irritating to eyes and skin (rabbits), and non-sensitizing to skin (guinea pigs). Some granular formulations may contain clays as inert ingredients that may act as eye irritants. In acute inhalation toxicity tests with rats, the airborne concentration of imidacloprid that resulted in mortality to half of the test organisms (LC_{50}) is > 69 mg/meters cubed air in the form of an aerosol, and >5323 mg/meters cubed air in the form of dust. These values represent the maximum attainable airborne concentrations (Kidd and James, 1994).

Signs and Symptoms of Poisoning
Although no account of human poisoning was found in the literature, signs and symptoms of poisoning would be expected to be similar to nicotinic signs and symptoms, including fatigue, twitching, cramps, and muscle weakness including the muscles necessary for breathing (Doull et. al., 1991).

Chronic toxicity
A 2-year feeding study in rats fed up to 1,800 ppm resulted in a No Observable Effect Level (NOEL) of 100 ppm (5.7 mg/kg body weight in males and 7.6 mg/kg in females). Adverse effects included decreased body weight gain in females at 300 ppm, and increased thyroid lesions in males at 300 ppm

and females at 900 ppm. A 1-year feeding study in dogs fed up to 2,500 ppm resulted in a NOEL of 1,250 ppm (41 mg/kg). Adverse effects included increased cholesterol levels in the blood, and some stress to the liver (measured by elevated liver cytochrome p-450 levels) (Federal Register, 1995).

Reproductive Effects
A three generation reproduction study in rats fed up to 700 ppm imidacloprid resulted in a NOEL of 100 ppm (equivalent to 8 mg/kg/day) based on decreased pup body weight observed at the 250 ppm dose level (Federal Register, 1995).

Teratogenic Effects
A developmental toxicity study in rats given doses up to 100 mg/kg/day by gavage on days 6 to 16 of gestation resulted in a NOEL of 30 mg/kg/day (based on skeletal abnormalities observed at the next highest dose tested of 100 mg/kg/day) (Pike et. al., 1993). In a developmental toxicity study with rabbits given doses of imidacloprid by gavage during days 6 through 19 of gestation, resulted in a NOEL of 24 mg/kg/day based on decreased body weight and skeletal abnormalities observed at 72 mg/kg/day (highest dose tested) (Federal Register, 1995).

Mutagenic Effects
Imidacloprid may be weakly mutagenic. In a battery of 23 laboratory mutagenicity assays, imidacloprid tested negative for mutagenic effects in all but two of the assays. It did test positive for causing changes in chromosomes in human lymphocytes, as well as testing positive for genotoxicity in Chinese hamster ovary cells (Federal Register, 1995).

Carcinogenic Effects
Imidacloprid is considered to be of minimal carcinogenic risk, and is thus categorized by EPA as a "Group E" carcinogen (evidence of noncarcinogenicity for humans). There were no carcinogenic effects in a 2-year carcinogenicity study in rats fed up to 1,800 ppm imidacloprid (U.S. Environmental Protection Agency, 1995).

Organ Toxicity
In short-term feeding studies in rats, there were thyroid lesions associated with very high doses of imidacloprid (Federal Register, 1995).

Fate in Humans and Animals
Imidacloprid is quickly and almost completely absorbed from the gastrointestinal tract, and eliminated via urine and feces (70-80% and 20-30%, respectively, of the 96% of the parent compound administered within 48 hours). The most important metabolic steps include the degradation to 6-chloronicotinic acid, a compound that acts on the nervous system as described above. This compound may be conjugated with glycine and eliminated, or reduced to guanidine (Kidd and James, 1994).

2.4.2.3 Ecological effects

Effects on Birds
Imidacloprid is toxic to upland game birds. The LD_{50} is 152 mg/kg for bobwhite quail, and 31 mg/kg in Japanese quail (Meister, a995; Kidd and James, 1994). In studies with red- winged blackbirds and brown-headed cowbirds, it was observed that birds learned to avoid imidacloprid treated seeds after experiencing transitory gastrointestinal distress (retching) and ataxia (loss of coordination). It was concluded that the risk of dietary exposure to birds via treated seeds was minimal. Based on these studies, imidacloprid appears to have potential as a bird repellent seed treatment (Avery et. al., 1993, 1994).

Effects on Aquatic Organisms
The toxicity of imidacloprid to fish is moderately low. The 96-hour LC_{50} of imidacloprid is 211 mg/l for rainbow trout, 280 mg/l for carp, and 237 mg/l for golden orfe. In tests with the aquatic invertebrate Daphnia, the 48- hour EC_{50} (effective concentration to cause toxicity in 50% of the test organisms) was 85 mg/l (Kidd and James, 1994). Products containing imidacloprid may be very toxic to aquatic invertebrates.

Effects on Other Animals
Imidacloprid is highly toxic to bees if used as a foliar application, especially during flowering, but is not considered a hazard to bees when used as a seed treatment (Kidd and James, 1994).
Oral LD_{50} is between 49 and 102 ng/bee (Nauen et al., 2001).

2.4.2.4 Environmental fate

Breakdown of Chemical in Soil and Groundwater
The half-life of imidacloprid in soil is 48-190 days, depending on the amount of ground cover (it breaks down faster in soils with plant ground cover than in fallow soils) (Scholz and Spiteller, 1992). Organic material aging may also affect the breakdown rate of imidacloprid. Plots treated with cow manure and allowed to age before sowing showed longer persistence of imidacloprid in soils than in plots where the manure was more recently applied, and not allowed to age (Rouchard et. al., 1994). Imidacloprid is degraded stepwise to the primary metabolite 6-chloronicotinic acid, which eventually breaks down into carbon dioxide (Hellpointer, 1994). There is generally not a high risk of groundwater contamination with imidacloprid if used as directed. The chemical is moderately soluble, and has moderate binding affinity to organic materials in soils. However, there is a potential for the compound to move through sensitive soil types including porous, gravelly, or cobbly soils, depending on irrigation practices (Jenkins, 1994).

Breakdown of Chemical in Surface Water
The half-life in water is much greater than 31 days at pH 5, 7 and 9. No other information was found.

Breakdown of Chemical in Vegetation
Imidacloprid penetrates the plant, and moves from the stem to the tips of the plant. It has been tested in a variety of application and crop types, and is metabolized following the same pathways. The most important steps were loss of the nitro group, hydroxylation at the imidazolidine ring, hydrolysis to 6-chloronicotinic acid and formation of conjugates (Kidd and James, 1994).

2.4.3 Thaicloprid

Thiacloprid [3-[(6-chloro-3-pyridinyl)methyl]-2-thiazolidinylidene]cyanamide was first registered as pesticide in Brazil 1999. It uses on the agricultural crops cotton and pome fruits for control of a variety of sucking insects. The primary target pests for thiacloprid on cotton are aphids and whiteflies; Psylla, codling moth and plum Curculio are the primary pests on pome fruits. The two formulated products consist of a flowable concentrate at 40.4% and a wettable granular (WG) at 70%. Both formulated products are diluted in water and applied by ground or air as a full coverage foliar spray to cotton and pome fruits. They may also be applied as a concentrate foliar spray to pome fruits. The maximum single application rates are 0.25 lb. active ingredient per acre (a.i./A) for pome fruits and 0.09375 lb. a.i./A for cotton. The maximum seasonal application rates are 0.50 lb a.i./A for pome fruits and 0.28 lb a.i./A for cotton.

2.4.3.1 Physical properties

Thiaclporid is yellowish crystalline powder with molar mass 252,7 g/mol and density 1,46 g/ cm^3.
Solubility in water 185 mg/L. Melting point 136 °C. Partition coefficient(n-octanol/water):
K_{ow} = 18.0; log P_{ow} = 1.26 at 20°C. Vapor pressure: 23 X 10^{-12} hPa at 20°C; 8 X 10^{-12} hPa at 25°C (U.S. Environmental Protection Agency, 2003: 2).

2.4.3.2 Toxicological effects

Acute toxicity
All toxicity tests were performe on rats. The oral dose of technical grade thiacloprid that resulted in mortality to half of the test animals (LD_{50}) is 621 mg/kg in males; 396 mg/kg in females. The dermal LD_{50} is 2000 mg/kg in males and females. It is considered non-irritating to eyes and skin. In acute inhalation toxicity tests, LC_{50} is > 0.481 mg/L (U.S. Environmental Protection Agency, 2003: 3).

Chronic toxicity
The 90-Day oral dosing rodents NOAEL was 7.3 mg/kg/day for male and 7.6 mg/kg/day for females. For mice NOEL was 27.3/ 102.6 mg/kg/day (F/M)
90-Day oral dosing nonrodents NOAEL was 8.5 for males and 8.9 mg/kg/day for females (U.S. Environmental Protection Agency, 2003: 3-4).

Mutagenic Effects
Thiacloprid tested negative for mutagenic effects in a battery of 23 laboratory mutagenicity assays (U.S. Environmental Protection Agency, 2003: 4).

Carcinogenic Effects
Based on liver toxicity and microscopic lymph node changes in both sexes, and increased X-zone vacuolization of the adrenal glands in female mice, carcinogenicity test resulted in NOAEL 5.7 mg/kg/day for males and 10.9 mg/kg/day for females (U.S. Environmental Protection Agency, 2003: 4).

Fate in Animals
Thiacloprid was quickly and completely absorbed from the gastrointestinal tract, followed by a fast and uniform distribution to the organs and tissues of the rat. The major portion of the administered dose was quickly eliminated with the urine and faeces. There was no indication of an accumulative behaviour in rats. Besides the parent compound, 26 metabolites were identified in urine and faeces. In goats, the compound was also quickly excreted, mainly with the urine. Only a very small amount was secreted with the milk. Similarly in poultry, only a minute amount was found in the eggs (U.S. Environmental Protection Agency, 2003: 5).

2.4.3.3 Ecological Effects

Aquatic organisms
There is no concern for acute risk to freshwater fish and invertebrates nor for chronic risk to freshwater fish and invertebrates. It is predicted that the degradates will pose minimal risk to freshwater organisms. The test demonstrated that the LC_{50} values were higher than the highest concentrations tested which also indicated that the degradates were slightly toxic to practically non-toxic to aquatic organisms.
There is concern for risk to marine/estuarine invertebrate species, both acute (all the proposed uses) and chronic (for apple and cotton uses). This is because of the close proximity of the use sites to marine/estuarine habitats, the potential for thiacloprid to be washed off the use sites into these habitats after a rainfall event, the high toxicity (acute and potential for adverse reproductive effects to these species), and the Agency's risk quotients (RQ) predict that thiacloprid may contaminate surface water at concentrations that exceed the Agency's level of concern (U.S. Environmental Protection Agency, 2003: 9-10).

Terrestrial Organisms
There is no concern for birds on an acute oral basis or on a subacute basis. There is concern for chronic risks to birds for all the proposed uses. There is concern for acute risks to only the very smallest sized mammal species for all the proposed uses, and chronic risks to all small mammals for all the proposed uses (U.S. Environmental Protection Agency, 2003: 10).

Plants
Based on the submitted data, it is not expected that plant species will be adversely effected by the proposed uses (U.S. Environmental Protection Agency, 2003: 10).

Beneficial Insects
Based upon the results of core bee toxicity tests, it is predicted that thiacloprid will not adversely affect bees. In addition, thiacloprid toxicity is unlike other neonicotinoid insecticides (i.e.: imidacloprid, and clothianidin) which have demonstrated very high acute toxicity to bees (U.S. Environmental Protection Agency, 2003: 10). LD_{50} for thiacloprid is 14,6 µg/bee (Iwasa et al., 2004)

2.4.3.4 Environmental Fate

Degradation/Dissipation; Soil
The main route for dissipation of Thiacloprid in soil is through microbial degradation (from 0.6 to 3.8 days half-life). It is stable in anaerobic aquatic conditions (half life of over 1 year), and degrades under aerobic aquatic conditions with a half-life of 10-63 days. The only two major degradates (greater than 10% of applied radioactivity) were YRC 2894 amide which is the metabolite of concern in drinking water and YRC 2894 sulfonic acid. In an aerobic soil system, the calculated DT50 for the amide and the sulfonic acid metabolites were from 32-142 days and 12 - 73 days, respectively. There are no toxicological concerns with the YRC 2894 amide metabolite (U.S. Environmental Protection Agency, 2003: 9).

Field
The submitted field studies showed that thiacloprid degrades with a half life range from 2.4 to 27.4 days, and major metabolites were YRC 2894 Amide and YRC 2894 sulfonic acid. The major route of dissipation under terrestrial field conditions was transformation (U.S. Environmental Protection Agency, 2003: 9).

Leaching
Both the parent and the drinking water metabolite of concern, YRC 2894 amide, have low-medium potential to leach to ground water. Though the other of the two major metabolites, sulfonic acid, is expected to be more persistent and mobile than the parent, its toxicity is likely to be much less than the parent due to its increased polarity and expected ease of excretion. In addition, the amide is a much larger percentage of the applied dose (74%) than is the sulfonic acid (19.7%). There are incomplete environmental fate data for YRC 2894 amide, so conservative assumptions were made about its fate based upon the fate of the parent (U.S. Environmental Protection Agency, 2003: 9).

Ground and Surface Water
The modeling predicts that both thiacloprid and its major degradate, YRC 2894 amide, will not be found in significant concentrations in groundwater. However, YRC 2894 sulfonic acid is expected to be more persistent and mobile, and, thus, a groundwater advisory will be required on the label. Because of limited mobility, thiacloprid is not likely to run off from the use site to contaminate surface water. However, thiacloprid has a high water solubility that results in the potential contamination of surface water following rainfall events (U.S. Environmental Protection Agency, 2003: 9).

2.4.4 Acetamiprid

Acetamiprid (E)-N1-[(6-chloro-3-pyridyl)methyl]-N2-cyano-N1-methyl acetamidine
is a systemic insecticide uses for control of sucking-type insects on leafy vegetables, fruiting vegetables, cole crops, citrus fruits, pome fruits, grapes, cotton, and ornamental plants and flowers. Application rates a maximum of 0.55 pounds active ingredient per acre per season.

2.4.4.1 Physical properties

Acetamiprid is solid, white powder insecticide with molar mass 222,68 g/mol and relative density 1,330 (20°C), octanol/water partition coefficient Log Kow = 0.8 at 20°C.
Solubility in water is 4.25×10^3 mg/L at 25°C. Vapor pressure is lower than 1×10^{-6} at 25°C and Henry's constant is $<5{,}3 \times 10^{-8}$ Pam^3/mol (25°C) (EPA. Pesticide Fact Sheet, 2002: 1-2).

2.4.4.2 Toxicological effects

Tests of acute and chronic toxicity were performe on rats.

Acute toxicity
The oral LD_{50} is 417 mg/kg for male and 314 mg/kg for female. The dermal LD_{50} is >2000 mg/kg, inhalation LC_{50} > 1,15 mg/L air (European Comission, Health&Consumer protection Cirectorate, 2003: 9).

Chronic toxicity
A 13-week feeding study in rats resulted in a NOEL of 12.4/14.6 mg/kg/day (M/F)
A 13-week feeding study in mice resulted in a NOEL of 106.1/129.4 mg/kg/day (M/F). Adverse effects included decreased glycerol and cholesterol levels, reduced absolute organ weights. (EPA. Pesticide Fact Sheet, 2002: 7).

Reproductive Effects
A two generation reproduction study in rats fed up to 6,5mg/kg daily resulted in no changes in body weight (European Comission, Health&Consumer protection Cirectorate, 2003: 10).

Mutagenic Effects
Acetamiprid is considered to be no mutagenic.

Carcinogenic Effects
Acetamiprid pesticide has been classified as a “unlikely” human carcinogen, there was no evidence of carcinogenicity in mammals. (EPA. Pesticide Fact Sheet, 2002: 3-4).

Fate in animals
Tests were performed on rats. Acetamiprid is extensively and rapidly metabolized. Metabolites 79-86% of administered dose. Profiles similar for males and females for both oral and intravenous dosing. Three-seven percent of dose recovered in urine and feces as unchanged test article. Urinary and fecal metabolites from 15-day repeat dose experiment only showed minor differences from single-dose test. Initial Phase I biotransformation: demethylation of parent. 6-chloronicotinic acid most prevalent metabolite. Phase II metabolism shown by increase in glycine conjugate (EPA. Pesticide Fact Sheet, 2002: 8).

2.4.4.3 Ecological effects

Effects on Birds
The LD_{50} is 98 mg/kg for mallard in short term exposure to acetamiprid, daily feeding study resulted in LD_{50} 741 mg/kg. (European Comission, Health&Consumer protection Cirectorate, 2003: 20).

Effects on Aquatic Organisms
In short term exposure (96 hour) EC_{50} >100 mg/L (*Oncorhynchis mykiss*), study of long term exposure (35 days) and concentration of 19,2 mg/kg resulted in no effluence (*Pimephales promelas*) (European Comission, Health&Consumer protection Cirectorate, 2003: 20).

Effects on Other Animals
Acetamiprid has negative effect on bees in concentration higher than microgram per bee. LD_{50} 7,1 µg/bee (24 hour after application of acetamiprid on bee) is 400 times higher than LD_{50} for imidacloprid. (Iwasa et. al., 2004).

2.4.4.4 Environmental Fate

Degradation/Dissipation; Soil
Acetamiprid is a mobile, rapidly biodegradable compound in most soils. The primary degradation pathway is aerobic soil metabolism with short half lives ranging from <1 day to 8.2 days. The major degradate –methyl(6-chloro-3-pyridyl)methyl amine, was substantially more persistent than the parent

acetamiprid, reaching a maximum of 73.3% of the applied material after 121 days (EPA. Pesticide Fact Sheet, 2002: 12).

Field
The submitted field studies showed that acetamiprid is non persistent with dissipation half-lives of less than 18 days. Leaching to lower depth was not significantly observed for the parent acetamiprid. Surface water contamination is more of a concern than ground water contamination due to overland runoff (EPA. Pesticide Fact Sheet, 2002: 13).

Ground and Surface Water
Available data indicate that acetamiprid is relatively non persistent and though it is mobile rapid degradation will reduce its potential to leach to groundwater. The primary degradation pathway for the compound is aerobic soil metabolism, which results in rapid biodegradation in soil. It is stable to hydrolysis at environmental temperatures, and photodegrades relatively slowly in water which makes it more persistent in water. Acetamiprid is a moderately to highly mobile in most soils and is not expected to bind strongly to aquatic sediments.
The potential for the degradation products to leach to groundwater is significantly higher being more persistent than the parent acetamiprid. The mobility and persistence of the major degradation product in the environment may result in groundwater contamination. However, all indications are that such contamination will not be of toxicological significance. Acetamiprid could potentially reach surface water via spray drift or runoff under certain environmental conditions (EPA. Pesticide Fact Sheet, 2002: 13).

2.4.5 Thiametoxam

Thiametoxam 3-(2-chloro-1,3-thiazol-5-ylmethyl)-5-methyl-1,3,5-oxadiazinan-4-ylidene(nitro)amine discovered by Ciba (now Syngenta AG) in 1991, was introduced in New Zealand in 1997. Uses for control of aphids, whitefly, thrips, ricehoppers, ricebugs, mealybugs, white grubs, Colorado potato beetle, flea beetles, wireworms, ground beetles, leaf miners and some lepidopterous species, at application rates from 10 to 200 g/ha (Tomlin, 2003: 959). Major crops for foliar and soil treatments are cole crops, leafy and fruity vegetables, potatoes, rice, cotton, deciduous fruit, citrus, tobacco and soya beans; for seed treatment use, maize, sorghum, cereals, sugar beet, oilseed rape, cotton, peas, beans, sunflowers, rice and potatoes.

2.4.5.1 Physical properties

Thiametoxam is crystalline powder insecticide with molar mass 291,7 g/mol and relative density 1,57 g/ cm^3. Solubility in water 4,1 g/L (25°C). Melting point 139.1°C . Partition coefficient(n-octanol/water): log Pow = –0.13 (25°C). Vapor pressure: 6.6 x 10^{-6} mPa at 25°C, Henry 4.70 x 10^{-10} Pa m^3 /mol (25°C) (Tomlin, 2003: 959).

2.4.5.2 Toxicological effects

Toxicity test were made on rats.The 90 days oral dosing of acetamiprid NAOEL (no observed adverse effect level) is 1,74 mg/kg for male and 92,5 mg/kg for female. LOAEL (lowest observed adverse effect level) values are 17,64 for male nad 182,2 mg/kg for female.
The 28 days dermal treating NOAEL was 250 mg/kg daily (male) and 60 mg/kg daily (female), LOAEL values were 1000 and 250 mg/kg daily (M/F) (U.S. EPA. Federal Register Environmental Documents, 2005).

Reproductive Effects
Reproductive tests were performed on rats. Study resulted in decreased of body weight and distortion of a bons. NOAEL is 200 mg/kg daily and LOAEL is 750 mg/kg daily. (U.S. EPA. Federal Register Environmental Documents, 2005).

Fate in Animals
In oral dosing of rats thimethoxam was quickly and almost completely absorbed and eliminated with the urine. Same metabolism was for goats and chickens. Most of thiamethoxam was eliminated in primary form, there is only one important degradate product (Norvatis, 1997).

2.4.5.3 Ecological effects

Effects on Birds
The toxicity of thiametoxam to fish is moderately low. The LD_{50} of thiametoxam is 1552 mg/kg for partridge, and 576 mg/kg for mallard. Test with chronically exposure shows that thiametoxam extract fast and there is no accumulation in body (Syngenta Crop Protection, 2005).

Effects on Aquatic Organisms
LC_{50} for xxxx was >100 mg/kg and LC_{50} > 111mg/kg for xxxx (Syngenta Crop Protection, 2005).

Effects on Other Animals
LD_{50} is 29,9 ng/bee in case that bee come into the contact with pesticide (Iwasa et. al., 2004), in a case of oral dosing LD_{50} is lower 5 ng/bee (Syngenta Crop Protection, 2005).
EC_{50} for earthworm was >1000 mg/kg earth (Syngenta Crop Protection, 2005).

2.4.5.4 Environmental fate

Breakdown of Chemical in Soil and Groundwater
Thiamethoxam is hydrolysis stable at pH 5. Thiamethoxam and his degradate products are moderately mobile in soil (log P_{ow} = -0.13) with the half-life ranging from 7-28 days. In water thiamethoxam photodegrades fast with half-life of 1 our at alkaline medium. In dark water/sediment environment half-life time ranging from 24 to 44 days in anaerobic conditions and from 8 to 16 days in aerobic conditions (Novartis, 1997).

Breakdown of Chemical in Vegetation
Thiametoxam penetrates the plant, and moves from the seed or root to the other parts of the plant. The test of metabolism in plants has been performed in a tomato. The most important step was photodegradation and the most of the dose was washed of with the rain. Thiametoxam degrades slowly in plants so the time of acting is longer (Novartis, 1997).

2.4.6 Detection methods

Recently, various analytical methods have been proposed for the determination of neonicotinoids in food, water and soil, including liquid chromatography with UV detction (HPLC/UV) (Tsamura et al., 1998; Rossi et. al., 2005), liquid chromatography-mass spectrometry (LC/MS) (Obana et al., 2003), gas chromatography-mass spectrometry (GS/MS) (Navalon et al., 1997; Rosi et al., 2005), and liquid chromatography-electrosprey mass spectrometry (Fidente et al., 2005).
GC requires extensive clean-up and derivatization because of the poor volatility, high polarity, and/or thermal instability of these compounds (Vilchez, 1996).
LC technique is most commonly used. The application of LC with diode array detection (DAD) is restricted by detector insensitivity and unspecificity, and the large amounts of interferences from biologic and vegetables extracts (Blasco, 2002; Fernandez-Alba et al., 1996). LC coupled to mass spectrometry (MS) with atmospheric pressure ionization (API) interfaces, mainly atmospheric pressure chemical ionization (APCI) and electrospray (ES), has overcome many of the disadvantages associated with other detectors. Imidacloprid (Fernandez-Alba et al., 2000; Pous et al., 2001), were analyzed in fruits and vegetables by LC–MS using either APCI or ES.
Hence, liquid chromatographic methods such as HPLC/DAD (Obana et al., 2001; Mandič et al., 2005), HPLC/MS (Obana et al., 2003; Fidente et al., 2005; Secca et al., 2005), and HPLC/post-column photoactivation /electrochemical detection (Rancan et al., 2006) appeared to be advantageous for the determination of neonicotinoids in various matrices.

3 EXPERIMENTAL

3.1 Reagents and solutions

All the materials were used as obtained from the suppliers and no further purification of the chemical was performed. Deionised water was prepared using a Milli-Q water purification system, MilliRO 5 PLUS.

Methanol:	J. T. Baker, (HPLC gradient grade)
Acetone:	J. T. Baker, (HPLC gradient grade)
Acetonitrile:	J. T. Baker, (HPLC gradient grade)
Dichlorometane:	J. T. Baker, (HPLC gradient grade)
$K_2Cr_2O_7$:	Riedel-de Haën
1.5-diphenylcarbazide:	Sigma-Aldrich
H_3PO_4:	Riedel de Haën
Thiamethoxam:	Riedel de Haën, 99.4%
Imidacloprid:	Riedel de Haën, 99.9%
Thiacloprid:	Riedel de Haën, 99.9%
Acetamiprid:	Dr Ehrenstorfer GmbH, 99.0%
Bilirubin:	Sigma, bilirubin Ixá min 93%
DMSO:	Riedel de Haën, 99,5%
HNa_2PO_4:	Fluka, ≥99%
H_2NaPO_4:	Fluka, ≥99%
NaCl:	Carlo Erba

3.1.1 Sample preparation

Stock standard solution (1000 mg/L) of Cr(VI) was prepared by dissolving 2.8280 g of potassium di-chromate (min 99.8% Riedel-de Haën, Germany) in 1.0 L of water. Solutions of lower concentrations were prepared daily by appropriate dilution.
Stock solution of 1,5 diphenylcarbazide (DPC) (Sigma-Aldrich) was prepared by dissolving 0.1 g of DPC in 10 mL of acetone.
H_3PO_4 solution was prepared by diluting 120 ml of 85% H_3PO_4 with 280 ml of water.
The standard solutions (10 ml) were treated with 0.8 ml of DPC and 0.4 ml of phosphoric acid and allowed to stand for 20 minutes prior to measurements.
DPC solution (10 ml) for on-line generation of Cr-DPC was prepared by diluting 0.8 ml DPC stock solution with 8.8ml water and 0.4 ml 25% H_3PO_4 .
The mobile phase consisted of water, acetone and 25 % H_3PO_4 in the volume ratio of
22 : 2 : 1.

Phosphate buffer saline (PBS) solution was prepared by dissolving 0,86 g of HNa_2PO_4, 0,54 g of H_2NaPO_4 and 8,12 g of NaCl in 1 L of distilled water. The pH was adjusted to 7,4 with 1M HCl.
The bilirubin solution was prepared in three steps. Firstly, a 10 mM stock solution was prepared by dissolving 5,847 mg of bilirubin in 1 mL of DMSO. The soobtained solution was further diluted (5 µL of the stock solution + 995 µL of DMSO) in order to obtain a 50 µM solution. The final 50 nM solution was obtained by adding 7 µL of the 50 µM solution to 6,993 mL of PBS. The solution was prepared fresh and kept wrapped in aluminium foil in a cold place in order to avoid photodegradation. Solutions of lower concentrations were prepared by appropriate dilution with the phosphate buffer.
The human endothelial cells (Ea.hy 926) were used as a model. Cell cultures were put in contact with a 50 nM bilirubin solution. Concurently, cells were incubated for 30 min with specific anti-bilitranslocase antibody (anti-sequence 65-75) and when the transport assay started they were put in the contact with a bilirubin solution. 600 µL samples were taken at time intervals ranging from 0 to 120

seconds in order to establish the time course of uptake. Samples were mixed with 600 µL of methanol in order to improve their optothermal properties. The experiment was performed in duplicate.

Individual stock solutions (200 µg/mL) of each neonicotinoid were prepared in mobile phase. The single compound standard solutions (20 µg/mL) were prepared by diluting each primary standard solution with the mobile phase.
Mobile phase consisted of 3:7 (v/v) water (0.2% phosphoric acid) : acetonitrile.
Multicomponent solutions of appropriate concentrations of neonicotinoids (2.5-2500 µg/L) were prepared daily by mixing the single compound solutions and diluting the standard multi-component solution with the mobile phase.

3.2 Apparaturs

3.2.1 Flow injection with TLS UV-Vis detection

The flow-injection analysis manifold is shown schematically in Figure 7. It consists of a HPLC pump (Shimadzu LC10Ai), injection valve (Rheodyne model 7725) with sample loop, reaction coil and detection unit. The eluent was pump through the system at different flow-rates (0.5 – 3.5 mL/min). The volume of the sample injection loop was 20, 100, 200 and 500 µL.

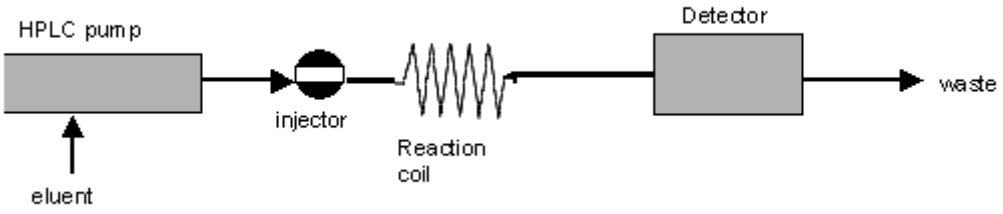

Figure 7: *Flow injection analysis manifold*

The TLS detection was preformed on a dual-beam TLS instrument (Figure 8). The excitation source (pump beam) is an argon ion laser (Coherent, Innova 90) operating at 514.5 nm or 476 nm, modulated by a mechanical chopper (Scientific Instruments, Model 300) and focused onto the sample cell by a 250 mm focal length lens. A He-Ne laser (Uniphase, Model 1103P, 632.8 nm) focused by 80 mm focal length lens in front of the sample provided the probe beam. Collinear propagation of pump and probe beam was obtained with dichroic mirror, which directed the two laser beams through an 8 µL (1 cm path-length) flow-through cell (Hellma) connected with reaction coil. The changes in the probe beam center intensity were detected with a silicon photodiode (Laser Components, OSD 5-E). The photodiode connects to a lock-in amplifier (Stanford Research Systems, Model SR830), which amplifies only the component of the input signal that appears with the frequency of the reference signal from the modulation. The signals were monitored and stored on a personal computer.

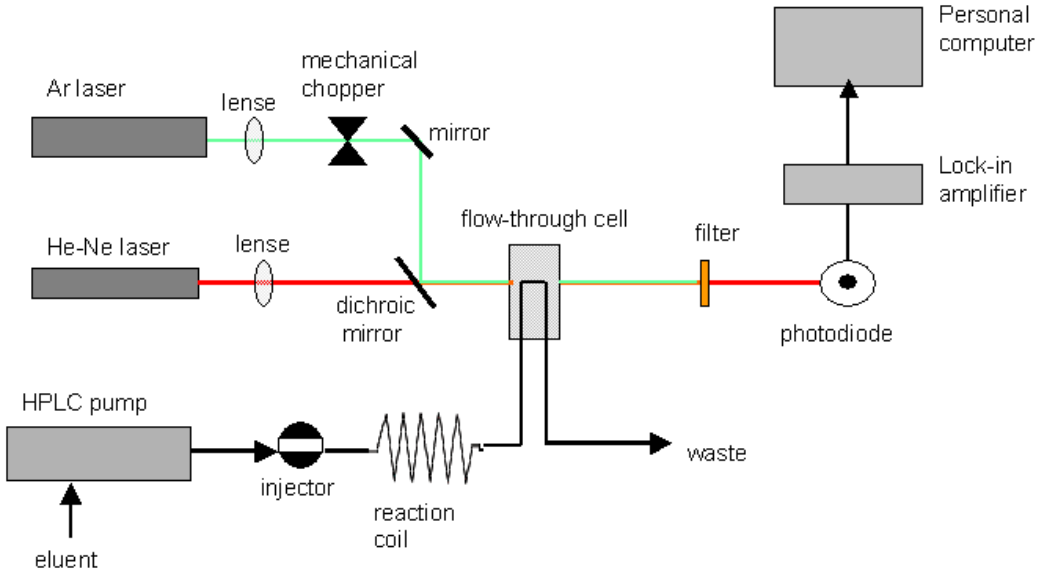

Figure 8: *FIA manifold with TLS detection*

3.2.2 HPLC with TLS UV detection

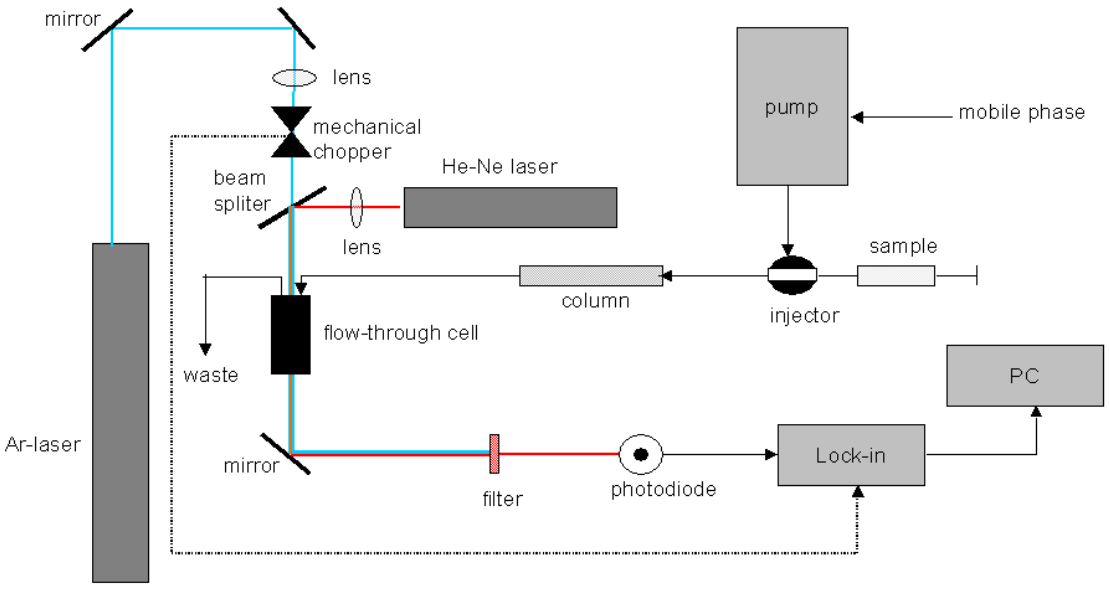

Figure 9: *A schematic diagram of the HPLC with TLS as a detection unit*

The sample is first introduced into the sample loop. The mobile phase than carries the sample from the sample loop to the chromatographic column (Pinnacle ODS, 250 mm × 4.6 mm, 5 µm) (Restek

Corporation, Cally 911457) using a high pressure chromatographic pump (Shimadzu LC10Ai). The eluting compounds are then detected by TLS.
The TLS measurements were made on a dual beam (pump/probe configuration) thermal lens spectrometer. A frequency doubled Ar–ion laser (Coherent, Sabre MotoFred) operating at 244 nm (100 mW) was used as excitation source (pump beam). The pump beam was modulated with a variable speed mechanical chopper (Scientific Instruments, Model 300). A He-Ne laser (Uniphase, Model 1103P) provided the probe beam. After focusing the pump beam with a 100 mm focal length quartz lens, collinear propagation of pump and probe beams was obtained by a beam-splitter, which directed the two laser beams through an 8 μL (1 cm path-length) flow-through cell (Hellma) connected to the output of an HPLC column. The fluctuation in the probe beam intensity was measured with a silicon photodiode (Laser Components, OSD 5-E). A red filter and a pinhole were located in front of the photodiode. The output of the photodiode was fed to a lock-in amplifier (Stanford Research, Model SR830) connected to a personal computer, where the HPLC/TLS chromatograms, represented as time-dependent changes in the probe beam intensity, were recorded.

4 RESULTS AND DISCUSSION

4.1 Flow injection thermal lens spectrometric detection of hexavalent chromium

It was noticed that TLS measurements of photolabile analytes in batch mode (Pedreira et al., 2004) are hindered due to degradation of analytes induced by intensive excitation laser source.
Pedreira et al., 2004 observed that the thermal lens effect was strongly reduced during the measurements of Cr-DPC in solution and the amplitude of the TL signal decreased for each consecutive shot. This indicated that the amount of absorbing species in the region where the beam is passing through was significantly reduced due to photochemical reaction. They showed that photochemical reaction of the Cr-DPC complexes is much slower than the thermal diffusion with a time constant higher than 50 ms. Therefore, fast response techniques, which minimize the exposure of photolabile analytes to irradiation, contribute to minimization of influence of photochemical processes on the TL signal.
Flow injection analysis is widely used as a simple and convenient approach to rapid analysis. It has several attributes, which would appear useful in trace level determinations, including small volume sampling, low risk of contamination and a large dynamic range for a given expenditure of time and reagent. A disadvantage is that the continous operation might led to excessive use of reagents.
In this work attempts were made to develop a FIA-TLS method for determination of trace levels of Cr(VI). Cr(VI) was determined following on-line generation of Cr(VI)-DPC complexes or by injection of Cr(VI)-DPC into the FIA system after complete development of color (20 min). The applicability of the developed method was tested on spiked drinking water.

4.1.1 Flow injection system with on-line Cr(VI)-DPC reaction

Initial experiments confirmed the difference in stability of TLS signals under flowing and static (stop flow) sample conditions. For static sample the signal decreased with laser radiation time, because of photodegradation of the analyte during exposure to intense optical power (140 mW). As shown in Figure 10 flowing the sample at constant flow rate (0.2 mL/min) through the detection cell averted the steady decrease of sample's absorbance. The experiment under the flowing conditions was performed by loading the sample into 1 mL injection coil, and injecting the sample into the flowing carrier buffer at – 200 s (200 s before time 0). The signal from flowing sample shows only slight variation over time.

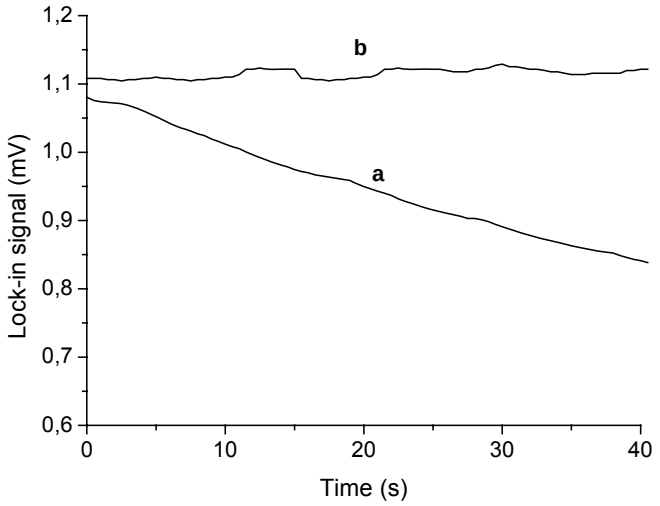

Figure 10: *Time dependence of thermal lens signal for static (a) and flowing (b) sample. Sample is Cr-DPC in water, 15 µg/L. Flow rate 0.2 mL/min, injected sample volume 1 mL.*

The concept of reversed FIA (rFIA) was used for further experiments in order to minimize reagent consumption and to enhance analytical sensitivity (Johnson and Petty, 1982). While in regular FIA the sample is injected into a continous flow of reagent solution (carrier), dispersed and transported to detector, rFIA consists of injecting volumes of reagent into the flowing sample stream. The reagent and sample mix in exactly the same manner as in conventional FIA apparatures so that the fundamental principles of FIA (reproducibility of timing, injection and dispersion) apply to rFIA as well..
In FIA technique, where the reagent solution is a carrier stream and the sample is injected into this stream, an increase in the sample volume decreases dispersion. Thus, increase in sample volume enhances the analytical sensitivity. Johnson and Petty 1982, showed that by reversing the roles of sample and reagent the relationsheep between dispersion and sensitivity is also reversed. In rFIA the amount of sample in the zone of the reagent increases as the dispesion increases. For successufully performed analysis by this technique, sample concentration in the zone of the reagent should be in the range from 67 to 90 % of the sample concentration in the carries stream. The sample will become well mixed with the reagent as its concentration increases so that well-formed peaks wiil result (Johnson and Petty, 1982).
From Figure 11 it is evident that by the simple reversed roles of sample and reagent, the sensitivity increased approximately 3 times relative to conventional FIA.

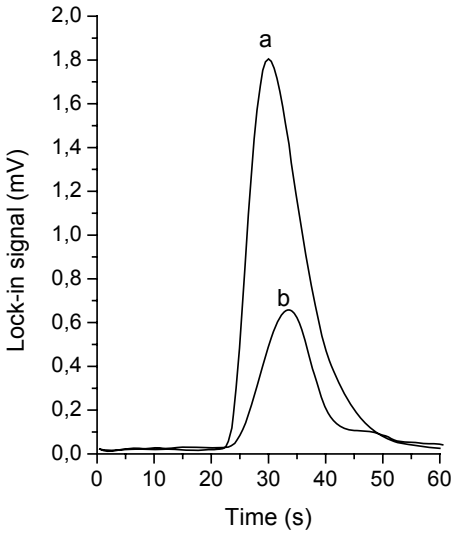

Figure 11: *TLS signal in flow injection analysis (a) and reversed flow injection analysis (b). Flow rate 2.5 mL/min, 20 µg/L Cr(VI). Injected reagent volume is 0.02 mL, injected Cr(VI) volume is 0.5 mL*

In this system the reagent is introduced into the continuous stream of sample, through a 20 µL injection coil. The color is developed in the reaction coil and the passage of the colored zone through the flow cell results in a transient signal measured at 514.5 nm. The peak height was used for all calculations.

Owing to the strong dependence of photothermal response on solvent composition, the TLS method is highly sensitive to non homogeneous composition of binary liquids, as demonstrated recently (Logar et al., 2002). As shown in Figure 12 for the FIA-TLS system, changes in solvent composition lead to large signal fluctuations and even distortion of the peak shape. This arises from a non-homogeneous solvent composition due to the difference in composition of the carrier solvent in the FIA system (sample in the described case) and injected DPC reagent.

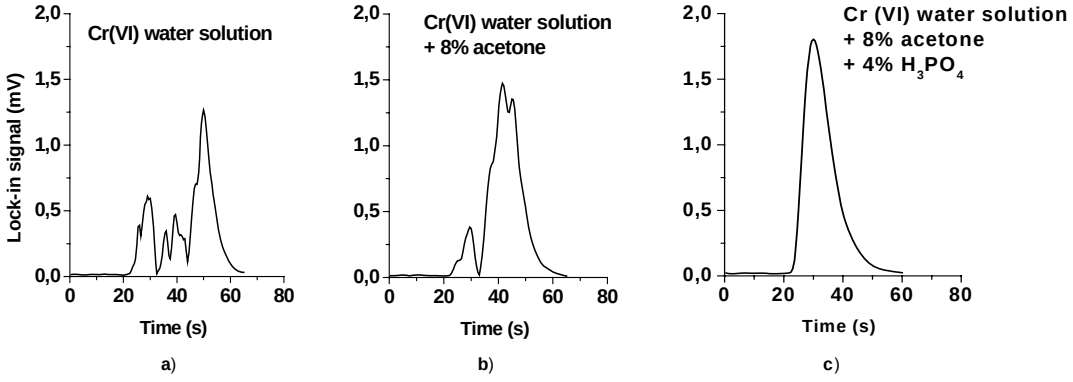

Figure 12: *Influence of the carrier composition on thermal lens signal. (20 µg/L Cr(VI), 20 µL injection coil, 2.5 mL/min)*

Fluctuations of the signal are clearly evident between 25 and 50 seconds for an aqueous Cr(VI) as carrier solution (Figure 12a) and are due to probe beam distortion (visible by naked eye) from non-homogeneous refractive index distribution (Logar et al., 2002). When 8% acetone is added to the flowing sample to better match the optical properties with those of DPC reagent, the initial signal fluctua-

tion is significantly reduced (Figure 12b). Finally a desired signal peak-shape (Figure 12c), affected only by the dispersion of the Cr-DPC passing the detection cell, is obtained when besides acetone, a 4% H_3PO_4 is added to the flowing sample (carrier solution) to match completely the composition of DPC reagent.
Figure 13 shows FIA-TLS signals for acidified diphenylcarbazide injected into the system with carrier without chromium (a) and carrier spiked with chromium (b). No detectaible signal was observed in the case when carrier contained no Cr(VI).

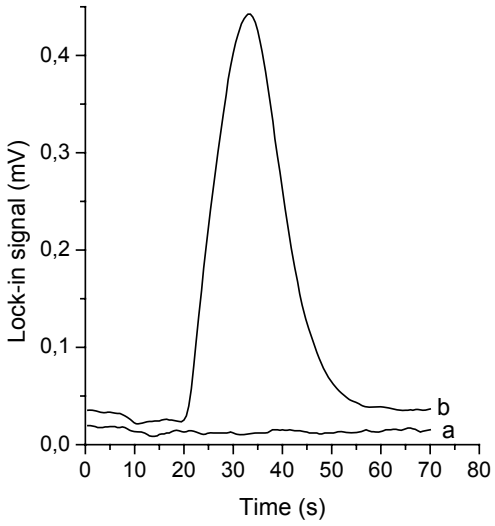

Figure 13: *Thermal lens signal of DPC (a) and Cr-DPC (b). (6 µg/L Cr(VI), 20 µL injection coil, 2.5 mL/min)*

Chemical and flow variables were optimized in order to obtain the best sensitivity. The DPC concentration was studied in the range 1- 5 mM, and the best sensitivity was obtained with a concentration of 3 mM. The influences of carrier solution flow rate and reagent volume were examined since these parameters have similar effects on the sensitivity of the method, affecting the sample zone dispersion and thermal lens signal.
The carrier solution flow rate was varied from 0.5 to 3.5 mL/min. Signal decreased with increasing flow rate (Figure 14). Diminished signal with sample flow is due to the heat loss through mass transfer out of the region irradiated by the excitation source. At the flow rate of 3.5 mL/min the time of analysis was about 3 times shorter (35 s) compared to 1mL/min flow rate (110 s) but the sensitivity decerased by 36% (according to peak areas). At the flow rate of 2.5 mL/min sensitivity was 21 % lower and time of analysis was 2.2 times shorter than at flow rate of 1 mL/min Thus, as a compromise between sensitivity and sampling frequency 2.5 mL/min flow rate was selected for further studies.
As known from literature, the TLS signal in flowing samples depends on the sample's residence time in the flow through cell (volume of the cell divided by the flow rate) and the characteristic time constant of thermal lens which is defined as $t_c=w^2\rho C_p /4k$. Assuming that ρ, C_p and *k* are linear functions of the volume fractions of each solvent in solution a time constant of 3.15 ms was calculated for the experimental conditions used in determination of Cr(VI) while the corresponding sample's residence time was 192 ms at 2.5 mL/min flow rate. Since the time constant is much shorter compared to the residence time (61 times) axial flow (in direction of laser beam propagation) doesn't have a significant contribution to the therml lens (Dovichi and Harris, 1981). The decrease in the TLS signal must therefore be associated with the turbulence generated inside the cell, which has similar effects as reported previously, when decreases in TLS signals of 15-35% were observed for flow rates similar to those used in this work (1.5 - 3.5 mL/min) (Dovichi and Harris 1981; Proskurnin et al., 1999). Another important parameter in TLS analysis of flowing samples is the modulation frequency, which should be selected based on the minimum signal to noise ratio. Still, the modulation frequency must be fast enough to avoid undetected samples or their fractions. It should be noted that modulation frequencies (8-12 Hz) were always higher than the sample exchange frequency, which ranged from 2 Hz for the flow rate of 1 mL/min to 7.5 Hz at 3.5 mL/min flow rate. Furthermore the period of a single laser irradiation at 10

Hz modulatin is 50 ms is also shorter compared to the sample's residence time and allows at least one irradiation of each volume passing the sample cell. Most importantly, the smallest injected sample (20 µL) requires over 20 seconds at 3.5 mL/min flow rate to pass the cell due to dispersion (Fig. 14), while undergoing about 200 duty cycles of chopper modulation at 10 Hz.

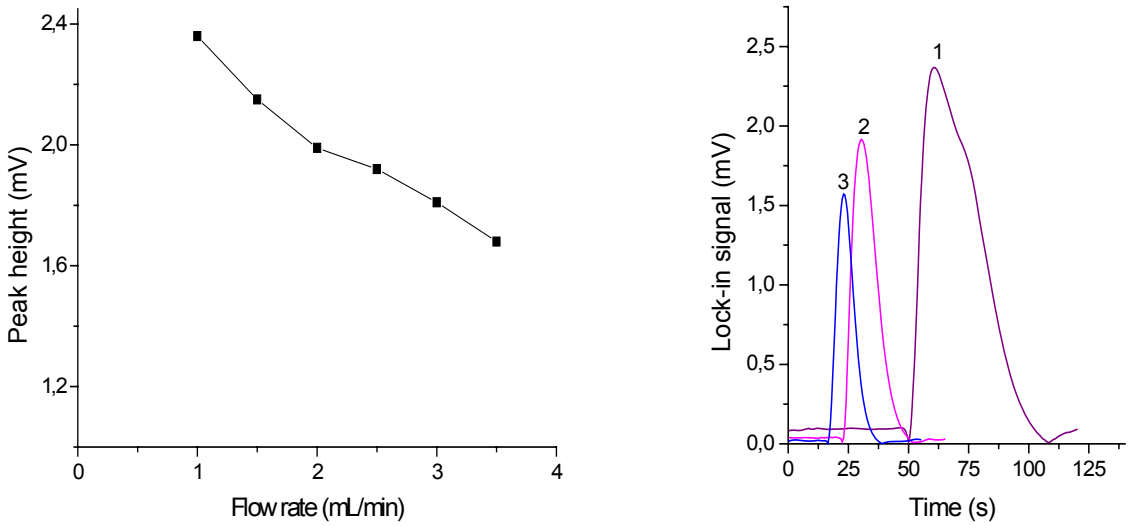

Figure 14: *Influence of carrier solution flow rate on the peak height (1 = 1mL/min, 2 = 2.5 mL/min and 3 = 3.5 mL/min). Conditions: 20 µg/L Cr(VI), 20 µL injection coil.*

Four different injection coil volumes of the DPC solution (20 – 500 µL) were examined. The signal variation with the coil volume indicates that large volumes of DPC solution are not required. The time dependent thermal lens signals show distortions from the expected peak shape, which are reflected in double peak shape (Figure 15). This is in agreement with previously described characteristics of rFIA, where higher volumes of injected reagent disable the quantitative mixing of injected reagent with sample in the center of reagent zone and cause the formation of two peaks. Therefore an injection coil volume of 20 µL was chosen for further experiments.

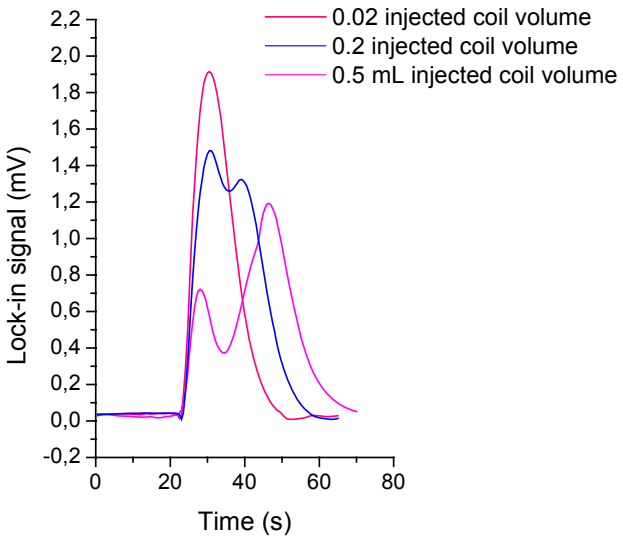

Figure 15: *Influence of the injected reagent volume on the thermal lens signal. (20 µg/L Cr(VI); 2.5 mL/min flow rate)*

4.1.1.1 Analytical features of the system

Under optimized conditions (2.5 mL/min flow rate, 20 µL injection coil) a linear fit (y = 0.015 + 0.09[Cr(VI) (µg/L)]) was derived for peak height dependence on Cr(VI) concentration between 1 and 20 µg/L (Figure 16) with a correlation coefficient r^2 = 0.9991.

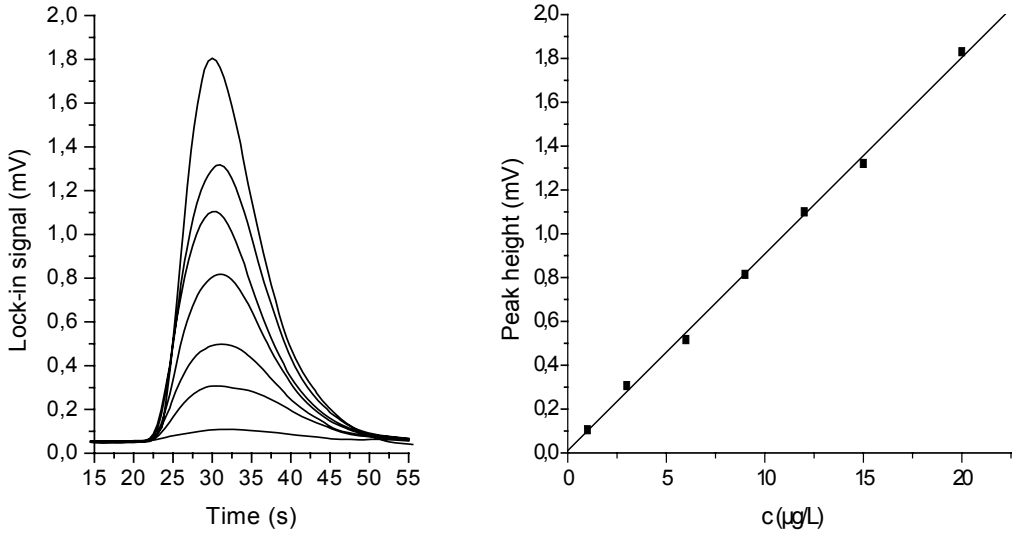

Figure 16: *Thermal lens signals (left) and calibration curve (right) for on-line Cr(VI)-DPC reaction (injected volume 20 µL , eluent flow rate 2.5 mL/min).*

Analytical features of the method are summarized in Table 2. The LOD (limits of detection) was calculated as a quotient between 3 fold standard deviation of blank devided by slope of calibration line and it was 0.067 µg/L., whereas the quantification limit was calculated as a quotient between 10 fold standard deviation of blank devided by slope of calibration line. The RSD observed at 1 µg/L level was 2.4% (n=5).

Table 2: *Analytical features of the optimized FIA system with on-line Cr-DPC reaction*

	Chromium concentration (µg/L)						
	1	3	6	9	12	15	20
Mean (n = 5)	0.123	0.269	0.466	0.804	0,905	1,087	1.54
S.D. ±	0.003	0.006	0.010	0.012	0.011	0.019	0.03
R.S.D. (%)	2.4	2.2	2.1	1.5	1.2	1.7	1.9
LOD (µg/L)	0.067						
LOQ (µg/L)	0.223						

4.1.2 Flow injection system with detection of pre-reacted Cr-DPC

In this case the carrier was not spiked with Cr(VI) and Cr-DPC was injected directly through sample loop after it was prepared off-line in batch mode and allowed for complete development of color (20 min). The operational conditions of the system were optimized in order to reach compromise beetwen sensitivity and frequency analysis. A 20 µg/L Cr(VI) solution was used for the optimization.
The effect of the carrier solution flow rate was checked over the range 0.5-3.5 mL/min. The signal decreased with increasing flow rate (Figure 17).
At the flow rate of 3.5 mL/min and 2.5 mL/min sensitivity decreased 37% and 19% (according to peak areas), the time of analysis abbreviated 3.2 and 2.5 times, respectively compared to flow rate of 1 mL/min. Therefore, the flow rate of 2.5 mL/min was selected for the method.

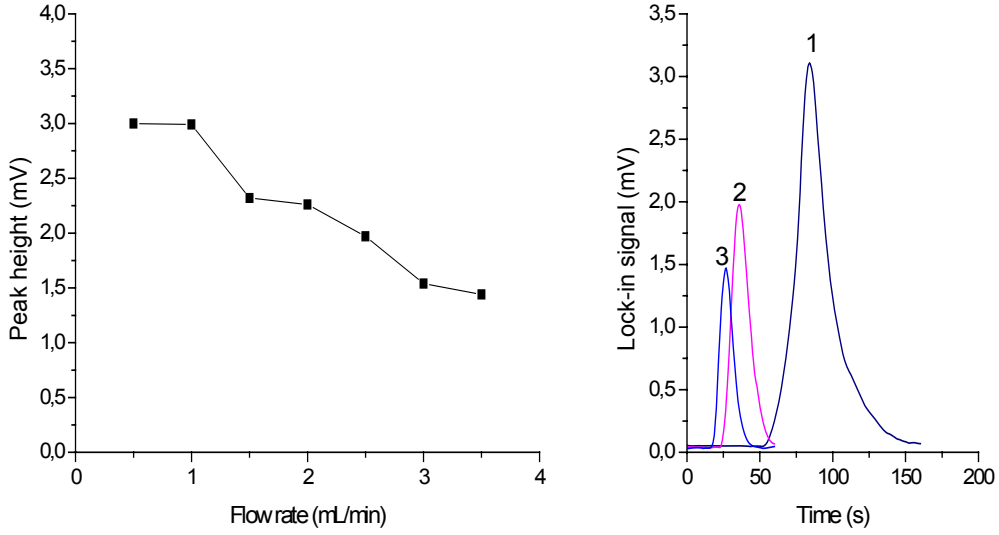

Figure 17: *Influence of the carrier solution flow rate on the peak height (left) and on the time of analysis (right).*
(1 = 1 mL/min; 2 = 2,5 mL/min and 3 = 3.5 mL/min). Conditions: 20 µg/L Cr(VI), 500 µL sample loop

The influence of sample volume on the signal was studied at a constant flow rate 2.5 mL/min. The peak height increase with increasing sample injection volume in the range 0.1-1 mL (Figure 18), But this increasing caused broadening of the peaks and lower sample throughput. Therefore, 500 µL sample volume was chosen in order to obtain a better compromise between sensitivity and analytical throughput.

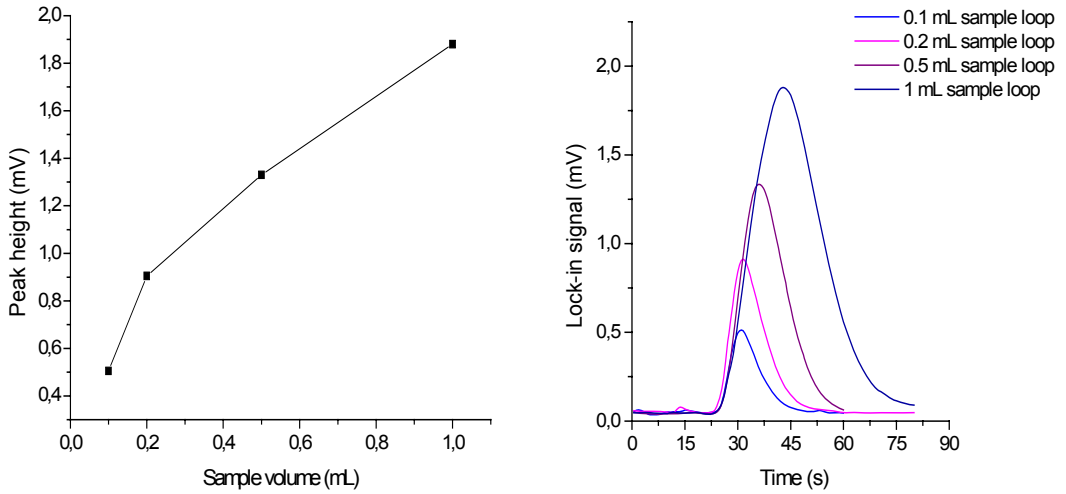

Figure 18: *Influence of the sample volume on the peak height (left) and the shape of the signal (right). (20 µg/L Cr(VI), 2.5 mL/min)*

After extrapolation of the data, presented on Figure 18, up to sample volume of 9 mL a steady-state signal of 3.15 mV was calculated. In FIA optimal signal is ½ steady- state signal therefore 0.5 mL injection coil volume was selected as optimum for further work, producing 44% of the steady state signal.

4.1.2.1 Analytical performance

Under optimized conditions (2.5 mL/min flow rate, 500 µL injection loop) a linear calibration was found in the range of 1 - 20 µg/L (Figure 19), described by the equation: y = 0.045 + 0.134 [Cr(VI) (µg/L)] and correlation coefficient r^2 = 0.9984.

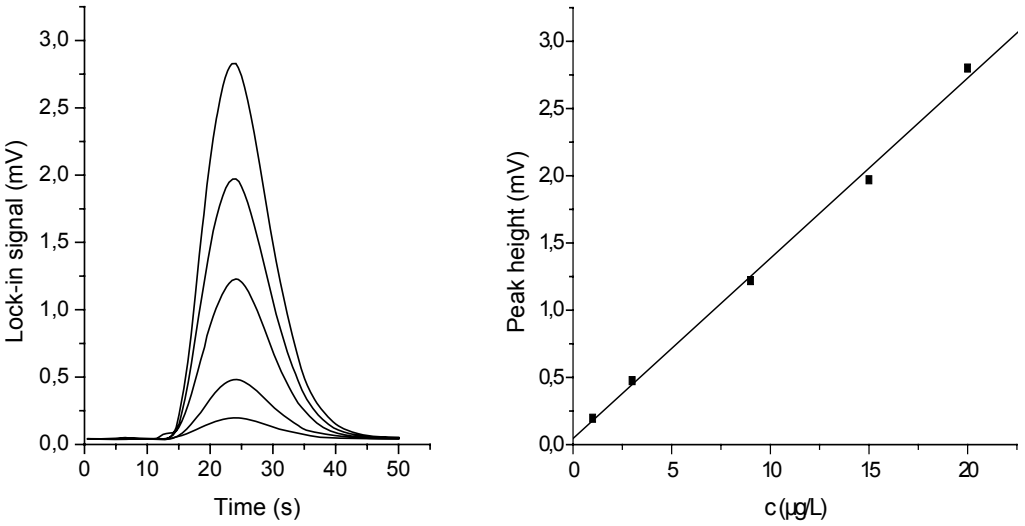

Figure 19: *Thermal lens signals (left) and calibration curve (right) for pre-reacted Cr(VI)-DPC. (injected volume 500 µL, eluent flow rate 2.5 mL/min).*

The LOD (limits of detection) was calculated as a quotient between 3 fold standard deviation of blank devided by slope of calibration line and it was 0.065 µg/L., whereas the quantification limit was calculated as a quotient between 10 fold standard deviation of blank devided by slope of calibration line. The RSD observed at 1 µg/L level was 2.5% (n=5) (Table 3).

Table 3: *Analytical features of the optimized FIA system with pre-reacted Cr-DPC*

	Chromium concentration (µg/L)				
	1	3	9	15	20
Mean (n = 5)	0,201	0,481	1,227	1.968	2,83
S.D. ±	0.005	0.005	0.015	0.010	0.014
R.S.D. (%)	2.5	0.95	1.22	0.5	0.5
LOD (µg/L)	0.065				
LOQ (µg/L)	0.215				

Obtained LODs for Cr(VI) are approximately same in both procedures. The results indicate that in case of on-line Cr-DPC reaction the time of reaction is sufficient to obtain adequate sensitivity, comparable to the case of prereacted Cr-DPC reaction where 20 min. are allowed for full colour development, according to recommended batch mode procedure (Die Untersuchung …, E. Merck AG). Therefore, time of analysis in FIA system with on-line reaction of Cr-DPC is 20 min. shorter compared to detection of prereacted Cr-DPC.

4.1.3 Determination of Cr(VI) in drinking water

In order to validate the developed methodologies, both procedure were applied to determine hexavalent chromium in drinking water, spiked with different chromium levels. The procedures were carried out in water samples without any previous treatment. The results presented in table 4 and 5 shows good agreement between added chromium and recoveries.

Table 4: *Determination of chromium in spiked drinking water samples by FIA method with on-line Cr-DPC reaction*

Concentration added (µg/L)	Concentration found (mean ± S.D., n=4) (µg/L)	Precision (%RSD)	Recovery (%)
1	0.984 ± 0.001	1.43	98.4
9	9.243 ± 0.002	0.24	102.7
15	14.675 ± 0.005	0.38	97.8

Table 5: *Determination of chromium in spiked drinking water samples by FIA method with pre-reacted Cr-DPC*

Concentration added (µg/L)	Concentration found (mean ± S.D., n=4) (µg/L)	Precision (%RSD)	Recovery (%)
1	0.988 ± 0.001	0.42	98.8
9	9.954 ± 0.008	0.67	110.6
15	14.775 ± 0.015	1.05	98.5

Another important feature of all methodologies that must be emphasized is the amount of waste generated at the end of the application. In the present study the system generates approximately 150 mL of effluent per hour of operation. The sampling rate was 50 h^{-1} in the case of detection of prereacted Cr-DPC and nearly 20 h^{-1} in the case of on line generation of Cr-DPC complexes.
For spectrophotemetric measurements of Cr(VI) with DPC method in batch mode, samples are usually prepared in 10 or 25 mL volumetric flasks. Amount of waste generated when analysing 50 samples in batch mode would be 500 or 1250 mL. Therefore, with appliance of FIA technique waste is reduced 3.3 or 8.3 fold.

4.2 FIA-TLS determination of bilirubin

TLS showed up to be capable of detecting physiological concentrations of bilirubin (Margon et al., 2005). Since, bilirubin is known as photolabile analyte (Bonnet, 1976), it was predicted that TLS measurements of bilirubin in batch mode with high power excitation beam (60 – 100 mW) are obstructed by photochemical reaction that occurs during the measurements. FIA-TLS determination of bilirubin was investigated to overcome the problems associated with photodegradation.
Besides the laser power and the solute concentration, the TL signal is sensitive to the thermo-optical properties of the medium, namely the temperature dependent refractive index and thermal conductivity. Owing to its low $\partial n/\partial T$ and high k values, water is a poor solvent for thermal lens spectrometry. On the contrary, organic solvents have better thermo-optical properties due to higher $\partial n/\partial T$ and lower k values. Therefore, it may be advantageous to use water-solvent mixtures to improve the sensitivity of the TLS method (Dovichi and Harris, 1979).
In order to attain best performance for the analytical flow system in terms of sensitivity the influence of added organic solvent and flow variables that could affect the performance were studied by the univariante method.

4.2.1 Study of FIA variables

Influences of carrier solution flow rate and sample volume were examined. A 50 nM bilirubin solution was injected directly through sample loop into the carrier stream, which consisted of 1:1 (v/v) PBS phosphate buffer : methanol. The signal was measured at 476 nm and the peak height was used for all calculations.
The peak height depends on the residence time of the sample zone in the system, e.g. on the total flow rate. The effect of the pump flow rate was checked over the range 0.5-3 mL/min. The results demonstrate that the signal decreases when the carrier flow rate is increased (Figure 20).
At the flow rates of 2 and 3 mL/min sensitivity decreased 15 and 24% respectively but the time of analysis was 2 and 2.4 times shorter compared to flow rate of 1 mL/min. Therefore, the carrier flow rate was set at 2 mL/min for further measurements.

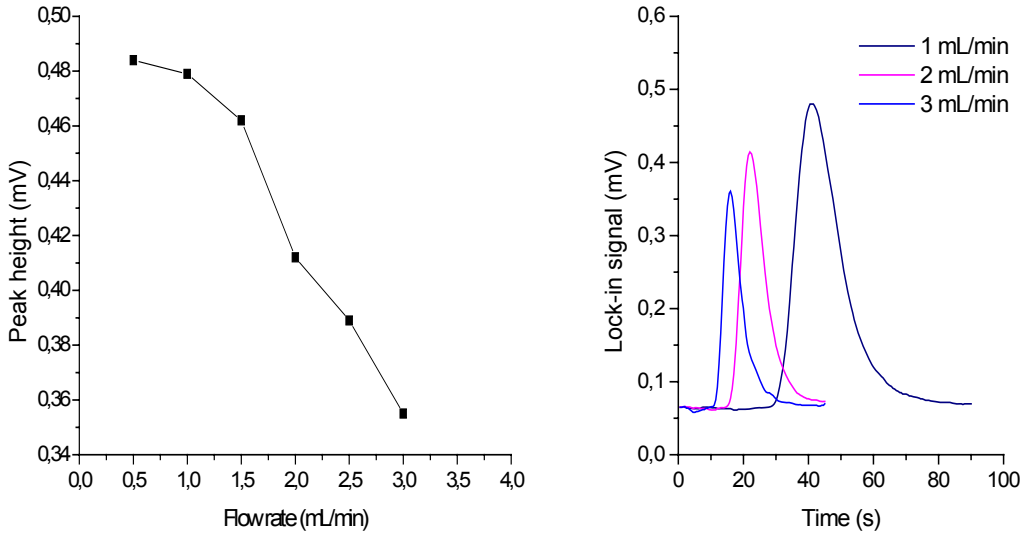

Figure 20: *Influence of the carrier solution flow rate on the peak height. Conditions: 50 nM bilirubin solution, 200 µL sample loop, P = 50 mW*

The influence of sample volume on the signal was studied at a constant flow rate 2 mL/min. The peak height increased with increasing sample injection volume in the range 0.1- 0.5 mL, since the dispersion of the sample zone is inversely proportional to injection volume. But increasing of injection volume caused broadening of the peaks. Thus, 200 µL sample volume was selected for further work (Figure 21).

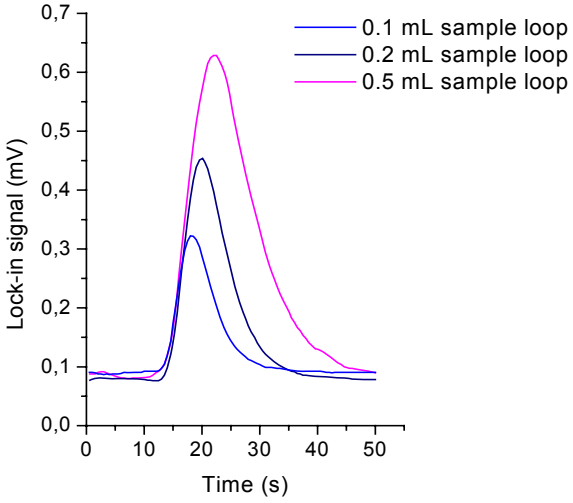

Figure 21: *Influence of the sample volume on the peak height. Conditions: 2 mL/min flow rate, 50 nM bilirubin solution, P = 50 mW.*

4.2.2 Analytical performance

Calibration graph was linear over the range of 2, 5 - 50 nM, with a typical equation: y = 0.1824 + 0.0062[bilirubin (nM)] and correlation coefficient r^2 = 0.995 The LOD calculated from the slope of calibration line (S/N = 3 basis) was 0.4 nM.
An analytical throughput of 60 h^{-1} was achieved with the system operating at optimal conditions (2 mL/min, 200 µL sample volume).

4.2.3 Influence of added organic solvent (methanol) on TL signal

4.2.3.1 Changes in the enhancement factor

The enhancement of the cw-laser thermal lens signal in methanol with respect to that in water is due to an increase in ∂n/∂T and a decrease in *k*. The change in ∂n/∂T increases the enhancement factor (Eq. 30) by 4.3 times, whereas the change in k increases the enhancement factor 3 times (Table 1). For liquid mixtures, the composition dependent thermal lens signal is difficult to calculate precisely since one needs information on the thermo-optical properties of the mixtures. Most often, the relationship between enhancement factor and solvent composition is estimated assuming that ∂n/∂T and *k* are linear functions of the volume fraction of each solvent (Weimer and Dovichi, 1986)

$$\frac{\partial n/\partial T}{k} = \frac{F_{H_2O}\left(\partial n/\partial T\right)_{H_2O} + F_{MeOH}\left(\partial n/\partial T\right)_{MeOH}}{F_{H_2O}k_{H_2O} + F_{MeOH}k_{MeOH}} \tag{31}$$

where F is the volume fraction of the specified solvent. However, the composition dependence of the refractive index gradient is generally a more complicated function (Li et al., 1994) and reliable values must come from experiments. Such determination of ∂n/∂T or thermal conductivity have been made using the thermal lens method (Franko and Tran, 1991; Snook et al., 1998) but precise determination of ∂n/∂T requires knowledge of the thermal conductivity, the sample absorbance and a reference medium to calibrate the experimental set-up if the optical and geometrical parameters of this set-up are not known (Fisher et al., 1996). In addition, it is necessary that the refractive index of the solution is not influenced by other factors than the temperature.
For the purpose, the ∂n/∂T values have been estimated as a linear function of the volume fraction and the thermal conductivities have been estimated using the Filippov equation

$$k = F_{H_2O}k_{H_2O} + F_{MeOH}k_{MeOH} - 0.72F_{H_2O}F_{MeOH}\left(k_{MeOH} - k_{H_2O}\right) \tag{32}$$

Thermal conductivities and ∂n/∂T of the pure solvents were taken from literature (Table 1).
Adding of methanol to aqueous solution of bilirubin improves the experimental enhancement factor but concomitant it decreased bilirubin concentration. From the curve shown in Figure 22 it is obvious that the increase in enhancement factor, derived from the theoretical fit, is maximal at 55% of methanol added. The sensitivity is increased up to 1.5 and 2.4 times with the addition of 20 and 50 % of methanol. Addition of higher volume fraction of methanol decreased the sensitivity due to sample dilution.

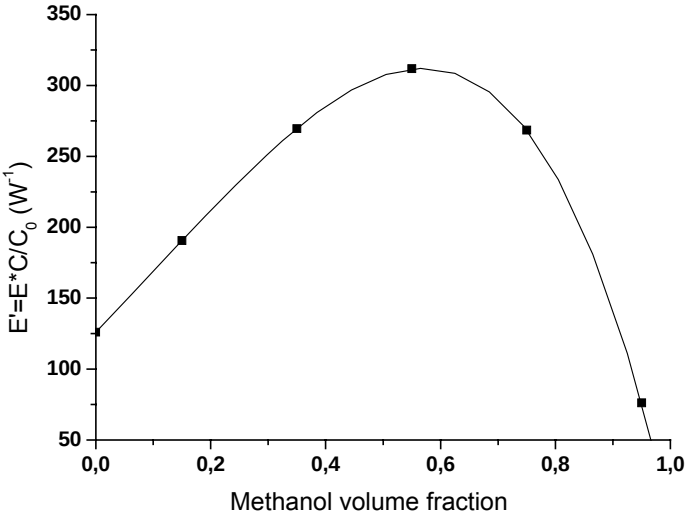

Figure 22: *Plot of the theoretical enhancement factor as a function of the methanol volume. The curve is plot of the E values calculated with Eq. (36) and multiple by bilirubin concentration fraction.*

4.2.3.2 Relative sensitivity of the TLS method

The effect of the addition of different amounts of methanol (0-50%) on TLS signal and the sensitivity of detection was tested. All experiments were carried out under the optimal experimental conditions (carrier flow rate 2 mL/min, injected sample volume 200 µL). The same volume of methanol was carefully added to the sample and to the carrier to avoid a mismatch in their composition.
Calibration curves (Figure 23) were prepared in the concentration range of 2.5-50 nM with the addition of different amounts of methanol (0, 20 and 50%). Enhancement factors calculated as slope of calibration line with added solvent against the slope of calibration with no addition were 1.2 for 20 and 2.9 for 50% of methanol added. Experimentally obtained values for enhancement factors differ from theoretically calculated by 20%. This could be attributed to the fact that in our calculations the enhancement factors were not calculated with reliable values of thermo-optical properties.

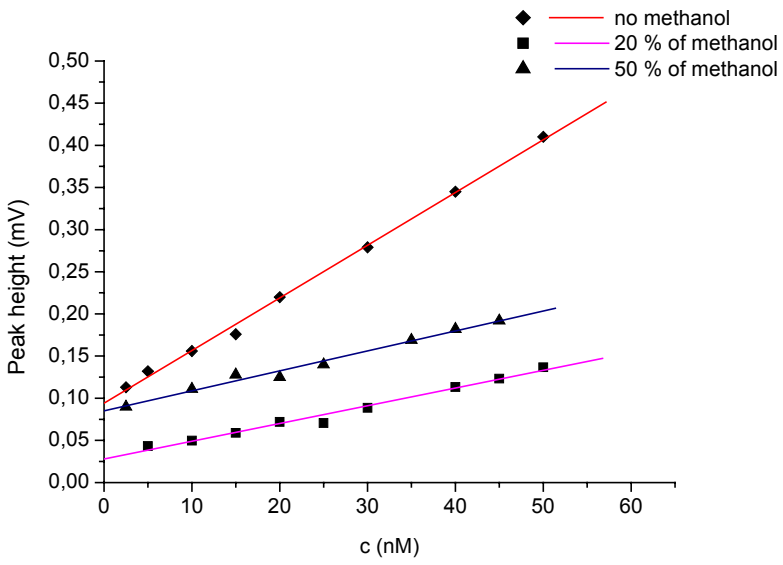

Figure 23: *Calibration curves for the bilirubin determination with different amounts of methanol*

The measurement of each concentration was repeated four times. The regression coefficients (r^2) of the plotted lines were higher than 0.995. The LOD calculated from the slope of calibration lines (S/N = 3 basis) were 1.43 nM for bilirubin in PBS phosphate buffer, 0.91 nM for bilirubin in 8:2 (v/v) PBS:MeOH mixture and 0.4 nM for bilirubin in 1:1 (v/v) PBS:MeOH mixture. The RSD for all measurements are summarized in Table 6.

Table 6: *Analytical features of measurements*

Bilirubin in PBS phosphate buffer				Bilirubin in PBS:MeOH 8:2 (v/v)			Bilirubin in PBS:MeOH 1:1 (v/v)		
nM	TL signal (mV)	STDEV	RSD (%)	TL signal (mV)	STDEV	RSD (%)	TL signal (mV)	STEDV	RSD (%)
2,5				0,077	0,0044	5,7	0,169	0,015	8,7
5	0,043	0,0021	4,8	0,136	0,015	11,1	0,192	0,010	5,2
10	0,050	0,0012	2,3	0,082	0,0032	3,9	0,216	0,005	2,3
15	0,059	0,0026	4,5				0,225	0,008	3,6
20	0,072	0,0046	6,4	0,142	0,0078	5,6	0,258	0,005	2,0
25	0,071	0,0029	4,1	0,135	0,001	0,7	0,313	0,001	0,5
30	0,089	0,0031	3,4	0,162	0,0046	2,8	0,391	0,004	1,1
35	0,108	0,0069	6,4	0,176	0,0087	4,9	0,378	0,002	0,5
40	0,113	0,0064	5,7	0,19	0,001	0,5	0,454	0,001	0,2
45	0,123	0,0021	1,7	0,21	0,007	3,3	0,519	0,002	0,3
50	0,137	0,0076	5,5	0,237	0,022	9,3	0,523	0,012	2,3

4.2.4 Bilirubin uptake in endotheliail cells

The applicability of the developed methodology was studied by analyzing the role of bilitranslocase (a membrane protein) in transport of bilirubin in endothelial cells. A histochemical analysis has demonstrated the positivity of endothelial cells (from a fragment of a rat aorta) to the response of a treatment with antibilitranslocase antibody. The expression of bilitranslocase in Ea.hy 926 cell line has been demonstrated by means of different analysis, such as Western blot and immunocytochemistry, both techniques use antibodies to detect the protein in cells. (Passamonti and Maestro, unpublished results).
It was shown that bilitranslocase plays a major role in the transport of free bilirubin (bilirubin-IXα) across the membrane of HepG2 cells (Margon et al., 2005).
We suppose a simmilar mechanism of bilirubin transport also in the case of model human endothelial cells (Ea.hy 926). We tried to assess bilirubin uptake at basal conditions with 50 nM bilirubin concentrations. The measurements were done in batch and flow injection mode. Samples taken from the cells incubated with the specific anti-bilitranslocase antibody (anti-sequence 65-75), which should block the activity of protein, were measured in a flow injection mode.

Both methods show (Figure 24) that there was no significant decrease in signal for samples taken at longer time of cell exposure to bilirubin and thus we assumed that the cells did not take up any bilirubin. Figure 24b shows that bilirubin was not enetering the cells incubated with anti-bilitranslocase antibody.

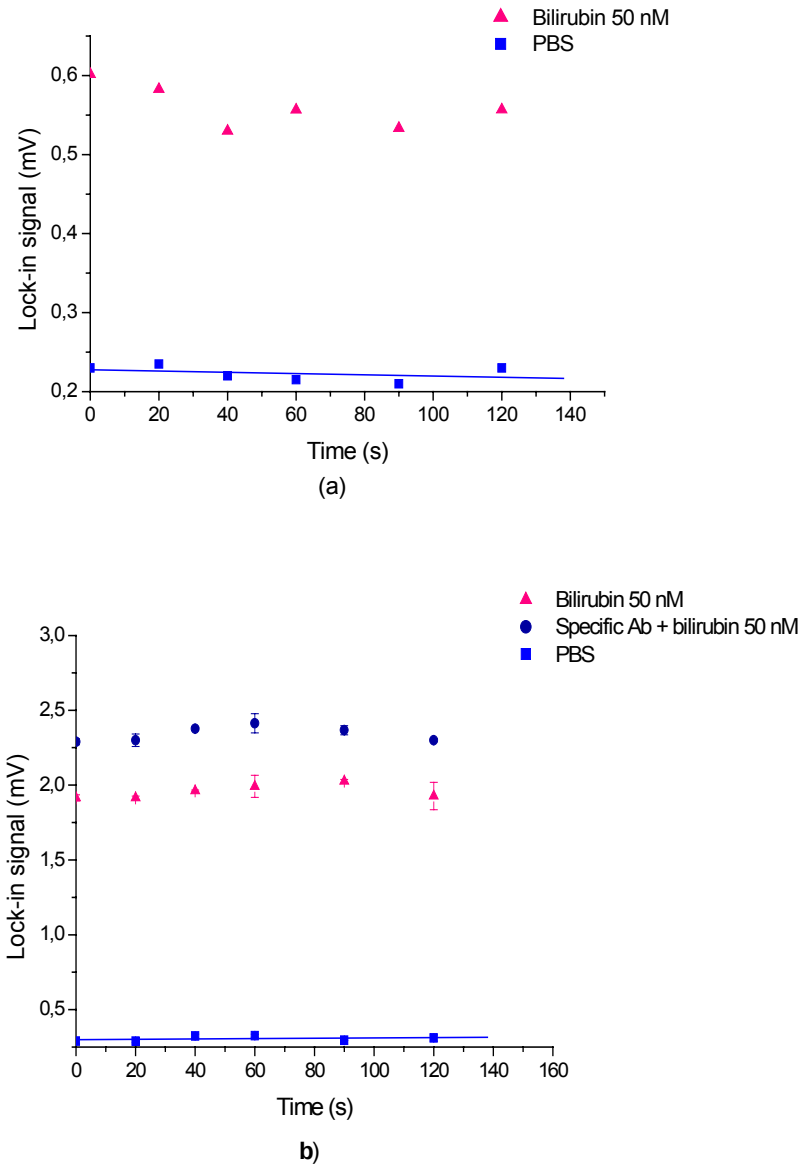

Figure 24: *Bilirubin uptake with time by endothelial cells at basal conditions. (a) Batch mode; (b) FIA-mode. PBS - phophate buffer saline*

It was shown that depending on the NADH/NAD^+ ratio the bilitranslocase changes from a low affinity form into its high affinity form (high NADH/NAD^+) (Margon et al., 2005). Thus, a reason why endothelial cells are impermeable to bilirubin could be related to the low NADH/NAD^+ ratio in cells kept at basal conditions.

The obtained results show that FIA-TLS method could be used for analysis of real samples with phisiological bilirubin concentrations. Since the available sample volume is 1.2 mL, flow injection mode enables up to five replicate measurements, whereas batch mode enables only one measurement of a particular sample. Reproducibility of the measurements at different times obtained in batch mode was 5%, whereas comparative FIA technique showed RSD of 2.3 and 2.1% for two experiments performed with 50 nM bilirubin (Fig. 24). Reproducibilities of the respective FIA TLS signal values assessed by four replicate measurements at each sampling time ranged from 0.3 to 6%.

Therefore, FIA offers several adventages in terms of: considerable decrease in required sample volume, reproducibility and reliability.

4.3 Determination of Selected Neonicotinoid Insecticides by Liquid Chromatography with Thermal Lens Spectrometric Detection

4.3.1 Procedures

Chromatography. The chromatographic separation procedure was applied in combination with TLS and DAD techniques. The isocratic separation of neonicotinoids was performed on a Pinnacle ODS column (250 mm × 4.6 mm, 5 μm) (Restek Corporation, Cally 911457). The mobile phase was 7:3 (v/v) water (0.2% phosphoric acid): acetonitrile. The flow rate of the eluent was 1.0 mL/min. Aliquots of 20.0 μL were manually injected through an injection loop in the case of HPLC/TLS, while an auto sampler (Agilent 1100) was utilized for HPLC/DAD analysis. Due to differences in absorption spectra of studied insecticides all chromatograms were recorded at four wavelengths (254, 270, 245 and 242 nm) in case of DAD, whereas in case of TLS the wavelength of the excitation laser (244 nm) was used for detection.

Sample Preparation. The water samples were collected from the Vipava river (Slovenia) and stored in the dark at 4°C for one week before further treatment. Stability of samples under these conditions was found sufficient for the purpose of this work where analysis of neonicotinoids was done only on spiked river samples. The aliquot of river water sample was spiked with the standard mixture of four neonicotinoids and kept in dark at 4ºC for 1 h before analysis without any kind of sample pre-treatment.
For all measurements, the solutions were filtered through 0.45-μm membrane filters (Millipore, USA).

4.3.2 Optimization of the HPLC/TLS method

TLS with single excitation wavelength is a non-specific detection technique, and therefore requires prior separation of analyte species. A mixture of water and acetonitrile is commonly used for the HPLC separation of different neonicotinoids on a reverse phase (Mandić et al. 2005, Rancan et al. 2006). The isocratic system 3:7 (v/v) water (0.2% phosphoric acid): acetonitrile was used to separate four insecticides as sharp, independent peaks.
An earlier study showed that the presence of phosphoric acid had a favourable effect on the shape of chromatographic peaks (Mandić et al. 2005), making them sharper and thus improving the separation.
The TLS parameters, such as modulation frequency and lock-in amplifier time constant, must be carefully optimized to increase the S/N ratio in HPLC-TLS measurements. Our experiments showed that by selecting longer lock-in time constants (up to 3 s), the signal noise was reduced due to averaging of the signal over longer time intervals. However, due to the longer averaging periods, the chromatographic peaks were broadened and also shifted to longer retention times The optimal time constant was therefore set at 1 s.
Additional improvements in the S/N were achieved by optimizing the modulation frequency (*f*) of the pump beam. The noise level of HPLC/TLS signals was reduced when the modulation frequency was changed from 12.5 to 120 Hz (Figure 25). On the other hand, a decrease of the peak height due to shorter excitation periods at higher modulation frequencies could also be observed. These contrary effects were equalized at 80 Hz and this frequency was used as optimal modulation frequency as it provided the optimal S/N ratio.

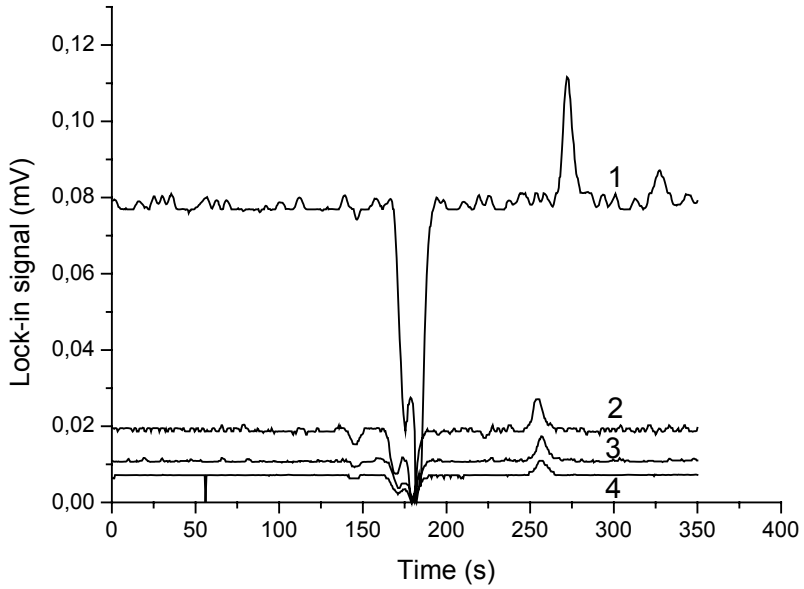

Figure 25: *Effect of modulation frequency on analytical signal and S/N ratio. Sample, 200 µg/L imidacloprid; P = 100 mW; time constant 1 s; f (1) = 12.5, (2) 60, (3) 80 and (4) 120 Hz. Mobile phase was 6:4, v/v water (containing 0.2% phosphoric acid) : acetonitrile*

4.3.3 Determination of neonicotinoid insecticides

Initial verification of the efficiency of the HPLC/TLS separation and determination procedure was performed under optimized TLS conditions.
The retention times for thiamethoxam, imidacloprid, acetamiprid and thiacloprid were 4.4, 5.7, 6.5 and 8.5 min., respectively (Table 7). Retention times (t_R) and reproducibility (RSD), determined individually for each compound. A comparison of the reproducibility with that of the comparative HPLC/DAD technique showed that comparable precision was obtained in both cases.

Table 7: *Retention times and reproductibility of individual neonicotinoid signals obtained by HPLC/TLS and HPLC/DAD techniques (n= 6)*

	Technique			
	HPLC/TLS		HPLC/DAD	
Insecticide	t_R (s)	RSD (%)	t_R (s)	RSD (%)
Thiamethoxam	261.0	0.12	257.8	0.10
Imidacloprid	342.4	0.66	337.4	0.12
Acetamiprid	391.9	0.33	373.1	0.10
Thiacloprid	510.6	0.57	511.6	0.22

In all cases the linearity of TLS detector response was checked with standard solutions in the range of 80-1000 ng/mL (Figur 26c). The r-square values of individual calibration lines ranged from r^2 = 0.995 for thiamteoxam to r^2 = 0.997 for thiacloprid.
The LOQs for acetamiprid and thiacloprid provided by TLS technique are however about 8.5 and 3 times lower compared to DAD (Table 8). Higher sensitivities found for acetamiprid (Figure 26a, c) and thiacloprid determination can be explained by the fact that the broad absorption band with maxima at 245 and 242 nm, respectively, matched well with the excitation laser wavelength of 244 nm. This is not the case for thiamethoxam (254 nm) and imidacloprid (270 nm) (Figure 26b,c).

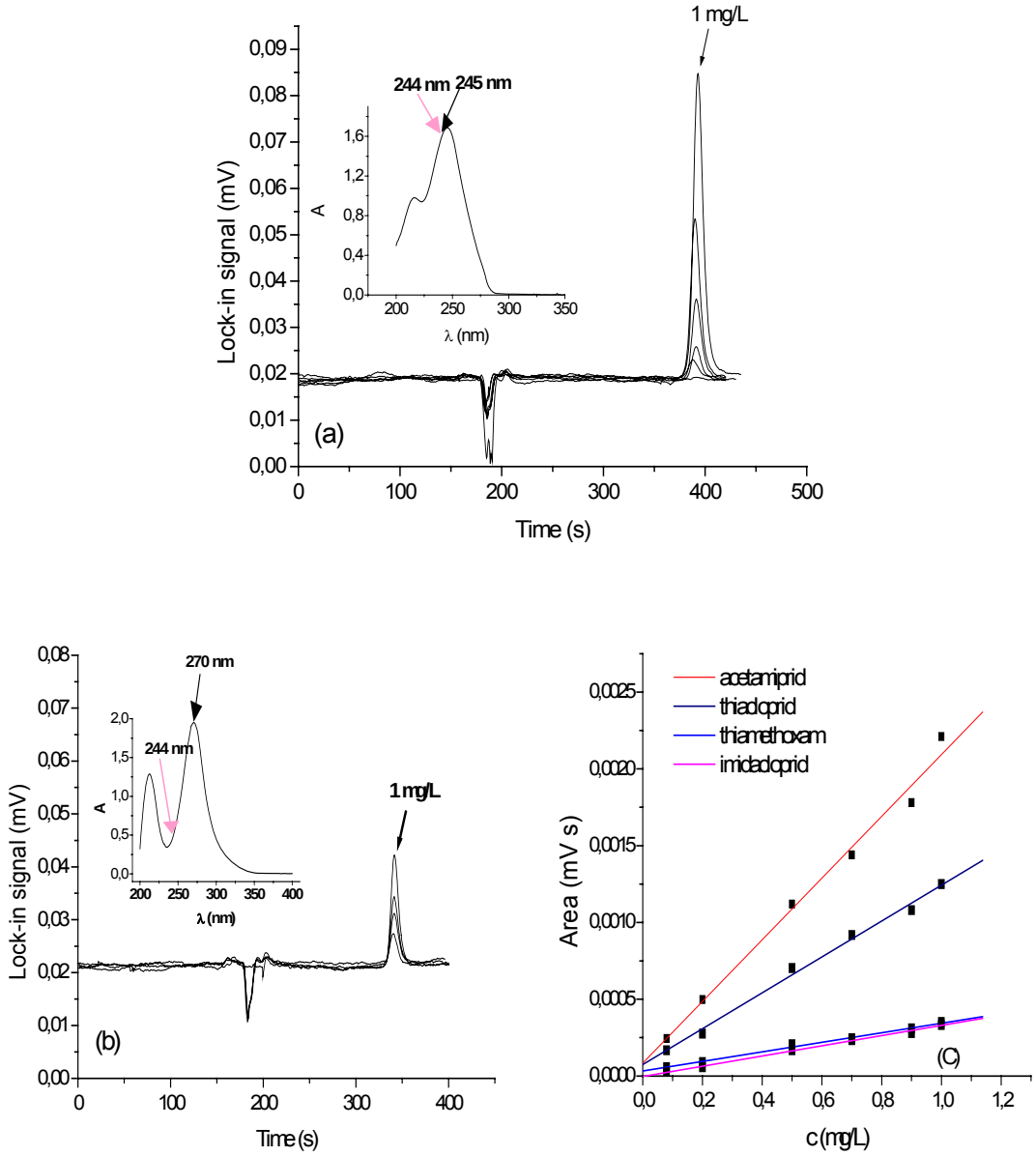

Figure 26: *HPLC-TLS chromatograms of diferenet concentrations of acetamiprid (a) and imidacloprid (b) and calibration curves for acetamiprid, thiacloprid, thiamethoxam and imidacloprid (c). Inserts in chromatograms represent the absorption spectra of analyte with indicated wavelengths of absorption maxima and laser excitation.*

Chromatogram of standard mixture of 4 neonicotinoids is shown in Figure 27.

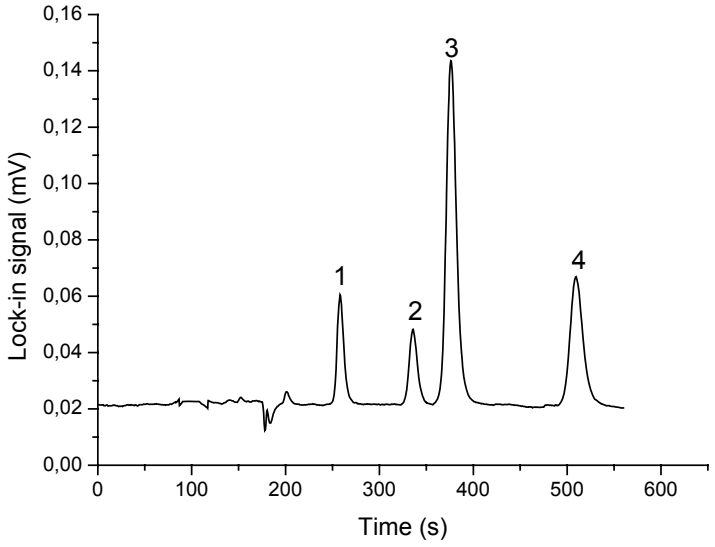

Figure 27: *HPLC/TLS chromatogram of 1.5 μg/mL level multi-residue analysis: (1) thiamethoxam; (2) imidacloprid; (3) acetamiprid and (4) thiacloprid. P = 100 mW, time constant 1 s; f = 80 Hz. Mobile phase: 7:3, v/v water (containing 0.2% phosphoric acid) : acetonitrile, v =1.0 mL/min*

Quantitative evaluation was based on the linear relationship between the peak area and concentration of neonicotinoids. The analytical parameters are presented in Table 8. Reproducibility of the responses obtained for the HPLC/TLS, assessed by six replicate measurements (100 μg/L) and the corresponding peak areas, were evaluated. A comparison of the reproducibility with that of the comparative HPLC/DAD technique showed that comparable precision was obtained in both cases.

Table 8: *Analytical parameters for the HPLC/TLS and HPLC/DAD determinations*

	Technique					
	HPLC/TLS			HPLC/DAD		
Insecticide	LOD (μg/L)	LOQ (μg/L)	RSD (%)	LOD (μg/L)	LOQ (μg/L)	RSD (%)
Thiamethoxam	15	50	0.9	39	130	0.9
Imidacloprid	27	89	1.1	27	89	1.0
Acetamiprid	3.2	10	0.8	26	85	0.8
Thiacloprid	7.5	25	0.7	23	76	0.9

4.3.4 Determination of neonicotinoide insecticides in river water samples

The applicability of the optimized HPLC/TLS was investigated by carrying out a recovery test on river water samples fortified at two levels (0.025 and 0.1 mg/L) as described in Experimental section, which is in agreement with the concentrations (0.01-0.3 mg/kg) quoted in the literatures (Di Muccio et al. 2006, Fernandez-Alba et al. 1996, Mandić et al. 2005, Obana et al. 2002, Obana et al. 2003) for the determination of neonicotinoids in different real samples (river water, pepper, potato, cucumber, apple

etc.). Figure 28 shows the HPLC/TLS signals obtained for the blank river water sample (curve S-1) and spiked one (curve S-2). As can be seen, after the separation steps there are no co-eluted compounds that could interfere with the determination of the investigated insecticides.

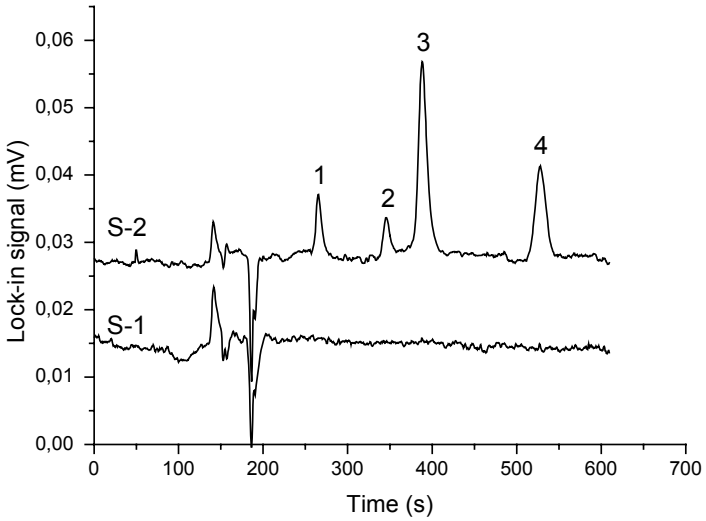

Figure 28: *HPLC/TLS chromatograms of non-treated river water sample (S-1); 100 µg/L level multi-residue analysis in spiked river water sample (S-2):*
(1) thiamethoxam; (2) imidacloprid; (3) acetamiprid and (4) thiacloprid; P = 100 mW, time constant 1 s; f = 80 Hz. Mobile phase: 7:3, v/v water (containing 0.2% phosphoric acid) : acetonitrile, v =1.0 mL/min. Curve S-1was evenly shifted in the vertical direction for clarity.

Results and recovery values are shown in Table 9. Average recoveries were in the range of 88–98% and reproducibility of the responses assessed by six replicate measurements ranged from 2 to 4.9%.

Table 9: *Determination of neonicotinoids in spiked river water samples by HPLC-TLS method*

Insecticide	Concentration added (µg/L)	Concentration found (mean ± S.D., n=6) (µg/L)	Precision (%RSD)	Recovery (%)
Thiamethoxam	100	98.3 ± 0.1	2.02	98.3
Imidacploprid	100	88.7 ± 0.5	4.08	88.7
Acetamiprid	100	95.3 ± 0.2	4.92	95.3
Thiacloprid	100	91.7 ± 0.4	4.78	91.7

LOQ limits of the method of 0.01 mg/L for imidacloprid or thiamethoxam, 0.002 mg/L for acetamiprid and 0.004 mg/L for thiacloprid were achieved. These levels are low enough to allow monitoring of the investigated neonicotinoid insecticides in real samples.

5 CONCLUSIONS

This work describes a sensitive and rapid FI assay for the determination of photochemicaly unstable analytes. Two developed procedures enabled accurate and precise determination of Cr(VI) at low µg/L levels, using a thermal lens spectrometric detector, without the need of any additional, time consuming pre-concentration step prior to the final measurement. The FIA-TLS procedure with on-line Cr-DPC reaction significantly reduced the time of analysis (50 s insteade of 20 min) and consumption of costly ultra-pure reagents relative to conventional spectrophotometric methods. With 10 mL of DPC solution 500 samples could be analysed instead of only 25 in case of batch mode measurement. For cases where the original sample size is limmited a second FIA procedure based in pre-reacted Cr-DPC complex is advantageous. Achieved LODs are approximately same (0.067 µg/L and 0.065 µg/L) in both procedures.
The presented results show that the thermal lens signal decreased with an increase in the flow rate within the whole range of the tested flow rates. This agrees with the published data (Dovichi and Harris, 1981) that flow increases the effective thermal conductivity of the sample due to the turbulence of the flow in the cell.

It has been demonstrated that the addition of methanol to the carrier (PBS phosphate buffer) and to sample enhances the TL signal from bilirubin. Consequently the sensitivity of FIA-TLS determination of bilirubin was improved by 2.9 times compared to FIA-TLS determination in aqueous solutions and an LOD of 0.4 nM was achieved. The high sample throughput of the system (60 samples per hour) makes it very suitable when rapid analysis is need and especially when the number of samples to be analyzed is significant.
The developed FIA-TLS system offers improved sensitivity, allowing the determination of Cr(VI) at levels under those established by batch mode TLS which offers LODs of 0.1 ng/mL (Šikovec et al., 1996; Margon et al., 2005). This stems from much shorter and highly reproducible time of exposure to excitation laser light (100 ms compared to several seconds), and therefore reduced photodegradation of Cr-DPC complex and bilirubin under given experimental conditions. As a results the standard deviation of FIA-TLS measurements is reduced by over two times compared to batch mode measurements and overcompensates the observed losses in sensitivity in flowing samples (up to 40 %) offering thus LODs on the order of 0.07 ng/mL for Cr(VI) in water.
The method was applied successfully to determination of Cr(VI) in drinking water samples and bilirubin in biological samples (endothelial cells).

A new HPLC-TLS method for simultaneous determination of four neonicotinoids (imidacloprid, thiamethoxam, acetamiprid and thiacloprid) in water samples was developed The retention times of thiamethoxam, imidacloprid, acetamiprid and thiacloprid were 4.4, 5.7, 6.4 and 8.5 min and the LODs were 15, 27, 3.2, and 7.5 µg/L, respectively. The LODs for imidacloprid compared well with those obtained by the same method using a DAD detector, while for the other investigated neonicotinoids the LODs provided by TLS technique were up to 8.5 times lower compared to DAD, with similar RSDs. The method was successfully tested for the determination of insecticides in spiked river water samples. For all analized neonicotinoides good recoveries (from 88 to 98%) have been obtained.
The method found further application in the analysis of real vegetable samples (potato) contaminated with these insecticides at a ppb level (Guzsvány et al., 2006). HPLC/TLS appears to be a promising technique for sensitive determination of neonicotinoids in biological samples as well. This would enable very much needed investigations of the physiological effects of low doses of neonicotinoids on honeybees, which are very much affected by the use of new insecticides.

6 REFERENCE

Al-Sabti K., Franko M., Adrijanič B., Knez S. 1994. Chromium-induced micronuclei in fish. Journal of Applaid Toxicology, 14: 333-336

Anderson R.A. 1989. Essentiality of chromium in humans. Science of the Total Environment, 86: 75-81

Arnaud N., Georges J. 2001. Investigation of the thermal lens effect in water-ethanol mixtures: composition dependence of the refractive index gradient, the enhancemant factor and the Sorret effect. Spectrochimica Acta Part A, 57: 1295-1301

Avery M.L., Decker D.G., Fischer D.L. 1994. Cange and Flight Pen Evaluation of Avian Repellancy and Hazard Associated with Imidacloprid-Treated Rice Seed. Crop Protection, 13: 535-540

Avery M.L., Decker D., Fischer D.L., Stafford T.R. 1993. Responses of Captive Blackbirds to a New Seed Treatment. J. Wildl. Manage. 57: 652-656.

Baesso M.L., Shen J., Snook R.D. 1994. Mode-mismatched thermal lens determination of temperature coefficient of optical path length in soda lime glass at different wavelengths. Journal of Applied Physics, 75: 3732-3737

Bailar J.C., Emeleus H.J., Nyholm R., Trotman-Dickenson A.F. 1973. Comprehensive Inorganic Chemistry. Permagon Press, Oxford

Barrett J., O'Brien P., De Jesus J.P. 1985. Chromium(III) and the glucose tolerance factor. Polyhedron, 4:

Beer H., Bernhard K. 1959. The effect of bilirubin and vitamin E on the oxidation of unsaturated fatty acids by ultraviolet irradiation [in German]. Chimia, 13: 291–292

Bendrusheva S.N., Ragozina N.Yu., Nedosekina D.A., Proskurnin M.A., Pyell U. 2006. Optimization of the instrumental parameters of the thermal lens detector for capillary electrophoresis. Moscow University Chemistry Bulletin, 60: 31-38

Bernard K., Ritzel G., Steiner K.U. 1954. On a biological significance of bile pigments: bilirubin and biliverdin as antioxidants for vitamin A and essential fatty acids [in German]. Helvetica Chimica Acta, 37: 306-313

Bialkowski S.E. 1996. Photothermal spectroscopy methods for chemical analysis. in: J.D. Winefordner (Ed.), Chemical Analysis, vol 134, Wiley, New York

Bicanic D., Franko M., Gibkes J., Gerkema E., Favier J.P., Jalink H. 1996. Applications of photoacoustic and photothermal non-contact methods in the selected areas of environmental and agricultural sciences, in: A. Mandelis (Ed.), Progress in Photothermal and Photoacoustic Science and Technology, vol. 3. Life and Earth Sciences, SPIE-Optical Engineering Press, Bellingham, 131–180

Blasco C. 2002. Simultaneus determination of imidacloprid, carbendazim, methiocarb, and hexythiazox in peaches and nectarines by liquid chromatography-mass spectrometry. Analytica Chimica Acta, 461: 109—116.

Bonnett R., Davis E., Hursthouse M.B., 1976. Structure of bilirubin, Nature, 262: 327–328

Bosma P.J. 2003. Inherited disorders of bilirubin metabolism. Journal of Hepatology, 38: 107-117

Brannon J.H., Magde D.J. 1978. Absolute quantum yield determination by thermal blooming fluorescein. Journal of Physical Chemistry, 82: 705-709

Braunwald E., Fauci Athony., Kasper D., Hauser S., Longo D., Jameson J. 2004. Harrison's principles of Internal Medicine. 16th ed. The McGraw-Hill's AccessMedicine

Buckingham S.D., Balk M.L., Lummis S.C.R., Jewess P., Sattelle D.B. 1995. Actions of nitromethylenes on an α-bungarotoxin-sensitive neuronal nicotinic acetylcholine receptor. Neuropharmacology, 34: 591-597

Caldera-Forteza A., Tomas-Mas C., Estela-Ripoll J.M., Cerda-Martin V., Ramis-Ramos G. 1995. Microchem. J. 52: 28

Chapman D. 1965. The Structure of Lipids by Spectroscopic and X-Ray Techniques. Methuen, London

Chartier A., Georges J., Mermet J.M. 1990. Abnormal signals in thermal lens spectrophotometry: determination of triplet lifetime of erytrosine, Specrchim. Acta. Part A, 46: 1737-1742

Chowdhury N.R., Arias I.M., Wolkoff A.W., Chowdhury J.R., 2001. Disorders of bilirubin metabolism. In: I.M. Arias, W.B. Jakoby, D. Schachter and D.A. Shafritz, Editors, The liver: biology and pathobiology (3rd ed), Raven Press, New York

Chromium. Micronutrient Information Center.
http://lpi.oregonstate.edu/infocenter/minerals/chromium/index.html (15. dec. 2006)

Chromium Toxicity: Environmental Medicine Case Study.
http://www.atsdr.cdc.gov/HEC/CSEM/chromium/docs/chromium.pdf (15. dec. 2006)

Clesceri L.S., Greenberg A.E., Trussel R.R. 1989. Standard Methods for the Examination of Water and Wastewaters. Port City Press, Baltimore

Cotton F.A., Wilkinson G.F. 1988. Advanced Inorganic Chemistry. 5th Ed. John Wiley & Sons, New York

Di Muccio A., Fidente P., Barbini A.D., Dommarco R., Seccia S., Morrica P. 2006. Application of solid-phase extraction and liquid chromatography-mass spectrometry to the determination of neonicotinoid pesticide residues in fruit and vegetables. Journal of Chromatogr A 1108: 1–6

Die Untersuchung von Wasser. Ein Auswahl chemischer Methoden für die Praxis, 5. Auflage, E.Merck AG·Darmstadt

Djousse L., Levy D., Cupples L.A., Evans J.C., D'Agostino R.B., Ellison R.C. 2001. Total serum bilirubin and risk of cardiovascular disease in the Framingham offspring study. American journal of cardiology, 87 :1196 –1200

Doull J., Klassen C.D., and Amdur M.O. 1991. Cassarett and Doull's Toxicology. The Basic Science of Poisons. Fourth Edition. Pergamon Press, Elmsford, NY

Dovichi N.J. 1987. Thermo-optical spectrophotometries in analytical chemistry. CRC Critical Reviews in Analytical Chemistry, 17: 357-423

Dovichi N.J., Harris J.M. 1979. Laser-induced therml lens effect for calorimetric trace analysis. Analytical Chemistry, 51: 728-731

Dovichi N.J., Harris J.M. 1980. Differentila thermal lens calorimetry. Analytical Chemistry, 52: 2338-2342

Dovichi N.J., Harris J.M. 1981. Thime resolved thermal lens calorimetry. Analytical Chemistry, 53: 106-109.

Edward H. Piepmeier. 1986. Analytical Applications of Lasers. in: J.D. Winefordner, P.J. Elving, I.M. Kolthoff (Ed.), Chemical Analysis, vol 87, Wiley, New York

Encyclopedia of Chemical Technology, Vol. 6, (1979), 3rd Ed., John Wiley & Sons, New York 1984

Erskine R.S., Bobbitt D.R. 1989. Obliquely crossed, differential thermal lens measurements under conditions of high background absorbance. Applied Spectrscopy, 43: 668-674

European Commission, Health&Consumer protection Directorate, 2003. Acetamiprid SANCO/1392/2001-Final. Appendix I-II: Identity, physical and chemical properties. www://ec.europa.eu/food/plant/protection/evaluation/newactive/acetamiprid.pdf (10. jan. 2007)

Faubel W. 1996. Detection of Pollutants in Liquids and Gases. in: A. Mandelis (Ed.), Progress in Photothermal and Photoacoustic Science and Technology, vol. 3. Life and Earth Sciences, SPIE-Optical Engineering Press, Bellingham, 289–328.

Faubel W., Schulz T., Seidel B.S., Ache H.J. 1994. Comparing the analytical potential of PAS, PDS, TL and PTPS for trace detection of pesticides in water. Journal De Physique IV, 4: C7–531-534.

Federal Register. Imidacloprid; Pesticide Tolerances. July 5, 1995. 60(128): 34943-24945.

Fernandez-Alba R.A., Valverde A., Aügera A., Contreras M., Chiron S. 1996. Determination of imidacloprid in vegetables by high-performance liquid chromatography with diode-array detection. Journal of Chromatography A, 721: 97–105

Fernández-Alba A.R., Tejedor A., Agüera A., Contreras M., Garrido J. 2000. Determination of imidacloprid and benzimidazole residues in fruits and vegetables by liquid chromatography-mass spectrometry after ethyl acetate multiresidue extraction. Journal of AOAC International, 83: 748-755.

Fidente P., Seccia S., Vanni F., Morrica P. 2005. Analysis of neonicotinoid insecticides residues in honey by solid matrix partition clean-up and liquid chromatography-electrospray mass spectrometry. J Chromatogr A 1094: 175–178

Fischer M., Georges J. 1996. Prediction of the calibration curves for the analysis of high absorbances using mode-mismatched dual-beam thermal lens spectrometry with chopped continuous wave laser excitation. Analytica Chimica Acta, 322: 117-130

Franko M., Tran C.D. 1996. Analytical thermal lens instrumentation. Review of Scientific Instruments 67: 1-18

Franko M., Bicanic D., van de Bovenkamp P. 1994. Dual beam infrared thermal lens spectrometry at 965 cm-1 absorption band as a measure of nonconjugated trans fatty acids content in margarine samples. Journal De Physique IV, 4: C7–479-482.

Franko M., Bicanic D., Gibkes J., Bremer M., Akkermans E. 1997. Thermal lens spectrometric detection and characterization of fatty acids. Food Technology and Biotechnology, 35: 39-43.

Franko M. 2001. Recent applications of thermal lens spectrometry in food analysis and environmental research. Talanta, 54: 1–13

Franko M., Bicanic D. 1998. Differential thermal lens spectrometry in the infrared. Israel Journal of Chemistry, 38: 175-179.

Franko M., Tran C.D. 1991. Thermal lens effect in electrolyte and surfactant media. Journal of Physical Chemistry, 95: 6688-6696

Franko M., Luterotti S., Van De Bovenkamp P., Bicanic D. 1998. 5th International Symposium Chromatography and Hyphenated Techniques, Bled Slovenia, Book of abstracts. Slovenian Chemical Society, 148.

Franko M., Van De Bovenkamp P., Bicanic D. 1998. Determination of trans-â-carotene and other carotenoids in blood plasma using high-performance liquid chromatography and thermal lens detection. Journal of Chromatography B: Biomedical Applications, 718: 47-54.

Geoerges J., Paris T. 1999. Influence of the Soret effect on the analytical signal in cw-laser thermal lens spectrometry of micellar solutions. Analytica Chimica Acta, 386: 287-296

Georges J. 1999. Advantages and limitations of thermal lens spectrometry over conventional spectrophotometry for absorbance measurements. Talant, 48: 501-509.

Gopinathan V., Miller N.J., Milner A.D., Rice-Evans C.A. 1994. Bilirubin and ascorbate antioxidant activity in neonatal plasma. FEBS Letters, 349: 197–200

Gourley G.R. 1997. Bilirubin metabolism and kernicterus. Advance Pediatrics, 44: 173 229

Greenwood N.N., Earnshaw A., Chemistry of the Elements. Permagon Press, Oxford

Gupta R. 1992. Principles of photothermal spectroscopy in fluids. in: A. Mandelis (Ed.), Principles and Perspectives of Photothermal and Photoacustic Phenomena, Elsevier Science publishing, New York, vol. 1, 95-152

Gupta R, Sell, J. A. 1989. In Photothermal Investigations in Solids and Fluids, ed., Academic Press, New York

Gutzman D.W., Langford C.H. 1993. Application of thermal lens spectrometry to kinetic speciation studies of metal ions in natural water models with colloidal ligands. Analytica Chimica Acta, 283: 773-783

Guzsvány V., Madžgalj A., Trebše P., Gaál F., Franko M. 2006. Determination of Some Neonicotinoid Insecticides by Liquid Chromatography with Thermal Lens Spectrometric Detection. Environmental Chemistry Letters (In press).

Hansen T.W.R., Bradtlid D. 1986. Bilirubin and brain toxicity. Acta Paediatrica Scandinavica, 75, 4: 513-522

Harata A., Kitamori T., Sawada T.J. 1995. Japan Soc. Colour Mater. 68: 606.

Hargreaves T. 1968. The Liver and Bile Metabolism, Appleton-Century-Crofts, New York, NY,

Harris J.M. 1982. Flow injection of ultratrace level samples into laser-based detectors. Analytical Chemistry, 54, 13: 2337-2340

Harris T.D. 1982. High-sensitivity spectrophotometry. Analytical Chemistry, 54, 6: 741A-750A

Hellpointer E. 1994. Degradation and Translocation of Imidacloprid (NTN 33893) Under Field Conditions on a Lysimeter. Miles Inc., Agricultural Division, PO Box 4913, Kansas City, MO. Miles Report No. 106426, 1-71.

Hordvik A. 1973. Applied Optics.16, 2827 (J. M. Harris iz knjige)

Hu C., Whinnery J.R. 1973. New thermooptical measurement method and a comparison with other methods. Applied Optics,12, 1: 72-79

Iwasa T., Motoyama N., Ambrose J.T., Michael Roe R. 2004. Mechanism for the different toxicity of neonicotinoid insecticides in the honey bee, *Apis mellifera*. Crop Protection, 23: 371–378

Jenkins J.J. 1994. Use of Imidacloprid for Aphid Control on Apples in Oregon. Potential for Ground and Surface Water Contamination. Department of Agricultural Chemistry. Oregon State University, Corvallis, OR.

Kagabu S. and Medej S. 1995. Stability comparison of imidacloprid and related compounds under simulated sunlight, hydrolysis conditions, and to oxygen. Biosci. Biotechnol Biochem. 59: 980–985

Kagabu S. 1997. Chloronicotinyl insecticides –discovery, application and future perspective. Reviews in Toxicology. 1: 75–129

Karp W.B. 1979. Biochemical alterations in neonatal hyperbilirubinemia and bilirubin encephalopathy. Pediatrics, 64: 361-368

Katz S.A. 1991. The analytical biochemistry of chromium. Environmental Health Perspect. 92: 13-16

Katz S.A, Salem H. 1994. The Biological and Environmental Chemistry of Chromium. VCH Publishers New York

Khuen Q.E., Faubel W., Ache H.J. 1994. Fresenius Journal of Analytical Chemistry, 348: 533

Kidd H. and James D. 1994. Agrochemicals Handbook. Third Edition. Royal Society of Chemistry. Cambridge, England

Kochar S.P., Rossell J.B. 1987. Int. Sci. 5: 23

Kozar-Logar J., Malej A., Franko M. 1999. Gordon Research Conference on Photoacoustic and Photothermal Phenomena, New London, New Hampshire

Kotaś J., Stasicka Z. 2000. Chromium occurrence in the environment and methods of its speciation. Environmental Pollution, 107: 263-283.

Laech R.A., Ružička J., Harris J.M. 1983. Spectrophotometric determination of metals at trace levels by flow injection and series differential detection. Analytical Chemistry, 55, 11: 1669-167

Laech R.A., Harris J.M. 1984. Real-time thermal lens absorption measurements with application to flow-injection systems. Analytica Chimica Acta, 164: 91-101

Li W.B., Segre P.N., Sengers J.V., Gammon R.W. 1994. Non-equilibrium fluctuations in liquids and liquid mixtures subjected to a stationary temperature gradient. Journal of Physics Condensed Matter, 6: 119-124

Liu M.Y., Lanford J., Casida J.E. 1993. Relevance of [3H]Imidacloprid binding site in house fly head acetylcholine receptor to insecticidal activity of 2-nitromethylene- and 2-nitroimino-imidazolidines. Pesticide Biochemistry and Physiology, 46: 200-206

Luterotti S, Franko M, Šikovec M, Bicanic D. 2002. Ultrasensitive assays of trans- and cis-â-carotenes in vegetable oils by high-performance liquid chromatography - Thermal lens detection. Analytica Chimica Acta, 460: 193-200

Lucey J.F. 1972. Neonatal jaundice and phototherapy. Pediatrics, 19: 827–839
Luteroti S, Markoviæ K, Franko M, Bicanic D, Vahèiæ N, Doka O. 2003. Ultratraces of carotenes in tomato pureìes: HPLC-TLS study. Review of Scientific Instruments, 74: 684-686

Mandić I.A., Lazić D.S., Ökrész N.Sz., Gaál F.F. 2005. Determination of the insecticide imidacloprid in potato (*Solanum tuberosum L*) and onion (*Allium cepa*) by high- performance liquid chromatography with diode-array detection. Journal of Analitical Chemistry, 60: 1134–1138

Margon A., Terdoslavich M., Cocolo A., Decorti G., Passamonti S., Franko M. 2005. Determination of bilirubin by thermal lens spectrometry and studies of its transport into hepatic cells, Journal De Physique IV, 125: 717-720

Meister, R.T. 1995. Farm Chemicals Handbook '95. Meister Publishing Company. Willoughby, OH.

Nauen R., Ebbinghaus-Kintscher U., Schmuck R. 2001. Toxicity and nicotinic acethylcholine receptor interaction of imidacloprid and its metabolites in *Apis Mellifera* (Hymenoptera: Apidae). Pesticide Management Science, 57: 577—586.

Newman T.B., Maissels M.J. 1992. Response to commentaries re: Evaluation and treatment of jaundice in the term newborn: A kinder, gentler approach. Pediatrics, 89: 831-833

Obana H., Okihashi M., Akutsu K., Kitagawa Y., Hori S. 2002. Determination of acetamiprid, imidacloprid and nitenpiram residues in vegetables and fruits by high-performance liquid chromatography with diode-array detection. Journal of Agricultural and Food Chemistry, 50: 4464–4467

Obana H., Okihashi M., Akutsu K., Kitagawa Y., Hori S. 2003. Determination of neonicotinoid pesticide residues in vegetables and fruits with solid phase extraction and liquid chromatography mass spectrometry Journal of Agricultural and Food Chemistry, 51: 2501–2505

Onishi S., Kawade N., Itoh S. 1980. High-pressure liquid chromatographic analysis of anaerobic photoproducts of bilirubin-IXá in vitro and its comparison with photoproducts in vivo. Biochemical Journal, 190: 527-532

Ostrow J.D., Mukerjee P., Tiribelli C. 1994. Structure and binding of unconjugated bilirubin: relevance for physiological and pathophysiological function. Journal of Lipid Reseach, 35: 1715-1736

Pedreira P.R B., Hirsch L.R., Pereira J.R.D., Medina A.N., Bento A.C., Baesso M.L., Rollemberg M.C.E., Franko M. 2004. Observation of laser induced photochemical reaction of Cr(VI) species in water during thermal lens measurements. Chemical Physics Letters. 396: 221-225.

Pedreira P.R.B., Hirsch L.R., Pereira J.R.D., Medina A.N., Bento A.C., Baesso M.L., Rollemberg M.C., Franko M., Shen J. 2006. Real-time quantitative investigation of photochemical reaction using thermal lens measurements: theory and experiment. Journal of Applaid Physics, 100 (4), art. no. 044906,

Philip T., Chen T.S., Nelson D.B. 1989. Detection of adulteration of California orange juice concentrates with externally added carotenoids by liquid chromatography. Journal of Agricultural and Food Chemistry, 37: 90-95

Pike K.S., Reed G.L., Graf G.T. and Allison D. 1993. Compatibility of Imidacloprid with Fungicides as a Seed-Treatment Control of Russian Wheat Aphid (Homoptera: Aphidae) and Effect on Germination, Growth, and Yield of Wheat Barley. J.Econ.Entomol, 86: 586-593.

Pritchard M.P., Hawaksworth G.M. 1990. Substrate-specific glucuronidation in rat hepatocytes. Biochemical Society Transactions, 18: 1215-1216.

Pogacnik L,, Franko M. 1999. Determination of organophosphate and carbamate pesticides in spiked samples of tap water and fruit juices by a biosensor with photothermal detection. Biosensors and Bioelectronics, 14: 569-578

Power J.F., Langford C.H. 1988. Optical absorbance of dissolved organic matter in natural water studies using the thermal lens effect. Analytical Chemistry, 60: 842-846

Pogačnik L., Franko M. 2003. Detection of organophosphate and carbamate pesticides in vegetable samples by a photothermal biosensor. Biosens Bioelectron,18: 1–9

Proskurnin M.A., Chernysh V.V., Kurzin M.A. 2000. Flow analysis of transition metals by thermal lensing. Journal of Analytical Chemistry, 56: 31-35

Rancan M., Sabatini G.A., Achilli G., Galletti C.G. 2006. Determination of imidacloprid and metabolites by liqid chromatography with an electrochemical detector and post column photochemical reactor. Analitica Chimica Acta, 555: 20–24

Rossi S., Sabatini A. G., Cenciarini R., Ghini S, Girotti S. 2005. Use of High-Performance Liquid Chromatography-UV and Gas Chromatography-Mass Spectrometry for Determination of the

Imidacloprid Content of Honeybees, Pollen, Paper Filters, Grass, and Flowers. Chromatographia, 61: 189—195

Rouchard J., Gustin F. and Wauters A. 1994. Soil Organic Matter Aging and its Effect on Insecticide Imidacloprid Soil Biodegradation in Sugar Beet Crop. Toxicology in Environmental Chemistry, 45:149-155.

Saito M., Kitamori T., Sawada T., in: Scudieri F., Bertolotti M. 1999. Photoacoustic and Photothermal Phenomena: 10th International Conference. AIP Conference Proceedings, 463: 214.

Sampietro M., Iolascon A. 1999. Molecular pathology of Crigler-Najjar type I and II and Gilbert's syndromes. Haematologica, 84: 150-157

Schiff L., Schiff E.R. 1993. Diseases of the liver. Lippincott Publisher, Philadelphia, PA

Seccia S., Fidente P., Barbini Attard D., Morrica P. 2005. Multiresidue determination of neonicotinoid insecticide residues in drinking water by liquid chromatography with electrospry ionisation mass spectrometry. Analitica Chimica Acta, 553: 21–26

Sedlak T.W., Snyder S.H. 2004. Bilirubin benefits: Cellular protection by a biliverdin reductase antioxidan cycle. Pediatrics, 113: 1776-1782

Shah V.P, Midha K.K., Dighe S., McGilveray I.J., Skelly J.P., Yacobi A., Layloff T., Viswanathan C.T., Cook C.E., McDowall R.D. 1992. Analytical methods validation: Bioavailability, bioequivalence and pharmacokinetic studies. International Journal of Pharmaceutics, 82: 1-7

Sheldon S.J., Knight L.V., Thorne J.M. 1982. Laser –induced thermal lens effect: a new theoretical model. Applied Optics, 21: 1663-1669

Snook R.D., Lowe R.D. 1995. Thermal lens spectrometry: A review. Analyst, 120: 2051.

Snook R.D., Lowe R.D., Baesso M.L. 1998. Photothermal spectrometry for membrane and interfacial region studies. Analyst, 123: 587-593

Soloways S.B. 1979. Nitromethylene insecticides. In Advances in Pesticides Science (Part II), Pergamon Press, 206-217

Stocker R., Yamamoto Y., McDonagh A.F., Glazer A.N., Ames B.N. 1987. Bilirubin is an antioxidant of possible physiological importance. Science, 235: 1043–1046

Tsamura Y., Nakamura Y., Tonogai Y., Kakimoto Y., Tanaka Y., Shibata T. 1998. Determination of neonicotinoid pesticide nitenpyram and its metabolites in agricultural products. Journal of the Food Hygienic Society of Japan, 39: 127—134

Šikovec M., Franko M., Cruz F.G., Katz S.A. 1996. Thermal lens spectrometric determination of hexavalent chromium. Analytica Chimica Acta, 330: 245-250

Šikovec M., Franko M. 1999. Gordon Research Conference on Photoacoustic and Photothermal Phenomena, New London, New Hampshire

Šikovec M., Noviè M., Hudnik V., Franko M. 1995. On-line thermal lens spectrometric detection of Cr(III) and Cr(VI) after separation by ion chromatography. Journal of Chromatography, A 706: 121-126

Šikovec M., Noviè M., Franko M. 1996. Application of thermal lens spectrometric detection to the determination of heavy metals by ion chromatography. Journal of Chromatography, A 739: 111-117

Šikovec M., Noviè M., Franko M. 2000. Determination of hexavalent chromium in drinking water by thermal lens spectrometry. Annali di Chimica, 90: 163-168

Šikovec M., Noviè M., Franko M., Veber M. 2001. Effect of organic solvents in the on-line thermal lens spectrometric detection of chromium(III) and chromium(VI) after ion chromatographic separation. Journal of Chromatography, A 920: 119-125

Scholz K., and Spiteller M. 1992. Influence of Groundcover on the Degradation of 14C-Imidacloprid in Soil. Brighton Crop Protection Conference. Pests and Diseases, 883-888.

Simpkins W., Harrison M. 1995. Trends Food Sci. Technol. 6: 321

Syngenta Crop Protection. Envirofacts. 2005. Thiamethoxam. http://www.syngentacropprotection-us.com/enviro/futuretopics/ThiomethoxamEnvirofacts_7-19-05.pdf. (13. jan. 2007)

Terazima M., Azumi T. 1989. Direct measure of enthalpy differences between enol and keto forms by the time resolved thermal lens method: 7-hydroxiqounoline. Journal of American Chemical Society, 111: 3824-3826

Thorne J.B., Bobbitt D.R. 1993. Comparison of Beer's law and thermal lens techniques for absorption measurements under conditions of high scattering backgrounds. Applied Spectroscopy, 47: 360

Tomlin C. 2000. The Pesticide Manual: a World Compendium, 12th edition, British Crop Protection Council, Farnham, United Kingdom

U.S. EPA. 1995. Imidacloprid; Pesticide Tolerance and Raw Agricultural commodities. 40 CFR Part 180 Section 472

U.S. EPA. Office of Prevention, Pesticides and Toxic Substances 2003. Pesticide fact sheet : Thiacloprid. Washington D.C., Sep.26.
http://www.epa.gov/opprd001/factsheets/thiacloprid.pdf (13. jan. 2007)

U.S. EPA. Office of Prevention, Pesticides and Toxic Substances 2002. Pesticide fact sheet : Acetamiprid. Washington D.C., Mar.15.,
http://www.epa.gov/opprd001/factsheets/acetamiprid.pdf (13. jan. 2007)

U.S. EPA. Federal Register Environmental Documents. 2005. Thiamethoxam: Pesticide Tolerance.
http://www.epa.gov/EPA-PEST/2005/January/Day-05/p089.htm. (13. jan. 2007)

Vilchez J.L. 1996. Determination of imidacloprid in water and soil samples by gas chromatography-mass spectrometry. Journal of Chromatography A , 389—294.

With T.K. 1968. Bile Pigments. Chemical Biological and Clinical Aspects. Academic Press, New York

Wu T.W. 1984. Bilirubin analysis—The state of the art and future prospects. Clinical Biochemistry, 17: 221-229

Weimer W.B., Dovichi N.J. 1986. Journal of Applaied Physics, 59: 225

Zucker S.D., Horn P.S., Serman K.E., 2004. Serum bilirubin levels in the US population: gender effect and inverse correlation with colorectal cancer. Hepatology, 40: 827–835.